UNIVERSIDAD MIGUEL HERNÁNDEZ DE ELCHE

PROGRAMA DE DOCTORADO EN RECURSOS Y TECNOLOGÍAS AGRARIAS, AGROAMBIENTALES Y ALIMENTARIAS

UNIVERSIDAD DE SONORA

DEPARTAMENTO DE INVESTIGACIÓN Y POSGRADO EN ALIMENTOS

PROGRAMA DE DOCTORADO EN CIENCIAS DE LOS ALIMENTOS

POTENCIAL ANTICANCERÍGENO DE COMPUESTOS AISLADOS A PARTIR DE TINTA DE PULPO (*Octopus vulgaris*)

MARTIN SAMUEL HERNANDEZ ZAZUETA

TESIS DOCTORAL

DIRECTOR DE TESIS:

DR. ÁNGEL ANTONIO CARBONELL BARRACHINA

CODIRECTOR DE TESIS:

DR. ARMANDO BURGOS HERNÁNDEZ

2024

UNIVERSITAS
Miguel
Hernández

POTENCIAL ANTICANCERÍGENO DE COMPUESTOS AISLADOS A PARTIR DE TINTA DE PULPO (*Octopus vulgaris*)

Martin Samuel Hernandez Zazueta
Estudiante de Doctorado

Director: Ángel Antonio Carbonell Barrachina

Codirector: Armando Burgos Hernandez

Thesis for the degree of Doctor from the Miguel Hernández University of Elche

Orihuela, Alicante, Spain 2024

UNIVERSITAS
Miguel
Hernández

El Dr. Ángel Antonio Carbonell Barrachina, director y el Dr. Armando Burgos Hernandez codirector de la tesis doctoral titulada **"Potencial anticancerígeno de compuestos aislados a partir de tinta de pulpo (*Octopus vulgaris*)"**

INFORMA/N:

Que D. Martin Samuel Hernandez Zazueta ha realizado bajo nuestra supervisión el trabajo titulado **"Potencial anticancerígeno de compuestos aislados a partir de tinta de pulpo (*Octopus vulgaris*)"** conforme a los términos y condiciones definidos en su Plan de Investigación y de acuerdo con el Código de Buenas Prácticas de la Universidad Miguel Hernández de Elche, cumpliendo los objetivos previstos de forma satisfactoria para su defensa pública como tesis doctoral.

Lo que firmo/firmamos para los efectos oportunos, en Orihuela a 15 de abril de 2024.

Director/a de la tesis	Codirector/a de la tesis
Dr. Ángel Antonio Carbonell Barrachina	Dr. Armando Burgos Hernandez

UNIVERSITAS
Miguel
Hernández

Profa. Dra. Juana Fernández López, Catedrática de Universidad y Coordinadora del Programa de Doctorado en Recursos y Tecnologías Agrarias, Agroambientales y Alimentarias (ReTos-AAA) de la Universidad Miguel Hernández de Elche (UMH),

CERTIFICA:

Que la Tesis Doctoral titulada **"Potencial anticancerígeno de compuestos aislados a partir de tinta de pulpo (*Octopus vulgaris*)"** del que es autor **Martin Samuel Hernandez Zazueta** ha sido realizada bajo la dirección del **Dr. Ángel Antonio Carbonell Barrachina,** profesor de la UMH y de la codirección del **Dr. Armando Burgos Hernández**, profesor de la Universidad de Sonora (UNISON, México), actuando como tutor el Dr. Daniel Valero Garrido (UMH). Considero que la tesis es conforme en cuanto a forma y contenido a los requerimientos del Programa de Doctorado ReTos-AAA, por tanto, es apta para su exposición y defensa pública.

Y para que conste a los efectos oportunos firmo el presente certificado en Orihuela a 22 de abril de de dos mil veinticuatro.

Profa. Dra. Juana Fernández López

UNIVERSITAS
Miguel
Hernández

ÍNDICE DE CALIDAD DE LAS PUBLICACIONES

UNIVERSITAS
Miguel
Hernández

La presente Tesis Doctoral, titulada "Potencial Anticancerígeno de Compuestos Aislados a partir de Tinta de Pulpo (*Octopus vulgaris*)", se presenta bajo la modalidad de **tesis por compendio** de las siguientes **publicaciones**:

- **Hernández-Zazueta, M.S.**, García-Romo, J.S., Noguera-Artiaga, L., Luzardo-Ocampo, I., Carbonell-Barrachina, Á.A., Taboada-Antelo, P., Campos-Vega, R., Rosas-Burgos, E.C., Burboa-Zazueta, M.G., Ezquerra-Brauer, J.M., Martínez-Soto, J.M., Santacruz-Ortega, H. del C., Burgos-Hernández, A., 2021. *Octopus vulgaris* ink extracts exhibit antioxidant, antimutagenic, cytoprotective, antiproliferative, and proapoptotic effects in selected human cancer cell lines. Journal of Food Science. https://doi.org/10.1111/1750-3841.15591.

- **Hernández-Zazueta, M. S.**, Luzardo-Ocampo, I., García-Romo, J. S., Noguera-Artiaga, L., Carbonell-Barrachina, Á. A., Taboada-Antelo, P., Campos-Vega, R., Rosas-Burgos, E. C., Burboa-Zazueta, M. G., Ezquerra-Brauer, J. M., & Burgos-Hernández, A. (2021). Bioactive compounds from Octopus vulgaris ink extracts exerted anti-proliferative and anti-inflammatory effects in vitro. Food and Chemical Toxicology, 151, 112119. https://doi.org/10.1016/J.FCT.2021.112119.

- **Hernández-Zazueta, M. S.**, García-Romo, J. S., Luzardo-Ocampo, I., Carbonell-Barrachina, Á. A., Taboada-Antelo, P., Rosas-Burgos, E. C., Ezquerra-Brauer, J.M., Martínez-Soto, J.M., Candia-Plata, M.C., Santacruz-Ortega, H.C. & Burgos-Hernández, A. (2023). N-(2-ozoazepan-3-yl)-pyrrolidine-2-carboxamide, a novel Octopus vulgaris ink-derived metabolite, exhibits a pro-apoptotic effect on A549 cancer cell line and inhibits pro-inflammatory markers. Food and Chemical Toxicology, 113829. https://doi.org/10.1016/j.fct.2023.113829.

UNIVERSITAS
Miguel
Hernández

***Octopus vulgaris* ink extracts exhibit antioxidant, antimutagenic, cytoprotective, antiproliferative, and proapoptotic effects in selected human cancer cell lines**

Autores: Martin Samuel Hernández-Zazueta, Joel Said García-Romo, Luis Noguera-Artiaga, Iván Luzardo-Ocampo, Ángel Antonio Carbonell-Barrachina, Pablo Taboada-Antelo, Rocio Campos-Vega, Ema Carina Rosas-Burgos, María Guadalupe Burboa-Zazueta, Josafat Marina Ezquerra-Brauer, Juan Manuel Martínez-Soto, Hisila del Carmen Santacruz-Ortega, Armando Burgos-Hernández.

Revista: *Journal of Food Sciences*

https://doi.org/10.1111/1750-3841.15591.

Editor: Richard W. Hartel

ISSN: 1750-3841

Ámbito de la publicación: Health, Nutrition, & Food

Categoría SCOPUS	Categoría del Cuartil	Rango	Factor de Impacto	Factor de Impacto de los Últimos Cinco Años
Food Science & Technology	Q2	57/144	2.991	0.33

UNIVERSITAS
Miguel
Hernández

Bioactive compounds from *Octopus vulgaris* ink extracts exerted anti-proliferative and anti-inflammatory effects *in vitro*

Autores: Martín Samuel Hernández-Zazueta, Iván Luzardo-Ocampo, Joel Said García-Romoa, Luis Noguera-Artiaga, Ángel Antonio Carbonell-Barrachina, Pablo Taboada-Anteloe Rocío Campos-Vega, Ema Carina Rosas-Burgosa, María Guadalupe Burboa-Zazueta, Josafat Marina Ezquerra-Brauera, Armando Burgos-Hernández.

Revista: *Food and Chemical Toxicology*

https://doi.org/10.1016/j.fct.2021.112119

Editor: José L. Domingo

ISSN: 0278-6915

Ámbito de la publicación: Food and Chemical Toxicology

Categoría JCR	Categoría del Cuartil	Rango	Factor de Impacto	Factor de impacto últimos 5 años
Toxicología	Q1	9/93	6.023	2.077

UNIVERSITAS
Miguel
Hernández

N-(2-ozoazepan-3-yl)-pyrrolidine-2-carboxamide, a novel *Octopus vulgaris* ink derived metabolite, exhibits a pro-apoptotic effect on A549 cancerous cell line and inhibits pro-inflammatory markers.

Autores: Martín Samuel Hernández-Zazueta, Joel Said García-Romo, Iván Luzardo-Ocampo, Ángel Antonio Carbonell-Barrachina, PabloTaboada-Antelo, Ema Carina Rosas-Burgosa, Josafat Marina Ezquerra-Brauera, Juan Manuel Martínez-Soto, Maria del Carmen Candia-Plata, Hisila del Carmen Santacruz-Ortega, Armando Burgos Hernández.

Revista: *Food and Chemical Toxicology*

https://doi.org/10.1016/j.fct.2023.113829

Editor: José L. Domingo

ISSN: 0278-6915

Ámbito de la publicación: Food and Chemical Toxicology

Categoría JCR	Categoría del Cuartil	Rango	Factor de Impacto	Factor de impacto últimos 5 años
Toxicología	Q1	9/93	6.023	2.077

UNIVERSITAS
Miguel
Hernández

Los autores agradecen a la Universidad Miguel Hernández de Elche por sus instalaciones y su excelente formación académica durante los 4 años de estudio. Agradezco al Consejo Nacional de Humanidades, Ciencias y Tecnologías (CONAHCYT) de México, que proporcionó el financiamiento para realizar mi doctorado (CVU: 786485) así como para llevar a cabo esta investigación (números de proyecto 241133 y 2174). Por ultimo y no menos importante, agradezco a la Universidad de Sonora por permitir desarrollarme en sus instalaciones como profesional y como persona.

UNIVERSITAS
Miguel
Hernández

ÍNDICE

UNIVERSITAS
Miguel
Hernández

ESTRUCTURA DE LA TESIS

Para la elaboración de la presente Tesis Doctoral se ha seguido la metodología basada en la publicación de artículos de investigación. Con esta Tesis Doctoral se pretende obtener el título de Doctor, para ello en la redacción de la misma, se ha seguido la normativa vigente de la Universidad Miguel Hernández de Elche.

La Tesis Doctoral se estructura en las siguientes partes:

1. Introducción.
2. Objetivos.
3. Metodología.
4. Publicaciones Científicas.
5. Resumen de Resultados y Discusión.
6. Discusión general.
7. Conclusiones generales e investigaciones futuras
8. Referencias.

La **Introducció**n contiene una breve revisión bibliográfica sobre productos naturales y su relación con actividad biológica benéfica para el ser humano. En la segunda parte se describen los **Objetivos** estimados en la presente tesis doctoral.

En la siguiente parte se detalla un **Resumen de la Metodología** utilizada, para la recopilación de los resultados y entender el diseño y la preparación de las muestras, además incluye los programas informáticos utilizados en los análisis estadísticos de los datos. A continuación, se recogen las publicaciones científicas publicadas que componen esta tesis doctoral.

- La **Primera Publicación** tiene la finalidad de reportar las evaluaciones realizadas sobre diferentes extractos y fracciones obtenidas a partir de la tinta de pulpo (*Octopus vulgaris*) mediante ensayos biodirigidos tales como, actividad antioxidante, citoprotectora, antiproliferativa y antimutagénica. Con base en los resultados obtenidos y mediante procesos de caracterización estructural, se obtuvo como resultado la identificación de un compuesto nuevo [N-(2-ozoazepan-3-yl)-pyrrolidine-2-carboxamide] (OPC) responsable de dicha actividad.
- La **Segunda Publicación** reporta los resultados que evidencian el potencial de los extractos y fracciones aisladas de la tinta de pulpo (*Octopus vulgaris*) y su efecto

antiproliferativo sobre líneas celulares humanas de cáncer de mama (MDA-MB435) y de colon (HT29 y HCT-116), además de un efecto antiinflamatorio, inhibiendo del desarrollo de especies reactivas de nitrógeno (NRS, siglas en Inglés) y de oxígeno (ROS, siglas en Inglés) y, al igual que un aumento en la expresión fluorométrica de IL-4 (antiinflamatoria) y disminución de NF-κB (proinflamatoria) en células mononucleares de sangre periférica (PBMC, siglas en Inglés).

- La **Tercera Publicación** da a conocer el nuevo compuesto denominado ozopromida [N-(2-ozoazepan-3-yl)-pyrrolidine-2-carboxamide] (OPC) como el responsable de la actividad antiproliferativa/pro-apoptótica sobre líneas de cáncer humano y antiinflamatorio mediante la modulación de citocinas pro y antinflamatorias. Al mismo tiempo, se describe el proceso para llevar a cabo su obtención a partir de síntesis química.

El **Resumen de la Discusión y Conclusiones** muestra un resumen con la discusión y conclusión de los resultados más interesantes e importantes conseguidos en los estudios, una discusión general de los mismos y las conclusiones de cada publicación. A continuación, se recogen las **Conclusiones Generales** obtenidas de los estudios realizados en esta Tesis Doctoral. En la siguiente parte se presentan las Investigaciones Futuras. Y en la última parte se recogen las **Referencias Bibliográficas** consultadas para la elaboración de esta memoria, sin tener en cuenta el apartado de publicaciones científicas.

Resumen

Abstract

RESUMEN

El cáncer es una enfermedad no transmisible de creciente preocupación en todo el mundo. Esta enfermedad se caracteriza principalmente por el crecimiento incontrolado y la diseminación de células anormales debido a la exposición de factores de riesgo comunes como infecciones por microorganismos, alto consumo de grasas, tabaquismo, factores hereditarios, etc. De manera similar, la inflamación crónica y persistente contribuye al desarrollo de cáncer y puede predisponer a la carcinogénesis. Es por eso que nos vemos en la necesidad de buscar nuevas alternativas que permitan la prevención y / o el tratamiento de esta enfermedad. Los productos alimenticios marinos como la tinta de *Octopus vulgaris* (OI) podrían ser fuentes de compuestos que aborden estas preocupaciones. Este estudio tuvo como objetivo evaluar los efectos antiproliferativos y antiinflamatorios de los extractos de tinta de *Octopus vulgaris* (extractos solubles en hexano, acetato de etilo, diclorometano (DM) y extractos solubles en agua) utilizando líneas celulares de cánceres tales como cancer colorrectal humano (HT-29/HCT116) y mama (MDA-MB-231) y células murinas (RAW 264.7) estimuladas con lipopolisacárido (LPS).

ABSTRACT

Cancer is a non-communicable disease of growing concern throughout the world. This disease is mainly characterized by the uncontrolled growth and spread of abnormal cells due to the exposure of common risk factors such as microorganism infections, high fat intake, smoking, hereditary factors, etc. Similarly, chronic and persistent inflammation contributes to the development of cancer and may predispose to carcinogenesis. That is why we need to find new alternatives that allow the prevention and / or treatment of this disease. Marine food products such as *Octopus vulgaris* ink (OI) could be sources of compounds that address these concerns. This study aimed to evaluate the antiproliferative and anti-inflammatory effects of OI extracts (hexane-soluble extracts, ethyl acetate, dichloromethane (DM) and water-soluble extracts using cancer cell lines such as human colorectal (HT -29/HCT116) and breast (MDA-MB-231) and murine cells (RAW 264.7) stimulated with lipopolysaccharide (LPS).

1. INTRODUCCIÓN

1. INTRODUCCIÓN

La segunda causa de muerte en el mundo es una enfermedad crónico-degenerativa denominada como cáncer (OMS, 2020) siendo los principales, de pulmón/bronquios, próstata y colon/recto para hombres y pecho, colon/recto y cérvix en el caso de mujeres (ACS, 2018). Muchos de estos se podrían prevenir evitando la exposición a factores de riesgo comunes como infecciones por microorganismos, alto consumo de grasas, tabaquismo, factores hereditarios, etc. Dichos factores pueden modificar los genes que están implicados directamente en la regulación del ciclo celular y dar lugar a la formación de nuevas células alteradas. Cuando estos genes sufren una mutación, las células proliferan en forma desmedida llegando a formar masas de tejido conocidas como neoplasias o tumores y en ciertos casos diseminarse a otros tejidos u órganos mediante el proceso de metástasis (Alberts et al., 2008). De esta manera el proceso de oncogénesis se da mediante la interacción entre la genética y el medio ambiente, después de que ésta se altera por agentes carcinógenos o por errores en la copia y la reparación de genes. Incluso si el daño genético se produce sólo en una célula somática, la división de la célula dañada se transmitirá a las células hijas, dando lugar a un clon de células modificadas (Lodish et al., 2008). A medida que las células se vuelven anormales, las células viejas o dañadas sobreviven cuando deberían morir y células nuevas se forman cuando no son necesarias. Estas células adicionales pueden dividirse sin interrupción y pueden formar masas denominadas tumores. Muchos tipos de cáncer forman tumores sólidos, los cuales son masas de tejido. Los cánceres de la sangre, como las leucemias, en general no forman tumores sólidos. Los tumores cancerosos son malignos, lo que significa que se pueden extender a los tejidos cercanos o los pueden invadir. Además, al crecer estos tumores, algunas células cancerosas pueden desprenderse y localizarse en diferentes órganos del cuerpo por medio del sistema circulatorio o del sistema linfático y formar nuevos tumores lejos del tumor original (NCI, 2015).

1.1. Clases de Tumores

Existen dos tipos de tumores, los tumores localizados e invasivos. Los tumores localizados se caracterizan por que están confinados a una región anatómica, ya sea un tejido o un órgano. Se encuentran delimitados por una membrana la cual no permite la invasión celular de las células malignas a tejidos vecinos, además no son considerados potencialmente peligrosos debido a que pueden removerse mediante cirugía (NIH, 2013).

Por el contrario, los tumores invasivos, pueden expandirse a distintas zonas anatómicas del cuerpo causando un daño generalizado. La invasividad viene dada por la producción de un grupo de proteínas llamadas proteasas, que ocasionan el rompimiento de las uniones célula-célula establecidas por las fibras de colágeno de matriz extracelular. Esto causa la liberación de la célula maligna del tumor primario, posteriormente esta pasa a circulación o vía linfática mediante extravasación, en esta zona algunas células son eliminadas por el sistema inmune pero otras logran sobrepasar esta barrera y mediante intravasación se establecen en nuevo tejido, donde logran reproducirse gracias a que activan la angiogénesis (formación de nuevos vasos sanguíneos) logrando así obtener los nutrientes y factores de crecimiento que le permitirán proliferar para formar un nuevo tumor (Lewis et al., 2000). A este proceso de invasión celular se le conoce como metástasis y es el causante del mayor número de muertes por cáncer (Plummer et al., 2016).

1.2. Epidemiología del Cáncer

Según la OMS, más del 70 % de los nuevos casos anuales de cáncer en el mundo se producen en África, Asia, América Central y Sudamérica representando el 70 % de las muertes por éste y se reporta que los casos anuales aumentaron de 14 millones en 2012 a 22 millones en el 2015 (OMS, 2015).

1.3. Inflamación y Cáncer

La inflamación crónica es una respuesta biológica del sistema inmune cuyo objetivo es proteger al organismo del daño externo; bajo ciertas condiciones, el proceso inflamatorio provee condiciones favorables para el desarrollo de varios pasos involucrados en la tumorigénesis, incluyendo la transformación celular, promoción, supervivencia, proliferación, invasión, angiogénesis y metástasis (Coussens y Werb, 2002).

Durante el 2008, alrededor del 25 % de todos los cánceres reportados estaban relacionados con la inflamación y se estima que 15 % de las muertes por cáncer están asociadas con ésta. Inflamaciones inducidas por infecciones están involucradas en la patogénesis de aproximadamente el 15-20 % de los tumores humanos. Sin embargo, incluso los tumores que no están vinculados epidemiológicamente a patógenos se caracterizan por la presencia de un componente inflamatorio en su microambiente (Allavena et al., 2008).

Características de la inflamación asociada a cáncer incluyen la presencia de leucocitos infiltrantes, citocinas, quimiocinas, factores de crecimiento, mensajeros de lípidos y enzimas que degradan la matriz. Hoy en día, es reconocido que la inflamación es un factor de riesgo para la mayoría de los tipos de cáncer. Se ha demostrado que TNF-α es uno de los principales mediadores de la inflamación, sin embargo, cuando éste presenta una desregulación y es secretado en la circulación, puede mediar una amplia variedad de enfermedades, incluyendo el cáncer (Aggarwal, 2003). Por otro lado, una de las moléculas más importantes implicada en el proceso inflamatorio y que juega un papel terapéutico en las células del sistema inmunológico es el óxido nítrico (ON) ya que regula la respuesta vascular, migración de leucocitos, producción de citocinas y proliferación celular. El ON es generado principalmente por la enzima Óxido Nítrico Sintasa (iNOS) a partir del aminoácido L-arginina (Bogdan, 2001). La expresión génica de iNOS y la traducción del mRNA está controlada por diversos agonistas, especialmente mediadores pro-inflamatorios. Las citoquinas más prominentes involucrados en la estimulación iNOS son TNF-a, IL-1b, y IFN-g. La expresión de iNOS está regulada por factores de transcripción incluyendo NF-kB. La enzima iNOS ha sido implicada en diferentes etapas de los cambios celulares que conducen a malignidad: la transformación de las células normales, crecimiento de células transformadas, angiogénesis desencadenada por factores angiogénicos liberados por células tumorales o del tejido circundante y metástasis de las células malignas (Taylor et al., 1998). Asimismo, es posible observar la expresión de esta enzima en una amplia variedad de tumores malignos humanos como cáncer de mama, pulmón, próstata, vejiga, cáncer colorrectal y melanoma maligno (Lirk, Hoffmann and Rieder, 2002). Entre los factores desencadenantes de la inflamación crónica que aumentan el riesgo de cáncer se encuentran las infecciones microbianas como *Helicobacter pylori* (HP); para el cáncer gástrico (Fuentes-Pananá, Camorlinga-Ponce y Maldonado-Bernal, 2009), el linfoma de la mucosa, enfermedades autoinmunes (enfermedad inflamatoria intestinal de cáncer de colon), y las condiciones inflamatorias criptogénicas (prostatitis para el cáncer de próstata). Por consiguiente, el uso de agentes anti-inflamatorios no esteroideos disminuye la incidencia de varios tumores (Guadagni et al., 2007).

La relación infección-inflamación-cáncer se comprende mejor en el cáncer gástrico, el cual resulta de la infección por HP de forma análoga (Kusters, van Vliet y Kuipers, 2006), el virus de Epstein-Barr daña el tejido epitelial del estómago de manera directa y

constante, quizá a través de la reacción inflamatoria a la infección (Imai et al., 1994). Por lo cual en la actualidad se reconoce un gran número de enfermedades entre ellas el cáncer que inician a partir de un proceso inflamatorio crónico (Coussens and Werb, 2002).

1.4. Terapias Contra el Cáncer

En la actualidad las terapias que reciben los pacientes afectados por cáncer suelen traerle repercusiones, debido a que afectan el desarrollo de las células tumorales y células normales no cancerígenas (Komen, 2010). En el caso de la quimioterapia los fármacos utilizados actúan bloqueando puntos específicos del ciclo celular, por lo que afectan el desarrollo de células que están en mitosis activa como las células cancerígenas, así mismo inhiben la proliferación de células normales no cancerígenas de crecimiento rápido como son las de médula ósea, folículos pilosos, células del sistema digestivo etc., provocando de esta manera la aparición de efectos secundarios (ACS, 2016). Aunado a este problema se encuentra la resistencia que presentan algunos tumores a la quimioterapia, se habla de resistencia innata cuando las células cancerígenas son resistentes a los fármacos aún sin haber tenido contacto previo y resistencia adquirida cuando ésta aparece después del contacto con la droga. La cinética de crecimiento y las mutaciones espontáneas son las características tumorales que determinan la resistencia (Paredes-Lario, Blanco-García y Echenique-Elizondo, 2006). Por ello la necesidad de indagar en la búsqueda de alternativas de origen natural con efecto terapéutico o quimiopreventivo ante esta enfermedad (Figueroa-Hernández et al., 2005).

1.5. Actividad Biológica en Productos Naturales

Los ecosistemas marinos representan la mayor parte de la superficie del planeta y comprenden un recurso continuo de compuestos con actividades biológicas ilimitados e inmensas entidades químicas. La fauna y la flora marinas suelen producir metabolitos secundarios con características estructurales distintas a los de otras fuentes naturales que son de interés por su uso potencial en la industria y en aplicaciones biomédicas (Braekman y Daloze, 1986; Stankevicins et al., 2008). Los organismos marinos han sido descritos como una fuente importante de sustancias bioactivas de gran valor para el tratamiento de enfermedades. Dichas sustancias contienen compuestos que han sido estudiados por su actividad biológica como, antibacterianos, antivirales, antimutagénicos, antiproliferativos, antitumorales, antineoplásicos y con beneficios en el sistema cardiovascular, entre otras. Solamente en el año 2000 fueron descubiertos alrededor de

143 productos marinos antitumorales de los cuales destacan: poliacetatos, terpenos, esteroides, y péptidos, entre otros. De igual manera fueron reportados 124 compuestos de origen marino con un potencial efecto citotóxico *in vitro* sobre células tumorales (Mayer y Gustafson, 2003). Numerosos estudios recientes han identificado compuestos con potencial biológico, como los alquilgliceroles aislados de aceite de hígado de tiburón con potencial anti-tumoral y anti-metastásico (Deniau et al., 2010); a su vez, se reportó un sulfoglicolípido de macroalgas marinas que inhibe el crecimiento de líneas celulares cancerígenas de humanos (Tsai y Sun Pan, 2012) al igual que terpenoides identificados en organismos marinos y esponjas (Gross y König, 2006), entre otros.

1.6. Compuestos Bioactivos en Cefalópodos

Algunos moluscos como los cefalópodos han sido ampliamente estudiados en cuanto a una variedad de actividades biológicas tales como la capacidad antioxidante, antitumoral, antimutagénica y antibacteriana (Cruz-Ramírez y col., 2015; Derby, 2014). En un estudio reciente, se aislaron y caracterizaron fracciones con actividad antimutagénica obtenidas a partir de extractos orgánicos crudos de músculo de pulpo (*Paraoctopus limaculatus*) en donde se obtuvo un porcentaje de inhibición mayor al 80 % inducida por 500 ng de AFB1 en ambas cepas de ensayo. Los datos de IR y RMN de ^{13}C y ^{1}H sugirieron la presencia de compuestos de tipo ftalato. El análisis de GC-MS reveló que el compuesto responsable de la alta actividad anti-mutagénica fue atribuida a la estructura de 1-butil-2-isobutil-ftalato (Cruz-Ramírez et al., 2015).

En otro estudio se evaluó la actividad antioxidante y antimicrobiana, así como estudios proximales del liofilizado de tinta de calamar de la India (*Loligo duvauceli*) donde se obtuvo 62.46 ± 0.62 % de proteína como contenido mayoritario seguido de 9.29 ± 0.05 % de cenizas 4.43 ± 0.29 % de humedad y 3.96 ± 0.08 % de grasa. Los resultados de la técnica de 2,2-Difenil-1-Picrilhidrazilo (DPPH) mostraron que el extracto acuoso del liofilizado de tinta de calamar tiene un alto potencial antioxidante de 94.87 ± 4.87 %, seguido del extracto etanólico con 67.57 ± 7.55 %, y el extracto de hexano con 2.10 ± 1.18 %. Tanto el extracto acuoso como el etanólico mostraron propiedades antimicrobianas con un halo de inhibición de 7.5 mm para *Bacillus subtilitis*, de 8 mm para *Staphylococcus aureus*, de 7 mm para *Salmonella sp.* y de 15 mm para *Escherichia coli* (Fahmy, 2013).

1.7. Generalidades del Pulpo

Los octópodos son del orden Octopda cefalópodos conocidos comúnmente como pulpos. Estos pertenecen al filo Mollusca los cuales se caracterizan por ser organismos invertebrados y de cuerpos blandos. Además, pertenecen a la clase Cephalopoda donde el pie característico de los moluscos aparece unido a la cabeza y se encuentra diversificado en varios tentáculos. Dichos organismos se incluyen en el orden Octopoda al cual pertenecen aquellos moluscos que poseen 8 tentáculos (Turgeon et al., 1998). Los hábitats del pulpo incluyen rocas, arrecifes y fondos submarinos; la mayoría se encuentran en áreas rocosas donde habitan en cuevas, grietas que funcionan como guaridas u hogares. Algunas especies viven en áreas arenosas y aparentemente no poseen un hogar permanente. Su alimentación consta de crustáceos, otros moluscos y peces pequeños (Rajasekharan Nair et al., 2011).

1.8. Tinta de Cefalópodos

Los cefalópodos se encuentran en todos los hábitats marinos del mundo. Éstos son famosos por sus mecanismos de defensas ante ambientes hostiles o bajo la amenaza de algún depredador, donde suelen responder con movimientos de escape, cambios de coloración producir toxinas e incluso eyección de tinta (Rajasekharan Nair et al., 2011). Esta última ha sido utilizada por los seres humanos en diversas formas durante miles de años y consiste mayormente en una suspensión de gránulos de melanina y proteoglicanos en un medio viscoso de color negro. Históricamente la tinta de calamar ha sido extraída directamente del saco de tinta de *Sepia officinalis*. Presenta una coloración oscura semitransparente que puede utilizarse como tinta para escribir o como colorante. Los usos de la tinta de calamar han sido reportados desde la década de los 70´s, pero no fue hasta la década de los 90´s que se volvió de uso común entre fotógrafos, artistas y pintores (López-Montes et al., 2009).

El conocimiento actual sobre la tinta de calamar explica los principales componentes que la constituyen, siendo la melanina uno de los mayoritarios por lo que se han investigado las vías bioquímicas involucradas en su producción, la neuroecología en el uso de la tinta en la interacción depredador-presa en su ambiente natural y el uso de tinta de calamar en particular para el desarrollo de fármacos con aplicaciones biomédicas y otros productos químicos con aplicaciones industriales, comerciales etc. (Derby, 2014). Existen estudios donde se evaluó la actividad antimicrobiana de los extractos de tinta y los tejidos del

cuerpo de los cefalópodos, *Euprymna stenodactyla* y *Octopus dollfusi* contra bacterias productoras de histamina (HPB) como *E. coli*, *Salmonella typhi* (*S. typhi*), *Klebsiella pneumoniae* entre otras, por el método de difusión en pocillo de agar donde como resultado se observó mayor actividad inhibidora frente a *Pseudomonas aeruginosa* con extractos metanólicos de tinta de *E. stenodactyla* y extractos etanólicos contra *S. typhi* (Sadayan, Thiyagarajan y Balakrishnan, 2013). Además, ya se ha reportado evidencia de actividad biológica en tinta de cefalópodos, encontrando potencial antioxidante, antimicrobiano, antiinflamatorio y citotóxico (Besednova, Zaporozhets, Kovalev, Makarenkova, y Yakovlev, 2017). Las actividades reportadas tienen el potencial de coadyuvar como un efecto protector contra el desarrollo del cáncer; los compuestos antioxidantes están asociados con la regresión y la inhibición del crecimiento de lesiones premalignas; los compuestos antimutagénicos tienen un efecto quimiopreventivo contra el ADN inducido por mutágenos y están asociados con una ralentización de las etapas iniciales del proceso de carcinogénesis. Además, la actividad antiproliferativa está directamente relacionada con el desarrollo de esta enfermedad y, por tanto, representa una herramienta en la identificación de nuevos candidatos con la habilidad de prevenir o desacelerar la división descontrolada de células cancerosas al interferir en el ciclo celular (García-Romo y col., 2020; López-Saiz, Suárez-Jiménez, Plascencia-Jatomea, y Burgos-Hernández, 2013). Por otro lado, la tinta de calamar ha sido ampliamente utilizada en la cultura medicinal China, debido a su efecto homeostático, antitumoral e inmunomodulador. Liu y colaboradores (2008) aislaron varios carbohidratos a partir de la tinta de calamar de las especies *Sepiella maidroni*, donde encontraron un nuevo polisacárido "SIP" (*S. maidroni* ink polysaccharide) al cual se atribuyó como un potencial y efectivo agente antimutagénico. En otro estudio evaluaron extractos de tinta *Sepia officinalis*, (IE) y extractos de *Coelatura aegyptiaca* (*C. aegyptiaca*) donde presentaron actividad en líneas celulares de carcinoma hepatocelular obteniendo una CI_{50} de 67 y 49.24 g/ml, respectivamente; donde concluyeron que, los extractos de tinta de *S. officinalis* y extractos de *C. aegyptiaca* tuvieron propiedades antioxidantes, anti-inflamatorias y citotóxicas por lo que los consideraron como fuente de medicamentos prometedores contra el cáncer (Fahmy, 2013). A pesar de las actividades biológicas encontradas en la tinta de cefalópodos, no hay informes de actividad antiproliferativa o proapoptótica *in vitro* de la tinta de pulpo (*Octopus vulgaris*) contra líneas celulares cancerosas como 22Rv1, HeLa y A549, un representante de las condiciones de cáncer primario (cáncer de próstata, cuello uterino y pulmón, respectivamente). La elucidación

estructural de los compuestos responsables de estas bioactividades se ha sugerido como un paso necesario en el proceso de su asociación con los beneficios para la salud observados (Fitahia y col., 2015). Por ejemplo, los polisacáridos ricos en ácido urónico, péptidos y carotenoides se identificaron como posibles candidatos de las propiedades antiproliferativas de la fracción de acetona de *Sepia pharaonis* contra dos líneas celulares de cáncer de cuello uterino (HeLa y Ca Ski) (Senan, Sherief y Nair, 2013). Sin embargo, particularmente para la tinta *O. vulgaris*, no hay informes de elucidación estructural de compuestos que muestren beneficios para la salud derivados de su tinta.

Debido a lo anterior y dada la presencia de compuestos activos presentes en la tinta de organismos marinos y, especialmente en pulpo, el enfoque de esta investigación es aislar, identificar y caracterizar química, bioquímica y funcionalmente los compuestos biológicamente activos producto de su metabolismo, en la búsqueda de compuestos con propiedades antimutagénicas, citoprotectoras, antiproliferativas y proapoptóticas de los extractos de tinta de *O. vulgaris* en las líneas celulares de cáncer 22Rv1, HeLa y A549. Además, esta investigación contribuye con la valorización de productos alimenticios marinos infrautilizados que presentan beneficios potenciales para la salud.

2. OBJETIVOS

2. OBJETIVOS

El **objetivo general** de esta Tesis Doctoral fue determinar el potencial anticancerígeno de los compuestos aislados a partir de la tinta de pulpo (*Octopus vulgaris*). Para alcanzar dicho objetivo principal se plantearon los siguientes **objetivos específicos**:

1. Determinar el potencial antiproliferativo y antiinflamatorio de los extractos y fracciones asiladas de la tinta de pulpo (*Octopus vulgaris*).

2. Caracterizar química y estructuralmente los compuestos aislados de las sub-fracciones activas de la tinta de pulpo.

3. Evaluar el efecto antiproliferativo y antiinflamatorio *in vitro* de los compuestos aislados sobre líneas cancerígenas, así como identificar las citocinas que están siendo reguladas por dichos compuestos.

3. METODOLOGÍA

3. METODOLOGÍA

3.1. Obtención de la Materia Prima, Generación de Extractos y Evaluación de su Actividad Biológica

3.1.1. Materia Prima

Con el propósito de llevar a cabo la presente investigación, se empleó la especie de pulpo *Octopus vulgaris*, obtenida mediante recolección en las costas de la zona de Bahía de Kino, situada en el Estado de Sonora, México, en el mes de agosto de 2018. Los sacos de tinta, esenciales para el estudio, fueron meticulosamente extraídos y posteriormente transportados a temperaturas subordinadas en hielo hasta las instalaciones del Laboratorio de Productos Marinos perteneciente al Departamento de Investigación y Posgrado en Alimentos de la Universidad de Sonora. En este entorno, se sometieron a procesamiento inmediato y se preservaron a una temperatura constante de -20 °C hasta su utilización subsiguiente. La obtención de los sacos de tinta se realizó mediante la aplicación de técnicas especializadas de lavado.

3.1.2. Elaboración de los Extractos

Con el fin de obtener los extractos de la tinta de pulpo, se procedió a poner en contacto dicha tinta con solventes de diferente polaridad, como, hexano (HX), diclorometano (DM), acetato de etilo (AcOEt) y agua (AG), en una relación de 1:10 (peso/volumen). La mezcla resultante se mantuvo en un recipiente hermético durante un período de 10 días, con agitación intermitente.

Al término de este período, se procedió a retirar la porción sobrenadante de las soluciones y posterior concentración utilizando un evaporador rotatorio a una temperatura de 40 °C bajo presión reducida. Los concentrados resultantes fueron almacenados de manera independiente a una temperatura de 4 °C, siguiendo el procedimiento establecido por Ebada et al. en el año 2008.

3.1.3. Evaluación de la Capacidad Antioxidante

3.1.3.1. Ensayo ABTS (Ácido 2,2 - azinobis-3-etilbenzotiazolina-6-sulfónico)

El ensayo de inhibición del radical ABTS se llevó a cabo siguiendo el protocolo establecido por Nenadis, Wang, Tsimidou y Zhang en el año 2004, empleando placas de 96 pocillos. En resumen, 20 µL de la muestra se mezclaron con 230 µL de una solución

de ABTS. La absorbancia se registró a una longitud de onda de 734 nm utilizando un lector de microplacas sintonizables Spectra Max (Molecular Devices Co., San José, CA, EE. UU.). Los resultados se expresaron en micromoles de equivalentes de Trolox (TE) por gramo de extracto. Todos los ensayos se realizaron en triplicado.

3.1.3.2. Ensayo DPPH (1,1 -difenil-2-picrilhidrazilo)

El ensayo de inhibición del radical DPPH se llevó a cabo siguiendo el procedimiento reportado por Fukumoto y Mazza en el año 2000, utilizando placas de 96 pocillos. Se añadieron 20 µL de la muestra a un pocillo y se mezclaron con 200 µL de una solución de DPPH en las placas de 96 pocillos. La absorbancia se leyó a los 30 minutos de incubación de los extractos en condiciones de oscuridad a temperatura ambiente (25 ± 1 °C) a una longitud de onda de 520 nm. Los resultados se expresaron en microgramos de equivalentes de Trolox (TE) por gramo de extracto. Todos los ensayos se realizaron en triplicado.

3.1.3.3. Ensayo FRAP (Poder Antioxidante Reductor del Ion Férrico)

La valoración del poder antioxidante reductor del ion férrico (FRAP) se llevó a cabo siguiendo el procedimiento descrito por Benzie y Strain en el año 1996, con algunas adaptaciones. Las soluciones madre se prepararon en condiciones ácidas, incluyendo una solución de tampón de acetato de sodio de 300 mmol/L (pH 3,6), $FeCl_3 \cdot 6H_2O$ de 20 mmol y una solución de 2,4,6-tripiridil-s-triazina (TPTZ), todas disueltas en una solución de HCl 40 mM. Una vez preparadas, estas soluciones se mezclaron en una proporción de 10:1:1 para obtener la solución de trabajo. Se combinaron 20 µL de esta solución con 280 µL para generar la solución FRAP en la placa de microtitulación y se incubó a temperatura ambiente (25 ± 1 °C). La absorbancia se registró después de 30 minutos a una longitud de onda de 638 nm para la medición indirecta del cambio de color del ion férrico. Se construyó una curva estándar en el rango de 0 a 200 µM de Trolox. Los resultados se expresaron en micromoles de equivalentes de Trolox (TE) por gramo de extracto. Todos los ensayos se realizaron en triplicado.

3.1.4. Cultivos Celulares y Bacterianos Utilizados

Para este estudio, se emplearon diversas líneas celulares que fueron donadas por el Laboratorio de Investigación sobre Alimentos Bioactivos y Funcionales (LIBAF) de la empresa Rubio Pharma y Asociados:

- ARPE-19 (ATCC CRL 2302): Línea celular epitelial de pigmento retiniano humano.

- A549 (ATCC CCL 185): Línea celular de carcinoma pulmonar humano.

- HeLa (ATCC CCL-2): Línea de adenocarcinoma de cuello uterino humano.

- 22Rv1 (ATCC CRL-2505): Línea celular de carcinoma de próstata humana.

Además, se utilizaron las siguientes líneas celulares proporcionadas por el Laboratorio de Cultivo de Células de Cáncer del Departamento de Investigaciones Científicas y Tecnológicas de la Universidad de Sonora (DICTUS):

-MDA-MB-231 (ATCC HTB-26): Línea de adenocarcinoma de mama humana.

-HCT-116 (ATCC CCL-247): Línea de carcinoma de colon rectal humana.

También, se adquirieron las siguientes líneas celulares de American Type Culture Collection (Manassas, Virginia):

-HT-29 (ATCC HTB-38): Células de adenocarcinoma colorrectal humano.

-RAW264.7 (ATCC TB-71): Línea de macrófagos murinos originada de un tumor inducido por el virus de la leucemia de Abelson.

Para el cultivo celular, se utilizó el medio DMEM (Medio del Águila Modificado de Dulbecco) suplementado con un 10 % de suero fetal bovino (SFB) y 15 % en el caso de la línea MDA-MB-231. Se añadieron 100 U/mL de penicilina, y las células se cultivaron en cajas de cultivo de 25 cm^2. Las células se mantuvieron en condiciones estándar, a una atmósfera de 5 % de CO2, a una temperatura de 37 °C y con un 85 % de humedad (Diagnosticos Roche, 2005). Para las líneas celulares cancerosas HT-29 y 22Rv1, se empleó medio RPMI (Medio del Instituto Memorial Roswell Park) suplementado con un 10 % de SFB. Los macrófagos, por su parte, se cultivaron en DMEM con un 10 % de SFB, un antibiótico antimicótico al 1 %, bicarbonato sódico a 1.5 g/L y piruvato sódico a 1 mM/L (1 mM) en placas de 60 mm. Se incubaron a 37 °C, en una atmósfera humidificada con un 5 % de CO_2.

Las cepas de *Salmonella typhimurium* TA98 y TA100 (Molecular Toxicology Inc.) fueron adquiridas y se sometieron a un control rutinario para confirmar las características genéticas, siguiendo el procedimiento detallado por Maron y Ames en 1983.

3.1.5. Evaluación de la Actividad Antimutagénica *In Vitro*

La evaluación de la actividad antimutagénica de los extractos derivados de la tinta de pulpo se llevó a cabo mediante la prueba de Ames, tal como fue descrita por Maron y Ames en 1983. En esta mencionada prueba, se emplearon dos cepas mutantes de *Salmonella typhimurium* (TA98 y TA100), las cuales son histidina-dependientes. Adicionalmente, se incorporó un extracto enzimático comercial derivado del hígado de rata (S9) para facilitar la biotransformación de compuestos que requieren activación metabólica. Este extracto metabólico fue empleado tanto para la activación de la aflatoxina B1 (utilizada como control positivo) como para posibles procesos de biotransformación que los compuestos antimutagénicos presentes en los extractos pudieran requerir. El procedimiento incluyó la adición de 2 mL de agar superior, el cual contenía histidina y biotina, a tubos de ensayo estériles, manteniendo la temperatura a 45 °C de acuerdo a las concentraciones especificadas en la metodología. A estos tubos se les añadieron 100 µL de cultivo fresco de la cepa, 100 µL de los extractos crudos a una concentración de 20 mg/mL y 500 µL de la mezcla enzimática S9. Cada una de las fracciones, así como sus diluciones, se contaminaron con aflatoxina B1 (AFB1) para asegurar la presencia de 500 ng por cada 100 µL de los extractos. Los tubos se agitaron y la mezcla resultante se dispuso en placas de agar mínimo glucosado; estas placas fueron incubadas en condiciones de oscuridad a 37 °C durante 48 horas, y se procedió a contar el número de colonias revertantes por placa. La antimutagenicidad se evaluó mediante la disminución del número de bacterias por placa como resultado de la inhibición del potencial mutagénico del mutágeno control por los posibles antimutágenos contenidos en el extracto de tinta. Los resultados obtenidos se representaron en gráficas de dosis-respuesta utilizando el paquete estadístico Infostat versión 2008. Todas las evaluaciones se realizaron en triplicado. La actividad antimutagénica de las muestras concentradas en comparación con la AFB1 se expresó en términos del porcentaje de inhibición de la mutagenicidad, calculado mediante la fórmula:

$$\% \text{ inhibición} = 1 - (M / C) * 100$$

Donde "M" representa el número de colonias revertantes por placa en presencia del mutágeno y el extracto a ser evaluado, mientras que "C" corresponde al número de colonias revertantes por placa en el control positivo, según lo descrito por Ames en 1983.

3.1.6. Evaluación del Efecto Citoprotector de los Extractos Contra el Daño Celular Oxidativo Inducido por H_2O_2

Se utilizó el kit de ensayo de bromuro de 3-(4,5-dimetiltiazol-2-il)-2,5-difeniltetrazolio (MTT) (kit de proliferación celular I, Roche, Cat. No. 11-465-007-001) con el propósito de evaluar el efecto protector de los extractos de tinta de pulpo en un contexto de daño celular oxidativo inducido por peróxido de hidrógeno (H_2O_2). Para llevar a cabo este estudio, se cultivaron células epiteliales pigmentarias de la retina humana [ARPE-19 (ATCC® CRL-2302TM)] en medio Eagle modificado por Dulbecco (DMEM, Sigma Aldrich, St. Louis, MO, EE. UU.), el cual contenía un 10 % de suero bovino fetal (FBS) (Corning, NY, EE. UU.), y se incubaron en condiciones de 37 °C y 5 % de CO_2. Las células fueron resuspendidas en una concentración de $1x10^4$ células por pocillo, utilizando un volumen de 100 µL de DMEM con 10 % de FBS, y posteriormente se sembraron en placas de 96 pocillos para su incubación. Luego de 24 horas, se adicionaron al medio de cultivo 100 µL de cada extracto diluido en DMSO a una concentración de 200 µg/mL (4 y 24 horas antes de la exposición a H_2O_2). Seguidamente, las células se lavaron dos veces con 100 µL de solución salina tamponada con fosfato (PBS) y el medio fue sustituido por H_2O_2 (100 µL, 10 mM), tras lo cual se incubaron durante un lapso de 30 minutos. Se incluyeron cultivos celulares de control positivo, los cuales fueron incubados con medio y 10 mM de H_2O_2 (sin extracto), y representaron el 15 % de la viabilidad celular, valor que fue deducido de los resultados de viabilidad obtenidos con los extractos. Por otro lado, los cultivos celulares de control negativo se incubaron exclusivamente con medio y DMSO al 0.5 % (v/v). Posteriormente, el medio fue reemplazado por uno nuevo que contenía 0.5 mg/mL de MTT, y se incubó durante 4 horas antes de la adición de 100 µL de dodecilsulfato de sodio (SDS). Después de una subsiguiente incubación de 12 horas, las placas se sometieron a lectura utilizando un lector de placas ELISA a una longitud de onda de 570 nm, con una longitud de onda de referencia de 650 nm. Los resultados obtenidos se expresaron como un porcentaje de viabilidad celular. Todas las evaluaciones se realizaron en tres experimentos diferentes, cada uno de ellos en triplicado.

3.1.7. Determinación de la Actividad Antiproliferativa (Ensayo MTT)

La evaluación de la actividad antiproliferativa se llevó a cabo utilizando el Kit de Proliferación Celular I (MTT) de Roche. Este método se basa en la capacidad colorimétrica de punto final, que se fundamenta en la propiedad intrínseca de las células

viables para reducir el colorante MTT (de color amarillo) a formazán (de color púrpura) a través de las deshidrogenasas mitocondriales. Se preparó una suspensión celular a partir de un cultivo en fase exponencial de crecimiento, con una concentración de 200,000 células/mL, ajustada utilizando un colorante de exclusión azul de tripano en una cámara de Neubauer. Luego, se inoculó una placa de ELISA de 96 pocillos con 100 µL de la suspensión celular en cada pocillo y se incubó durante 24 h a 37 °C en una atmósfera que contenía un 5 % de CO_2. Después de la incubación, se procedió al lavado de las células con PBS 1X, y se añadieron 100 µL de una concentración conocida del extracto a evaluar a cada pocillo. La incubación se prolongó durante 48 horas bajo las mismas condiciones. Luego, se retiró el sobrenadante, se realizó un lavado con 100 µL de PBS 1X y se añadieron 100 µL de medio fresco, junto con 10 µL de MTT en una proporción de 1:10. Esto fue seguido por una incubación de 4 horas. Después de la incubación, se agregaron 100 µL de SDS y se procedió a una incubación adicional de 24 horas antes de la lectura. Las absorbancias se registraron utilizando un espectrofotómetro con un lector de placas de tipo ELISA a una longitud de onda de 560 nm. Los datos de absorbancia se analizaron utilizando software especializado, como Excel, para calcular la viabilidad celular.

3.1.8. Fraccionamiento del Extracto Bioactivo

3.1.8.1. Cromatografía en Columna del Extracto de Tinta de Pulpo

Se tomaron 1.49 g del extracto de tinta de pulpo previamente liofilizado y se mezclaron con 50 mL de diclorometano de grado cromatográfico (J.T. Baker). La mezcla se mantuvo en agitación durante 24 horas a temperatura ambiente. Luego, se procedió a un filtrado al vacío utilizando una membrana de Nylon (Millipore) con un tamaño de poro de 0.45 µm, con el propósito de eliminar cualquier partícula en suspensión. El fraccionamiento se llevó a cabo empleando cromatografía en columna. Para la fase estacionaria, se utilizó gel de sílice con características similares, el cual se empaquetó en una columna de vidrio de 1.5 cm de diámetro y 15 cm de altura, utilizando 0.5 litros de hexano de grado cromatográfico (Sigma-Aldrich). La fase móvil consistió en una mezcla de disolventes, con una gradiente de polaridad gradual, empezando con hexano (Hx) y acetato de etilo (AcOEt) de grado cromatográfico en distintas proporciones, y aumentando la polaridad de la fase móvil hasta llegar a una elución final con acetato de etilo al 100 %.

3.1.8.2. Cromatografía en Capa Fina (TLC) Semipreparativa

En una etapa posterior, se aplicó una cromatografía en capa fina (TLC) preparativa para aislar compuestos de las fracciones bioactivas de DM obtenidas después de la cromatografía líquida de alta eficacia (HPLC). Esto se hizo utilizando la fracción de DM con mayor actividad biológica tras la prueba de MTT (fracciones de DM F1, F2 y F3). En resumen, las fracciones de DM se aplicaron en una placa de TLC de sílice (F254, 0.040-0.063 mm, Merck) y se desarrollaron utilizando una fase móvil compuesta por una mezcla de hexano y acetato de etilo en una proporción de 95:5 (v/v) (G. Liu et al., 2008). Las placas de TLC se examinaron bajo luz ultravioleta para supervisar el proceso de elución mediante HPLC y determinar la composición de las fracciones eluidas, lo que permitió su combinación en función de su composición.

3.1.9. Elucidación Química y Estructural de DM-F2

3.1.9.1. Espectroscopía Infrarroja de Transformada de Fourier (FTIR)

Para la elucidación química y estructural de las fracciones bioactivas, se llevó a cabo un análisis mediante Espectroscopía Infrarroja de Transformada de Fourier (FTIR) utilizando un espectrofotómetro Perkin Elmer FTIR Frontier (Waltham, MA, EE. UU.). Los espectros se obtuvieron promediando dieciséis exploraciones en un rango de 4000 a 400 cm^{-1}. Para registrar los espectros IR de las muestras, se emplearon gránulos de bromuro de potasio.

3.1.9.2. Espectrometría de Masas con Ionización por Electropulverización (ESI/MS)

Se obtuvo el espectro de masas de cada fracción bioactiva utilizando un espectrómetro de masas Agilent Technologies 6100 (Santa Clara, California, EE. UU.), operado en modo de iones negativos y positivos con ionización por electropulverización (un proceso no destructivo). La muestra se inyectó en una mezcla de metanol con acetonitrilo a 300 °C.

3.1.9.3. Resonancia Magnética Nuclear (RMN) de Carbono y Protones (RMN ^{13}C y RMN ^{1}H)

Se empleó un espectrómetro de RMN AVANCE 400 (Billerica, MA, EE. UU.) para analizar la muestra. La fracción más activa (DM-F2) se resuspendió en CDCl3/tetrametilsilano (500 µl; Sigma-Aldrich), que actuó como estándar interno, y se colocó en tubos de muestra de RMN de ultraprecisión con un diámetro de 5 mm. Se

realizaron espectros de RMN de carbono y protones a 100 y 400 MHz, respectivamente, y se registraron los cambios químicos en ppm.

3.1.9.4. Análisis de Compuestos Volátiles en los Extractos de DM y DM-F2 Mediante Cromatografía de Gases y Espectrometría de Masas (GC-MS)

Para la evaluación de los compuestos volátiles presentes en las fracciones bioactivas DM y DM-F2, se empleó la técnica de cromatografía de gases acoplada a espectrometría de masas (GC-MS), como se ha documentado previamente (Noguera-Artiaga et al., 2019). Este análisis se llevó a cabo utilizando un sistema Shimadzu GC-17A acoplado a un detector de masas Shimadzu QP-5050 (Shimadzu Corporation, Kyoto, Japón). La cromatografía de gases se ejecutó con una columna capilar SLB-5 ms (30 m x 0.25 mm, 0.25 μm, Supelco Inc., Sigma-Aldrich), empleando helio como gas portador a un caudal de 0.6 mL/min en modo splitless. La temperatura del horno inicial fue de 80 °C, seguida de un aumento de 2 °C/min hasta alcanzar 220 ºC. Luego, se aumentó a 25 °C/min hasta 300 °C, manteniendo esta temperatura durante 1.80 minutos. Las temperaturas del detector y del inyector fueron de 300 °C y 230 °C, respectivamente. La identificación de compuestos se realizó utilizando tres enfoques analíticos: índices de retención, índices de retención GC-MS y espectros de masas, consultando bibliotecas espectrales NIST05 y WILEY229. Es importante señalar que se consideró una identificación provisional cuando se basó únicamente en los datos espectrales de masas. Los resultados se expresaron como porcentajes del área total ocupada por cada uno de los compuestos.

3.1.10. Análisis Metabolómico No Dirigido

Se llevó a cabo un análisis global y no dirigido de los metabolitos identificados en DM y DM-F2 mediante cromatografía de gases y espectrometría de masas (GC-MS), siguiendo la metodología establecida por Gertsman y Barshop (2018). Todos los datos fueron sometidos a un proceso de normalización utilizando la herramienta informática MetaboAnalyst 3.0. Para visualizar los patrones de metabolitos presentes en cada muestra, empleamos un análisis de componentes principales (AMC). Además, se aplicó un análisis discriminante de mínimos cuadrados parciales (PLS-DA) con el fin de clasificar los metabolitos de las muestras. Este enfoque nos permitió considerar la cantidad de componentes y variables de cada modelo, siguiendo la metodología propuesta por Lê Cao y colaboradores en 2011. Para determinar la relevancia de cada metabolito en la diferenciación de las muestras, calculamos la Variable Importancia en las Puntuaciones

de Proyección (VIP). Utilizamos un valor VIP mayor o igual a 2 como criterio para evaluar la importancia de cada metabolito en la discriminación, de acuerdo con la regla de discriminación establecida por RoyChoudhury y colaboradores en 2017.

3.1.11. Evaluación del Efecto Proapoptótico de DM-F2 Mediante Citometría Celular

La evaluación del efecto proapoptótico de la fracción DM-F2 se llevó a cabo mediante el uso del Kit de Detección de Apoptosis con Anexina V marcada con isotiocianato de fluoresceína (FITC) de eBioscienceTM (n.º de catálogo 88-8005-74, Thermofisher Scientific, EE. UU.), siguiendo las instrucciones del fabricante. Se realizaron dos experimentos independientes, cada uno de ellos triplicado. Las células teñidas se analizaron utilizando un citómetro de flujo BD FACSVerseTM (BD Biosciences, NY, EE. UU.).

3.1.12. Evaluación Morfológica mediante Tinción Fluorescente

Para evaluar el efecto de DM-F2 en la morfología de las estructuras internas de la línea celular 22Rv1, se empleó una tinción con dilactato de 4',6'-diamidino-2-fenilindol (DAPI) (ID 329798905, Sigma-Aldrich) e isotiocianato de faloidina-tetrametilrodamina B (Phalloidin, MFCD00278840, Sigma-Aldrich), siguiendo una metodología basada en el trabajo de Van Vuuren, Botes, Jurgens, Joubert y Van Den Bout (2019), con ciertas adaptaciones. Las células de la línea 22Rv1 se cultivaron en placas de 96 pocillos y se les permitió crecer durante 24 horas antes de ser tratadas con DM-F2. Luego, las células se fijaron con una solución de formaldehído al 3.7 % en PBS después de 4, 12, 24 y 48 horas de incubación. A continuación, se permeabilizaron utilizando Triton X-100 al 0.2 % en PBS durante 15 minutos y se procedió a la tinción con DAPI y faloidina. Esto permitió visualizar las estructuras celulares, incluyendo el material nuclear a través de la tinción de ADN con DAPI y la actina-F con faloidina. Las microplacas se montaron en un microscopio de epifluorescencia invertido (Leica DMi8, Leica Microsystems, Wetzlar, Alemania) y se realizaron observaciones a 20x de aumento.

3.1.13. Evaluación de la Capacidad Anti-inflamatoria

3.1.13.1. Determinación de la Producción de Óxido Nítrico

Se cultivaron células RAW 264.7 en placas de 96 pocillos a una densidad de 2.5 x 10^5 células por pocillo a una temperatura de 37 ºC y una atmósfera de CO2 al 5 % durante 24 horas. Posteriormente, se indujo la producción de óxido nítrico (ON) en las células mediante la exposición al lipopolisacárido (LPS) de *Escherichia coli* (*E. coli*) a una concentración de 1 µg/ml, en presencia y ausencia de extractos, durante 24 horas. La producción de ON en el medio de cultivo se evaluó indirectamente midiendo la concentración de nitrito, utilizando la reacción de Griess. Se mezclaron 100 µl del medio sobrenadante con 100 µl de reactivo de Griess, que consiste en una solución al 1 % de sulfanilamida y un 0.1 % de dihidrocloruro de naftiletilendiamina, y se incubaron durante 10 minutos. La cantidad total de nitrito presente se determinó a partir de la absorbancia de la muestra medida a 540 nm. Para establecer el nivel de síntesis de ON inducido por los extractos, se utilizó una fórmula que compara la absorbancia de la muestra tratada con extractos con la absorbancia de la muestra tratada con medio de cultivo (DMEM), y se comparó con la absorbancia de la muestra tratada únicamente con LPS (1 µg/ml) como control positivo. El blanco de la prueba se realizó utilizando PBS. El cálculo de la cantidad de ON sintetizada en respuesta a la estimulación con LPS se expresó como un porcentaje utilizando la siguiente ecuación:

Síntesis de ON (%) = [(absorbancia de la muestra tratada con extractos - absorbancia de la muestra tratada con DMEM) / (absorbancia de la muestra tratada con LPS - absorbancia de la muestra tratada con DMEM)] x 100 %.

3.1.13.2. Perfil de Citocinas Inflamatorias

Para evaluar el efecto de DM-F2 en la modulación de citocinas asociadas a procesos inflamatorios, se utilizó el "Mouse Cytokine Antibody Array Panel A" (ARY0016, R&D Systems, Minneapolis, MN, EE. UU.). Se sembraron células RAW 264.7 (1 x 10^6) en placas de Petri de 60 mm y se les permitió crecer y adherirse durante un periodo de 48 horas. Posteriormente, se sometieron las células a tratamientos con LPS (lipopolisacárido) a una concentración de 1 µg/ml o LPS+DM-F2 (con una concentración inhibidora 50 (IC_{50}) de 87.33 µg/ml) en un medio sin suero fetal bovino (FBS) durante 24 horas. Después de los tratamientos, se procedió a la lisis de las células utilizando el inhibidor de proteasa Halt TM de Thermo Fisher Scientific a 4 ºC durante 30 minutos. La

concentración de proteína en los lisados se cuantificó mediante el ensayo de ácido bicinconínico (BCA) utilizando el kit Pierce TM BCA Protein Assay de Thermo Fisher Scientific para estandarizar todos los tratamientos. A continuación, se analizaron los lisados de proteínas utilizando el kit mencionado, siguiendo las instrucciones del fabricante. Los resultados se obtuvieron a través de un sistema de imágenes de células ChemiDoc XRS+ de BioRad Corp (Hercules, CA, EE. UU.). La expresión relativa de citocinas se comparó con el grupo control, que consistió en células RAW 264.7 desafiadas únicamente con LPS. La red de proteínas, necesaria para llevar a cabo un análisis *in silico* de las citocinas moduladas, se generó utilizando la plataforma STRING (von Mering et al., 2007) y se editó con el software Cytoscape. Los datos resultantes del análisis en STRING, incluyendo las vías de enriquecimiento según la Enciclopedia de Genes y Genomas de Kyoto (KEGG) y el proceso de enriquecimiento, se normalizaron utilizando los valores de tasa de descubrimiento falso (FDR) de proteínas.

3.1.14. Cuantificación de Especies Reactivas de Oxígeno (ROS) Intracelulares

Dado que la fracción DM-F2 se destacó como la más activa en las células de cáncer de próstata 22Rv1, se evluó su influencia en la generación de especies reactivas de oxígeno (ROS) intracelulares siguiendo el procedimiento descrito por Saleem y colaboradores en 2020. Inicialmente, se realizó una siembra de 1 x 10^4 células por pocillo en placas de cultivo de 96 pocillos y permitimos su crecimiento durante 24 horas. Posteriormente, se expuso las células a concentraciones de DM-F2 con base en la Concentración Letal 50 (LC_{50}) durante un período de 4 horas. Luego, las células fueron incubadas con 10 µM de diacetato de 2',7'-diclorodihidrofluoresceína (DCHF-DA) durante 30 minutos y se lavaron dos veces con solución salina tamponada con fosfato (PBS). La cuantificación de la intensidad de la señal fluorescente generada se realizó empleando un lector de placas FLUOstar Omega (BMG Labtech Inc., Ortenberg, Alemania), utilizando una longitud de onda de excitación/emisión de 488/525 nm, respectivamente. Los resultados se expresaron en unidades relativas de fluorescencia (RFU). Utilizamos las células tratadas con H_2O_2 como control positivo, mientras que las células no tratadas constituyeron el control negativo. Además, se aplicó el tratamiento con LC_{50} de cisplatino y docetaxel como controles farmacológicos en el experimento.

3.1.15. Evaluación de la Expresión Celular de IL-4 y NF-kB Mediante Citometría de Flujo

Para determinar el impacto de DM-F2 en la regulación de IL-4 y NF-kB, se empleó la técnica de citometría de flujo en células mononucleares aisladas de sangre periférica humana (PBMC), siguiendo el método de Chávez-Sánchez y colaboradores en 2010. Primero, se aislaron las PBMC utilizando un gradiente de densidad a través del agente Ficoll-Paque PLUS (GE Healthcare). La sangre se diluyó en una proporción de 1:2 con solución salina tamponada con fosfato (PBS). Luego, el sobrenadante superior se sometió a una centrifugación a 450 x g durante 30 min, nuevamente utilizando Ficoll-Paque. Posteriormente, las células se recogieron en un tubo estéril, se lavaron con 100 µl de PBS, se suspendieron en medio de cultivo y se cuantificaron. Antes y después de la activación con lipopolisacárido (LPS) durante 24 horas, se examinaron las células. A continuación, las células (1×10^6 células por pocillo) se trataron con LPS o DM-F2 y se marcaron con sondas fluorescentes para IL-4 humana utilizando el marcador isotiocianato de fluoresceína (FITC) (Cat. 500806, BioLegend, San Diego, CA, EE. UU.). También se aplicaron anticuerpos anti-IL-4 humana (MP4 25D2, BioLegend). Además, se evaluó el factor de transcripción nuclear NF-kB después de pretratar las células con anticuerpo NF-kB (Cat. B5681, Sigma-Aldrich) a una concentración de 15 mM durante 30 minutos. La intensidad de fluorescencia, expresada en unidades relativas de fluorescencia (RFU), se cuantificó utilizando un citómetro de flujo BD FACSVerse™ (BD Biosciences, NY, EE. UU.) tras analizar 10,000 eventos.

3.1.16. Docking Molecular

3.1.16.1. Análisis *in silico* de Interacciones entre Metabolitos de DM y Citocinas

Las estructuras 3D de ligandos seleccionados para la interacción *in silico* se descargaron de la base de datos PubChem: 4-metilcaprolactama (PubChem CID: 19242), ácido mirístico (PubChem CID: 11005), ácido hexadecanoico (PubChem CID: 985), hexadecanal (PubChem CID: 984), heptadecanal (PubChem CID: 71552) y octadecanal (PubChem CID: 12553). Para los receptores de proteínas, se descargaron estructuras 3D de NF-kB (1LE5) e IL-2 (4YUE) del banco de datos de proteínas. Las otras proteínas (IL-1α, IL-1β, IL-3, IL-4, IL-7, IL-16, CCL17 e IL-27) se modelaron en SwissModel basándose en sus secuencias FASTA de Uniprot ® (P01582, P10749, Q5SX77, P07750, Q544C8, O54824, F6R5P4 y Q8K3I6, respectivamente). Se seleccionó la mejor

estructura 3D en función de su porcentaje de identidad. Se siguió el procedimiento de atraque realizado por Luna-Vital, Weiss, & González de Mejía (2017). Los mejores sitios de unión se predijeron en la utilidad en línea MetaPocket 2.0 (Zhang, Li, Lin, Schroeder y Huang, 2011) y los cálculos de acoplamiento se realizaron en las herramientas AutoDock (Trott y Olson, 2010). La mejor conformación de acoplamiento se graficó en el software Discovery Studio Visualizer v. 19.1.0.18287 (Dassault Systèmes, Vélizy-Villacoublay, Francia).

3.1.16.2. Análisis *in Silico* de Compuesto identificado en DM-F2 con Objetivos Específicos de Muerte Celular

Con el propósito de evaluar el posible efecto del compuesto bioactivo identificado en DM-F2, se llevó a cabo un análisis *in silico* para determinar potenciales interacciones entre este compuesto (ligando) y objetivos específicos relacionados con la apoptosis en la línea celular 22Rv1 (Skjøth & Issinger, 2006). Primero, el ligando se representó usando Marvin Sketch y se verificó en tres dimensiones (3D) antes de someterlo al estudio de acoplamiento. Se descargaron los objetivos específicos de líneas cancerígenas desde la base de datos de proteínas, incluyendo ERK1 (4QTB), ERK2 (6GJB), y ACE2 (1R42). Otros objetivos, como Bad y Cyclin D1, se generaron en SwissModel 2.0 a partir de sus secuencias en formato Uniprot FASTA. Posteriormente, se construyeron los modelos respectivos (Q922934 y 2w99.1.A, para Bad y Cyclin D1, respectivamente). Para identificar las posibles ubicaciones de unión en los objetivos relacionados referenciados en líneas cancerígenas, se utilizó servidor MetaPocket 2.0. Realizamos cálculos de acoplamiento que incluyeron torsiones flexibles, enlaces de hidrógeno y energía de enlace, siguiendo el enfoque descrito por Luzardo-Ocampo, Campos-Vega, González de Mejía y Loarca-Piña (2020) con el uso de AutoDock Tools (Trott y Olson, 2010). Las representaciones de las conformaciones de acoplamiento más probables fueron generadas en el software BioVia Discovery v. 19.1.0.1.18287 (Dassault Systèmes, Vélizy-Villacoublay, Francia).

3.1.17. Síntesis de N-(2-ozoazepan-3-il) pirrolidina-2-carboxamida (OPC, ozopromida)

La síntesis de ozopromida se llevó a cabo mediante la adición gradual de diclorometano (DCM) a una mezcla que contenía N, N'-diciclohexilcarbodiimida (DCC) a 1.74 mM y L-prolina a 1.56 mM. Esta solución se mantuvo a 32 ºC durante 30 minutos en un

recipiente ubicado en un Sintetizador de Microondas (MS) (Discover© 2020, CEM Corporation, Matthews, NC, EE. UU.). Posteriormente, se agregaron gradualmente 3-amino-2-azepanona a 3.12 mM a los 3 ml de solución de DCM. La mezcla resultante se sometió a un tratamiento de 60 minutos a 32 °C en el MS y se filtró utilizando papel de filtro Whatman No. 1. El filtrado se enfrió a 4 ºC durante 24 h. Para finalizar, los solventes se eliminaron mediante destilación y el residuo se cristalizó a - 4 ºC, eliminando así los cristales de urea. La solución destilada se mantuvo a temperatura ambiente (25±1 ºC) durante 24 horas.

3.1.18. Caracterización Estructural de Ozopromida (OPC)

3.1.18.1. Espectroscopía Infrarroja Transformada de Fourier (FTIR)

La composición de OPC resultante fue sometida a análisis utilizando un espectrómetro FTIR Frontier de espectroscopía infrarroja transformada de Fourier (Perkin Elmer, Waltham, MA, EE. UU.). Se promediaron 16 exploraciones de espectro en un rango de 4000 a 400 cm^{-1}. Los espectros infrarrojos se registraron utilizando pastillas de bromuro de potasio.

3.1.18.2. Resonancia Magnética Nuclear (RMN) de Carbono y Protones (RMN 13C y RMN 1H) y Análisis de Espectroscopía Mononuclear Correlacionada Bidimensional (COSY-2D)

Para el análisis de la mezcla de OPC, se empleó un espectrómetro RMN AvanceCore de 400 MHz (Bruker, Billerica, MA, EE. UU.). Se resuspendieron aproximadamente 10 µl de la muestra en 500 µl de $CDCl_3$ con tetrametilsilano como estándar interno (Sigma-Aldrich, St. Louis, MO, EE. UU.), y se colocaron en tubos de RMN de 5 mm de diámetro. Se realizaron mediciones de resonancia magnética nuclear de carbono (RMN $_{13}C$ a 100 MHz) y protones (RMN $_{1}H$ a 400 MHz) para registrar los cambios en los desplazamientos químicos.

3.1.19. Evaluación *in silico* de las Propiedades de Absorción, Digestión, Metabolismo, Excreción y Toxicidad (ADMET) de la Ozopromida (OPC)

La valoración de las propiedades ADMET de OPC se llevó a cabo siguiendo el protocolo descrito por Cuellar-Nuñez et al. en 2022. En resumen, la estructura molecular de OPC fue dibujada utilizando el módulo MarvinSketch de SwissADME (Daina et al., 2017) y se tradujo a notación simplificada de estructura molecular conocida como SMILES

[SMILE: O=C(NC1CCCCNC1=O)C1CCCN1]. Esta notación se utilizó tanto en el software admetSAR 2.0 (disponible en http://lmmd.ecust.edu.cn/admetsar2/) para obtener información sobre sus propiedades fisicoquímicas y ADMET, como en el método de diagrama de huevo cocido para prever su absorción gastrointestinal y penetración a través de las membranas intestinales, según se informó previamente (Luzardo-Ocampo et al., 2020).

3.1.20. Análisis Estadístico

Los datos se presentaron en forma de media ± desviación estándar y se obtuvieron a partir de al menos dos experimentos independientes, cada uno repetido tres veces. Para evaluar las diferencias entre tratamientos para cada respuesta, se realizó un análisis de varianza (ANOVA), seguido de una prueba post-hoc de Tukey-Kramer, con un nivel de significancia establecido en $p < 0.05$. Las herramientas utilizadas para el análisis estadístico incluyeron SPSS Statistics (IBM Corp., Nueva York, EE. UU.) para la realización del análisis de varianza, GraphPad Prism v. 8.0 para la creación de gráficos y Number Cruncher Statistical Software (NCSS), versión 2001 (NCSS Statistical Software, EE. UU.) para cuantificar los valores de CL_{50}. En cuanto a los experimentos relacionados con las diferentes actividades, se llevaron a cabo en dos ocasiones, con tres réplicas por cada condición experimental. Se empleó la prueba de comparación de medias de Tukey con un intervalo de confianza del 95 % ($p < 0.05$) para realizar el análisis estadístico.

4. PUBLICACIONES

PUBLICACIÓN 1

Octopus vulgaris ink extracts exhibit antioxidant, antimutagenic, cytoprotective, antiproliferative, and proapoptotic effects in selected human cancer cell lines

Martin Samuel Hernández-Zazueta, Joel Said García-Romo, Luis Noguera-Artiaga, Iván Luzardo-Ocampo, Ángel Antonio Carbonell-Barrachina, Pablo Taboada-Antelo, Rocio Campos-Vega, Ema Carina Rosas-Burgos, María Guadalupe Burboa-Zazueta, Josafat Marina Ezquerra-Brauer, Juan Manuel Martínez-Soto, Hisila del Carmen, Santacruz-Ortega, and Armando Burgos-Hernández

Journal of Food Science. 2021. 86(2):587-601. Doi: 10.1111/1750-3841.15591

PUBLICACIÓN 1: TRANSCRIPCIÓN LITERAL

Octopus vulgaris ink extracts exhibit antioxidant, antimutagenic, cytoprotective, antiproliferative, and pro-apoptotic effects in selected human cancer cell lines

Running title: *O. vulgaris* ink inhibited cancer cells.

Martin Samuel Hernández-Zazueta[1], Joel Said García-Romo[1], Luis Noguera-Artiaga[2], Iván Luzardo-Ocampo[4], Ángel Antonio Carbonell-Barrachina[2], Pablo Taboada-Antelo3, Rocio Campos-Vega[4], Ema Carina Rosas-Burgos[1], María Guadalupe Burboa-Zazueta[5], Josafat Marina Ezquerra-Brauer[1], Juan Manuel Martínez-Soto[6], Hisila del Carmen Santacruz-Ortega[7], Armando Burgos-Hernández[1]*

1 Departamento de Investigación y Posgrado en Alimentos, Universidad de Sonora, 83000 Hermosillo, Sonora, México.

2 Escuela Politécnica Superior de Orihuela, Universidad Miguel Hernández de Elche, 03312 Alicante, España.

3 Grupo de Física de Coloides y Polímeros. Departamento de Física de Partículas, Universidad de Santiago de Compostela, 15782, Santiago de Compostela, España.

4 Research and Graduate Program in Food Science, School of Chemistry, Universidad Autónoma de Querétaro, 76010, Querétaro, México.

5 Departamento de Investigaciones Científicas y Tecnológicas, Universidad de Sonora, 83000 Sonora, México.

6 Departamento de Medicina y Ciencias de la Salud, Universidad de Sonora, 83000 Sonora, México.

7 Departamento de Investigación en Polímeros y Materiales, Universidad de Sonora, 83000, Sonora, México.

* Corresponding author at: Departamento de Investigación y Posgrado en Alimentos, Universidad de Sonora, Apartado Postal 1658, 83000 Hermosillo, Sonora, México. Tel.: +526-622-592-208; Fax: +526-622-592-209. E-mail address: armando.burgos@unison.mx

Abstract

Cancer is a non-communicable disease of rising worldwide concern. Marine food products such as *Octopus vulgaris*ink (OI) could be sources of compounds addressing these concerns. This study aimed to evaluate the antimutagenic, cytoprotective, antiproliferative, pro-apoptotic, and antioxidant capacity of OI extracts on human cancer cell lines (22Rv1, HeLa, A549). The ARPE-19 cell line was used as a reference human cell line to evaluate the ink's cytotoxicity. The water extract exhibited the highest antimutagenic and cytoprotective effect, but the dichloromethane extract (DM) showed the lowest half lethal concentration against 22Rv1 cells. Structural elucidation of purified DM fractions (F1, F2, F3) identified an unreported compound, N-(2-ozoazepan-3-yl)-pyrrolidine-2-carboxamide (OPC). DM-F2 showed high antiproliferative effect (LC_{50} = 27.6 µg/mL, reactive species modulation, early-apoptosis induction (43.2 %), and nuclei disruption in 22Rv1 cells. In silico analysis predicted high OPC affinity with Cyclin D1 (-6.70 kcal/mol), suggesting its potential impact on cell cycle arrest. These results highlight the antimutagenic, cytoprotective, and antiproliferative potential health benefits derived from underutilized marine food products such as OI. Further investigations at *in vitro* or *in vivo* levels are required to elucidate mechanisms and health benefits from OI.

Practical Application: *O. vulgaris* ink is an underutilized marine natural product that could be a source of biological compounds with potential health benefits such as antioxidant activity and cancer prevention.

1. Introduction

As cancer is the second cause of death in the world (WHO, 2020), the search for alternatives that may contribute to either preventing or treating this disease, such as natural food products (Vizetto-Duarte, Branco, & Custódio, 2020), has been the focus of scientific efforts around the world. In this sense, marine invertebrates such as corals, sponges, and cephalopods, have been reported as sources of bioactive compounds with promising therapeutic potential (Shinde, Banerjee, & Mandhare, 2019).

Cephalopods are a class of Mollusca that has been studied as sources of food components such as the ink, traditionally incorporated into the Mediterranean diet (Cucinotta & Pieroni, 2018) or south-Asian culinary preparations (Vate & Benjakul, 2016). Particularly for Octopus ink, there are no reports of its chemical composition, but the reported composition of squid or cuttlefish ink have indicated elevated contents of melanin, proteins and derivatives (peptides, glycosaminoglycans, and certain enzymes), lipids, and minerals (Derby, 2014; Liu, Luo, Chen, & Shang, 2011). For squid ink has been found fatty acids (1.34 %) displaying a profile of mainly saturated (56.6 %) fatty acids (Ayu Shazwani & Rabeta, 2020). Certain amino acids such as glycine, glutamic acid, and aspartic acid have also been identified on ink extracts from S. maindroni (Mimura, Maeda, Tsujibo, Satake, & Fujita, 1982)

Besides their use as food or food-ingredient, evidence of biological activity in cephalopods ink has already been reported mostly for cuttlefish and squid (Nair et al., 2011), finding antioxidant, antimicrobial, anti-inflammatory, and cytotoxic potential (Besednova, Zaporozhets, Kovalev, Makarenkova, & Yakovlev, 2017). The reported activities offer a protective effect against the development of cancer. For example, antioxidant compounds are associated with regression and growth inhibition of premalignant lesions. Besides, antimutagenic compounds exhibit a chemopreventive effect against mutagen-induced DNA and promote a slow cancer initiation. Furthermore, the antiproliferative activity is directly related to the development of this disease, representing a tool in the search for new candidate compounds that may either prevent or slow down uncontrolled cancer cell division by interfering with the cell cycle (García-Romo et al., 2020; López-Saiz, Suárez-Jiménez, Plascencia-Jatomea, & Burgos-Hernández, 2013).

Despite the ink-derived activities, there are no reports of *in vitro* antiproliferative or pro-apoptotic activity against several cancerous cell lines such as 22Rv1, HeLa, and A549, a representative from the primary cancer conditions (prostate, cervical, and lung cancer). The structural elucidation of the compounds responsible for these bioactivities has been suggested as a necessary step in the process of their association with the observed health benefits (Fitahia et al., 2015). For instance, polysaccharides rich in uronic acid, peptides, and carotenoids were identified as potential candidates of the antiproliferative properties of the acetone fraction of Sepia pharaonis against two cervical cancer cell lines (HeLa and Ca Ski) (Senan, Sherief, & Nair, 2013). However, particularly for *Octopus vulgaris*ink, there are no reports of structural elucidation of compounds exhibiting health benefits derived from the ink. Therefore, this research aimed to evaluate the antimutagenic, cytoprotective, antiproliferative, and pro-apoptotic effects of *Octopus vulgaris*ink extracts in 22Rv1, HeLa, and A549 cancer cell lines. Moreover, this research led to identifying a potential ink-derived compound that might be responsible for this effect. Besides, this research contributes to the valorization of underutilized marine food products exhibiting potential health benefits.

2. Material and methods

2.1. Biological material

Octopus (Octopus vulgaris) specimens were collected at shallow waters of the coast of Hermosillo, Sonora, Mexico (29°22′27″ N, 112°34′08″ W). The ink sacks were extracted from octopuses, transported in ice to the Marine Products Laboratory of the University of Sonora, and stored at -20 ºC until use.

2.2. Samples treatment and preparation of the ink extracts

The ink from the octopus sacs was extracted according to the methodology reported by Ebada, Edrada, Lin, & Proksch (2008). Approximately 1.30 kg of octopus waste material was obtained, from which 20 ink-sacks were obtained. After the ink removal from the sacs, 15 mL was homogenized 1:1 with water and frozen at -70 ºC. The mixture was then lyophilized in a Labconco freeze drier (Labconco Corporation, Kansas City, MO, US). This dried mixture (5 g from 15 mL from the original liquid octopus' ink) was prepared to obtain the four extracts; one with distilled water (WE), and the other three with organic solvents: hexane (HX), ethyl acetate (EA), and dichloromethane (DM). Reagents were HPLC-pure grade and used in a 1:10 ratio (w/v). All mixtures were kept closed containers

for 24 h with periodic stirring. After 24 h, stirring was stopped, the precipitates were discarded by decantation, and supernatants were collected. The supernatants were then filtered through a Whatman No. 1 filter paper (Whatman, Clifton, NJ, US) under vacuum and concentrated on a rotary evaporator at 40 °C under reduced pressure. Concentrates were stored at 4 °C until use.

2.3. Evaluation of the antimutagenic potential of the extracts by Ames assay

The antimutagenic potential of the octopus-ink extracts was tested using the plate incorporation procedure of Maron & Ames (1983). Salmonella Typhimurium TA98 and T100 histidine-dependent mutant strains (Molecular Toxicology Inc., N.C., U.S.) were used. The extracts were tested using a commercial S9 rat liver mixture (Aroclor 1254-induced, Sprague-Dawley male rat liver homogenized in 0.154 M KCl). Bioactivated aflatoxin B1 (AFB1) (Sigma-Aldrich, St. Louis, MO, U.S.) in the S9 rat liver mixture was used as a positive control of the potential biotransformation of S. typhimurium strains. The extracts were dissolved and diluted with DMSO and amended with sufficient AFB1 to achieve 500 ng of AFB1/100 µL at each diluted sample. AFB1 at different concentrations was used as a positive control. All assays were done in triplicate. Genetic markers of S. typhimurium strains were periodically verified.

2.4. Antioxidant capacity of the extracts

2.4.1. ABTS assay

The 2,2-azinobis-3-ethylbenzothiazoline-6-sulfonic acid (ABTS, Sigma-Aldrich) inhibition assay was conducted in 96-wells plates as reported by Nenadis, Wang, Tsimidou, & Zhang, (2004). Briefly, twenty microliters of the sample were mixed with 230 mL of ABTS solution. The absorbance was recorded at 734 nm using a Spectra Max Tunable Microplate reader (Molecular Devices Co. San Jose, CA, U.S.A.). Results were expressed as micromoles of Trolox equivalents (TE) per gram of extract. All assays were performed in triplicate.

2.4.2. DPPH assay

The 1,1-diphenyl-2-picrylhydrazyl inhibition assay was done as reported by Fukumoto & Mazza (2000) in 96-wells plates. Twenty microliters of the sample were added to a well and mixed in 96-well plates containing 200 µL of DPPH solution. The absorbance was read at 30 min of incubation of extracts in the dark at room temperature (25 ± 1 ºC) and

the DPPH reagent (λ= 520 nm). The results were expressed in µm TE/g extract. All assays were performed in triplicate.

2.4.3. FRAP assay

Determination of the ferric ion reducing antioxidant power (FRAP) was according to the methodology reported by Benzie and Strain (1996), with some modifications. The stock solutions were prepared in acidic conditions, including the 300 mmol/L sodium acetate buffer (pH 3.6), 20 mmol $FeCl_3 \cdot 6H_2O$, and TPTZ (2, 4, 6-tripyridyl-s-triazine) solution, all of them dissolved in 40 mM HCl solution. Once prepared, the solutions were combined at a 10:1:1 ratio to obtain the working solution. A 20-µL aliquot of this solution was combined with 280 µL to generate the FRAP solution at the microtitration plate and incubated at room temperature (25 ± 1 ºC). The absorbance was recorded after 30 min at 638 nm for the indirect measurement of the color change from the ferric ion. A standard curve was made from 0 to 200 µM of Trolox. Results were expressed as µM TE/g of extraction. All the assays were performed in triplicates.

2.5. Cytoprotective effect of the extracts against H2O2-induced oxidative cell damage

The 3-(4,5-dimethylthiazol-2-yl)-2,5-diphenyltetrazolium bromide (MTT) assay kit (Cell proliferation kit I, Roche, Cat. No. 11-465-007-001) was used to evaluate the protective effect of octopus-ink extracts. Human retinal pigment epithelial cells [ARPE-19 (ATCC® CRL-2302TM)] were cultivated in a Dulbecco's modified Eagle's medium (DMEM, Sigma Aldrich, St. Louis, MO, US) with 10 % fetal bovine serum (FBS) (Corning, NY, US) and were incubated at 37 °C at an atmosphere of 5 % CO_2. Later, the cells were resuspended (1x104 cells/well) in 100 µL of DMEM with 10 % of FBS and seeded in 96-wells plates and were incubated. After 24 h, 100 µL of the cultured medium was mixed with 200 µg/mL of each extract diluted in DMSO (4 and 24 h before H_2O_2 stimuli). Subsequently, cells were washed twice (100 µL PBS), and the medium was replaced with H_2O_2 (100 µL, 10 mM) and incubated for 30 min. The positive control cell cultures were incubated (without extract) with medium and 10 mM of H_2O_2 and represented 15 % of cell viability, a value subtracted from the viability values of the extracts. The negative control cell cultures were incubated only with medium and DMSO 0.5 % v/v. The medium was then replaced with fresh medium containing 0.5 mg/mL MTT and incubated for 4 h before 100 µL of sodium dodecyl sulfate (SDS) were added. After 12 h of

incubation, the plates were read in an ELISA plate reader at 570 nm and a reference wavelength of 650 nm. The results were expressed in percentage of cell viability. All the assays were conducted in three different experiments in triplicates.

2.6. Evaluation of antiproliferative potential

2.6.1. Cell lines

Human retinal pigment epithelium ARPE-19 (ATCC® CRL-2302TM), lung (carcinoma) A549 (ATCC® CCL-185TM), epithelioid cervix adenocarcinoma HeLa (ATCC® CCL-2TM), and prostate carcinoma 22Rv1 (ATCC® CRL-2505TM) cell lines were used.

2.6.2. MTT assay

The antiproliferative effect of the octopus-ink extracts and fractions was determined using the colorimetric MTT assay (Roche), following the manufacturer's instructions. Octopus-ink extracts were resuspended in DMSO and diluted in DMEM. Cells (1x104 cells/well) were seeded in 96-wells plates, allowed to grow (24 h, 37 ºC), washes twice with PBS, and treated with the ink extracts (25, 50, 100, and 200 µg/mL, 48 h, 37 ºC). Experimental control cell cultures were incubated only with DMSO (concentration not higher than 0.5 % v/v). DMEM-negative control cells were incubated without treatment. The plates were read using an ELISA plate reader (Benchmark Microplate Reader; Bio-Rad, Hercules, CA, US) at test a wavelength of 570 nm and a reference wavelength of 650 nm (Benchmark Microplate Reader; Bio-Rad, Hercules, CA, US). The percentage of cell proliferation was calculated considering the negative control cells and was used to calculate of the half lethal concentration of each extract (LC_{50}), using provided the equations of the survival analysis from the NCSS statistical software. Cisplatin and docetaxel at the same concentrations of the samples were used as drug controls.

2.7. DM fractioning and obtention of DM-F2

2.7.1. Open column chromatography

Since the DM extract showed the highest antiproliferative potential, purification of DM fractions was conducted to refine the screening of additional anti-cancer properties. The DM extract was dissolved in ethyl acetate and fractionated using an open silica gel column (3.5 cm × 60 cm using 60–120 mesh silica gel, Sigma-Aldrich) chromatography. The elution was performed using hexane: ethyl acetate (99:1) as a mobile phase, collecting 25-mL fractions in glass bottles. The liquid phases for the open column

chromatography can be found in Supplementary Table S1. Thirty-eight fractions were obtained, and those with similar contents (as determined by TLC monitoring) were combined to obtain DM fractions (F1, F2, and F3). These fractions were evaporated under vacuum and dried with N2. The eluents were monitored using thin-layer chromatography (TLC) plates coated with silica gel 60 containing F254 developer (Merck, Darmstadt, Germany). The chromatography was performed using the same solvent system in which they eluted from the column and observed under both 254- and 365-nm UV light.

2.7.2. Semi-preparative thin layer chromatography (TLC)

Preparative TLC was subsequently used to isolate compounds from the DM bioactive fractions obtained after HPLC using the most bioactive DM fraction after MTT test (F1, F2, and F3 DM fractions). Briefly, DM fractions were applied onto a silica TLC plate (F254 0.040-0.063 mm, Merck), and developed using 95:5 hexane:ethyl acetate (v/v) as mobile phase (G. Liu et al., 2008). The TLC plate were observed under UV light to monitor the HPLC elution process and determine the composition of the eluted fractions, which allowed its combination according to its composition.

2.8. Chemical and structural elucidation of DM-F2

2.8.1. Fourier-transformed infrared spectroscopy (FTIR)

The bioactive fractions were analyzed using a Perkin Elmer FTIR Frontier (Waltham, MA, US) with an average of sixteen spectra scans within a range of 4000–400 cm−1. Potassium bromide pellets were used to record the IR spectra from the samples.

2.8.2. Electrospray ionization mass spectrometry (ESI/MS)

The mass spectrum of each bioactive fraction was obtained using an Agilent Technologies 6100 Quadrupole LC/mass spectrometer (Santa Clara, California, US) operated in the negative and positive ion mode with electrospray ionization (non-destructive). The sample was injected into a mixture of methanol with acetonitrile at 300 °C.

2.8.3. Nuclear magnetic resonance (NMR) of carbon and proton (13C-NMR and 1H-NMR)

The AVANCE 400 NMR Spectrometer equipment (Billerica, MA, US) was used to analyze of the sample. The most active fraction (DM-F2) was resuspended in CDCl3/ tetramethylsilane (500 µL; Sigma-Aldrich) as an internal standard and placed in ultra-

precision NMR sample tubes (5-mm diameter). NMR of carbon and proton were measured at 100 and 400 MHz, respectively, and the chemical shifts were recorded in ppm.

2.9. Intracellular reactive oxygen species (ROS) levels.

Since DM-F2 was the most active fraction of the 22Rv1 prostate cancer cells, the impact of this fraction on the intracellular ROS generation was quantified following the reported procedure of Saleem et al. (2020). The cells (1 x 10^4 cells/well) were seeded in 96-wells plates and allowed to grow for 24 h. Afterward, the cells were treated with DM-F2 LC_{50} concentrations for 4 h. The cells were then incubated for 30 min with 10 µM of 2',7'-dichlorodihydrofluorescein diacetate (DCHF-DA) and washed twice with PBS. The fluorescent color development was quantified using a FLUOstar Omega plate reader (BMG Labtech Inc., Ortenberg, Germany) using an excitation/emission wavelength of 488/525 nm, respectively. The results were expressed in relative fluorescence units (RFU). Cells treated with H2O2 were used as the positive control, while the untreated cells were the negative control. Treatment with the LC_{50} of cisplatin and docetaxel was also conducted as drug controls.

2.10. Pro-apoptotic effect of DM-F2

2.10.1. Pro-apoptotic effect of DM-F2 evaluation by cell cytometry

The pro-apoptotic effect of the DM-F2 fraction was evaluated using the eBioscienceTM Annexin-V Apoptosis Detection Kit Fluorescein isothiocyanate (FITC) (Cat. No. 88-8005-74, Thermofisher Scientific, U.S.) following the manufacturer's instructions. Two independent experiments in triplicates were conducted. Stained cells were analyzed using a BD FACSVerseTM flow cytometer (BD Biosciences, NY, US).

2.10.2. Morphological evaluation by fluorescence staining

The effect of DM-F2 on the morphology of internal structures of 22Rv1 cell line was evaluated using 4',6'-diamidino-2-phenylindole dilactate (DAPI) (ID 329798905, Sigma-Aldrich) and phalloidin–tetramethylrhodamine B isothiocyanate (Phalloidin, MFCD00278840, Sigma-Aldrich) using the method of Van Vuuren, Botes, Jurgens, Joubert, & Van Den Bout (2019) with some modifications. The testing cells (22Rv1) were seeded in 96-wells plates, allowed to grow for 24 h, and treated with DM-F2. The cells were then fixed with 3.7 % formaldehyde in PBS after 4, 12, 24, and 48 h of incubation.

Further, the cells were permeabilized with 0.2 % Triton X-100 in PBS for 15 min and then stained with DAPI and phalloidin to visualize cell structures of the nuclear material through DNA and F-actin, respectively. The microplates were mounted on an inverted epifluorescence microscope (Leica DMi8, Leica Microsystems, Wetzlar, Germany) to conduct observations at 20x.

2.11. *In silico* analysis

To evaluate the potential effect of the bioactive compound identified in DM-F2, an *in silico* analysis was conducted to determine possible interactions between this compound (ligand) and selected apoptosis-involved targets from 22Rv1 cell line (Skjøth & Issinger, 2006). The ligand was drawn using Marvin Sketch and 3D-verified before the docking study. The cancer targets were downloaded from the Protein Databank: ERK1 (4QTB), ERK2 (6GJB), and ACE2 (1R42). Other targets such as Bad and Cyclin D1 were generated in SwissModel 2.0 using their Uniprot FASTA sequences, and respective models were built (Q922934 and 2w99.1.A, respectively for Bad and cyclin D1). The potential binding positions for the evaluated cancer targets were found using MetaPocket 2.0 server. Docking calculations selecting the flexible torsions, hydrogen bonds, and binding energy was conducted as reported by Luzardo-Ocampo, Campos-Vega, Gonzalez de Mejia, & Loarca-Piña (2020) using AutoDock Tools (Trott & Olson, 2010). Figures from the most probable docking conformations were generated in BioVia Discovery software v. 19.1.0.1.18287 (Dassault Systèmes, Vélizy-Villacoublay, France).

2.12. Statistical analysis

The data were expressed as the mean ± SD from at least two independent experiments in triplicates. An analysis of variance (ANOVA), followed by a post-hoc Tukey-Kramer's test, was conducted to establish differences ($p<0.05$) between treatments for each response. SPSS Statistics (IBM Corp., New York, U.S.) was used to obtain the analysis of variance, GraphPad Prism v. 8.0 to represent the graphics, and Number Cruncher Statistical Software (NCSS), version 2001 (NCSS Statistical Software, USA) was used to quantify (LC_{50}).

3. Results and discussion

3.1. Antimutagenic activity, antioxidant capacity, and cytoprotective effect of *Octopus vulgaris*ink extracts

The antimutagenic activity, antioxidant capacity, and the cytoprotective effect expressed as cell viability of *Octopus vulgaris*ink extracts are shown in Fig. 1A and B, C, and D, respectively. The extracts exhibited antimutagenic effect against AFB1 on S. Typhimurium TA98 tester strain (Fig. 1A), inhibiting more than 70% population even at the lowest concentration of the ink extract (0.005 mg/plate). The WE showed the highest ($p<0.05$) inhibition (93.2 % at the highest concentration tested) of the number of revertants/plate. A similar effect was observed when the TA100 strain was used (Fig. 1B), where the WE also exhibited the highest inhibition ($p<0.05$) (74.6 % at 5 mg/plate). These results suggest that the WE have compounds with the potential of protecting the genetic material from compounds (such as AFB1) that induce either type of mutation, considering the anti-reversive effect on base pair or frameshift, as intended by the Ames test. As the octopus' ink is often considered a waste material that has not been extensively used in the food industry (Rubaie, Idris, Kamal, & King, 2012), this property offers the potential to explore value-added benefits to valorize these by-products as a source of chemoprotective agents. There are no reports of the antimutagenic effect of octopus ink. However, a trypsin fractioning of isolated peptidoglycans of Sepiella maindroni ink yielded a hetero polysaccharide with strong antimutagenic activity evidenced in reducing the frequency of micronucleated cells in polychromate erythrocytes and reticulocytes induced by cyclophosphamide *in vivo* (Liu et al., 2008). A similar trypsin fractioning was also used to hydrolyze squid (Ommatresphes bartrami) squid oligopeptides for producing a pro-apoptotic tripeptide (Huang et al., 2012), suggesting that the ink hydrolysis by similar enzymes as those found in the gastrointestinal tract might potentiate the bioactivity of its components. Other parts from octopus have also shown antimutagenic activity, such as freeze-dried tentacles, attributed to the content of 1-butyl-2-isobutyl phthalate isolated from the lipid fraction of the muscle (Cruz-Ramírez et al., 2015).

The antimutagenic activity can be linked to the antioxidant potential of components (Aqil et al., 2011), considering their protective DNA properties against mutagens. Figure 1C shows the antioxidant capacity of the extracts, where the highest DPPH and FRAP values were produced by WE (37.6 ± 1.0 μM TE/g and 80.6 ± 0.7 μM TE/g, respectively), while it exhibited the same ABTS scavenging activity ($p>0.05$) than the other extracts. Water-,

hexane-, and ethanol-soluble extracts from squid ink were screened for antioxidant capacity. The water-soluble extract showed the highest DPPH and FRAP inhibition potential (up to 94.87 %) (Zaharah, 2017). Differences in the antioxidant behavior among extracts may be attributed to the specific mechanisms of actions of each radical, where electron and hydrogen transference is involved. For instance, melanin is a natural component of the ink from cephalopods that acts either way, as an antioxidant or reductive agent, stabilizing natural constituents from the ink and preventing its oxidation (Derby, 2014).

Figure 1D depicts the cytoprotective potential that extracts obtained from *O. vulgaris* ink have on ARPE-19 cells after 4 and 24 h of having received the treatment, expressed as percentages of cell viability above the positive control (15 % of cell viability of ARPE-19 cells after being treated with 10 mM H_2O_2). All the extracts showed the same trend at both incubation times. However, the overall values increased ($p<0.05$) from 4 to 24 h (5.73-57.05 %), while WE exhibited the highest increase (57.05 %). The WE showed the highest protection against cytotoxicity, preventing the damaging action of hydrogen peroxide-derived OH- radical over proteins, phospholipids, enzymes, or DNA (Kaczara, Sarna, & Burke, 2010). Water-soluble extracts have shown the ability to donate protons that may contribute to the OH- radical stabilization. In contrast, the cytoprotective capability of DM may be associated with the anion-receptor properties of polar aprotic solvents (Nayak, Seo, Park, & Park, 2007).

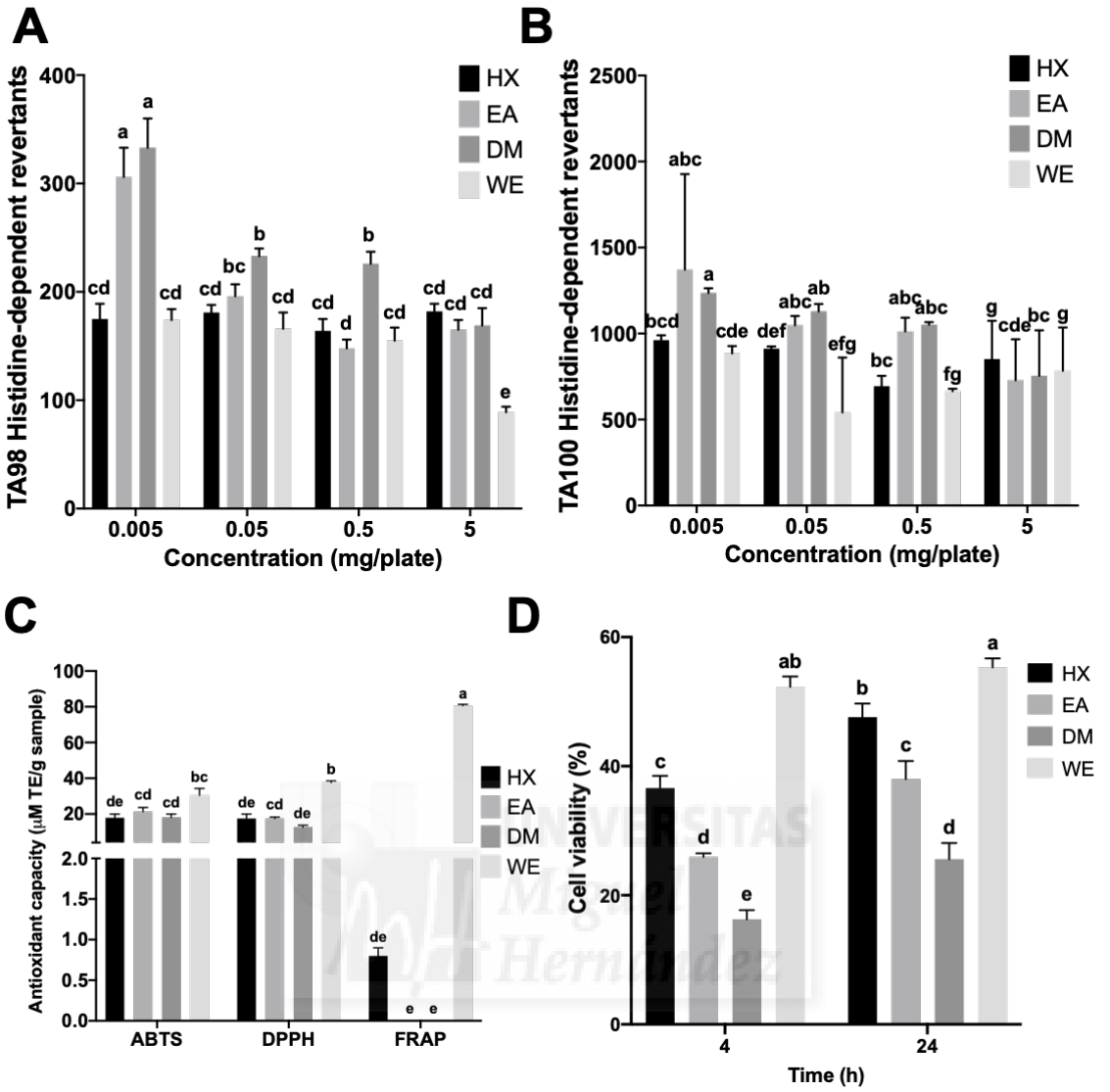

Figure 1. Antimutagenic and cytoprotective effect, and antioxidant capacity of *Octopus vulgaris*ink extracts. Antimutagenic effect against **(A)** TA98 histidine-dependent *Salmonella* Typhimurium strain and **(B)** TA100 histidine-dependent *S.* Typhimurium strain; **(C)** Antioxidant capacity of the extracts by ABTS, DPPH, and FRAP methods; **(D)** Cytoprotective effect against H_2O_2 from the extracts in ARPE-19 cells.

The values are the means ± S.D. from at least two independent experiments in triplicates. Different letters express significant differences ($p<0.05$) by Tukey-Kramer's test. **ABTS:** 2,2-azinobis-3-ethylbenzothiazoline sulfonic acid; **DPPH:** 1,1-diphenil-2-picrylhydrazil; **DM:** Dichloromethane extract of *O. vulgaris* ink; **EA:** Ethyl acetate extract of *O. vulgaris* ink; **FRAP:** Ferric ion reducing antioxidant power; **HX:** Hexane extract from *O. vulgaris* ink; **TE:** Trolox equivalents; **WE:** Water extract of *O. vulgaris* ink.

For the antimutagenic activity experiments (**A** and **B**), the spontaneous revertants were incubated only with vehicle (DMSO, 0.5 mL/100 mL) and represented 17 ± 1 and 96 ± 6 colonies of histidine-dependent revertants/plate for TA98 and TA100, respectively. In addition, the mutagenic control bacteria plates

incubated with AFB_1 (500 ng/plate) induced 1082 ± 105 and 1389 ± 89 colonies histidine-dependent revertants/plate for TA98 and TA100, respectively.

For the cytoprotective experiments (expressed in percentage of cell viability), the control cells were incubated with DMSO (0.5 mL/100 mL) and exhibited 15 % of cell viability, which was represented as the 100%. All the results from the extracts are the cell viability above this parameter.

3.2. Impact of *O. vulgaris* ink extracts and DM-fractions on cancer cells proliferation and ROS activity.

Figure 2A shows the antiproliferative effect of *O. vulgaris* ink extracts on 22Rv1, HeLa, and A459 cancer cells. Since the DM extract exhibited the highest impact on 22Rv1 cancer cell line, several fractions (F1, F2, and F3) obtained from DM were screened for their antiproliferative activity (Fig. 2B) and effect on ROS production (Fig. 2C) on the same cell lines. None of the extracts displayed antiproliferative effects on A459 cells (LC_{50} > 200 µg/mL), but both EA and DM exhibited the most potent activities against 22Rv1 and HeLa cell lines.

A

Treatments	LC_{50} Normal cells (µg/mL)	LC_{50} Cancer cells (µg/mL)		
	ARPE-19	22Rv1	HeLa	A459
HX	> 200[a]	154.9 ± 9[b]	> 200[a]	> 200[a]
EA	169.5 ± 6.4[b]	111.5 ± 8.3[c]	145.4 ± 5.9[b]	> 200[a]
DM	117.9 ± 9.8[c]	68.2 ± 3.8[d]	101.7 ± 5.8[c]	> 200[a]
WE	> 200[a]	> 200[a]	> 200[a]	> 200[a]
Cisplatin	92.6 ± 4.6[d]	1.6 ± 0.4[f]	7.4 ± 0.7[d]	3.8 ± 0.5[d]
Docetaxel	65.4 ± 3.9[e]	9.0 ± 1.3[e]	6.5 ± 2.7[d]	11.2 ± 4.5[c]

B

DM Fraction	ARPE-19	22Rv1
F1	> 200[a]	> 200[a]
F2	> 200[a]	27.6 ± 1.8[b]
F3	> 200[a]	> 200[a]
Cholesterol	> 200[a]	> 200[a]

C

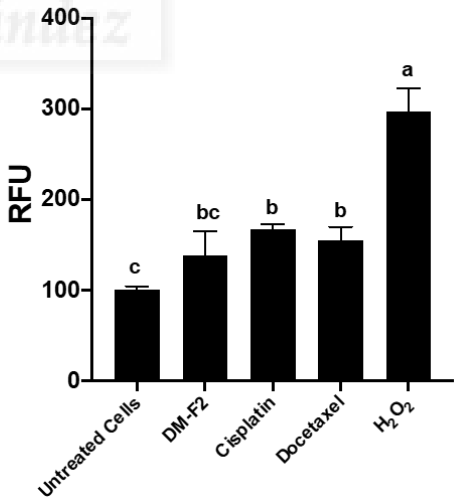

Figure 2. Antiproliferative and ROS-inductor activity of *Octopus vulgaris*ink extracts, drugs controls (cisplatin and docetaxel), and dichloromethane fractions on 22Rv1 and ARPE-19 cells. **(A)** Half lethal dose concentrations (LC_{50}) from *O. vulgaris* ink extracts against normal cells (ARPE-19) and cancer cells (22Rv1, HeLa, and A549) at 48 h of the treatment; **(B)** LC_{50} from dichloromethane purified fractions (F1, F2, and F3) against ARPE-19 and 22Rv1 cells at 48 h of the treatment; **(C)** Reactive oxygen species (ROS) modulation of DM-F2 and drugs controls in 22Rv1 cells.

The values are the means ± S.D. from at least two independent experiments in triplicates. Different letters express significant differences ($p<0.05$) by Tukey-Kramer's test. **DM:** Dichloromethane extract of *O. vulgaris* ink; **EA:** Ethyl acetate extract of *O. vulgaris* ink; **F1, F2, F3:** Fractions from DM; **HX:** Hexane extract from *O. vulgaris* ink; **RFU:** Relative fluorescence units; **WE:** Water extract of *O. vulgaris* ink.

For the antiproliferative effect (**A** and **B**), measured by MTT test, the control cells were incubated with DMSO (0.5 mL/100 mL) and represented 100% proliferation. All the LC_{50} concentrations were determined using several concentrations of the extracts, fractions, or drug controls (25, 50, 100, and 200 µg/ml). For the ROS experiments (**C**), DM-F2 corresponded to the LC_{50} of 22Rv1 cells (27.60 µg/ml). Cisplatin and docetaxel concentrations were also their LC_{50} (1.60 µg/ml and 9.00 µg/ml, respectively for cisplatin and docetaxel).

Since the LC50 values for ARPE-19 cells were higher than those obtained for 22Rv1 and HeLa cells, it could be inferred that the extracts are not cytotoxic to normal cells at the same lethal concentrations for cancer cells.

Cisplatin and docetaxel, commercially available chemotherapeutic agents, were used as controls for comparison purposes (Skjøth & Issinger, 2006). Notably, cisplatin showed the lowest LC_{50} for A549 cells, underlining the reported pro-apoptotic and pro-autophagy effects of this drug for this particular type of cells (Bade & Dela Cruz, 2020) by stimulating the mRNA upregulation and increased protein expression of the autophagy protein 5 and Beclin-1 (Chen et al., 2018). This pathway is hardly presented in 22Rv1 since lack of NF-kB pathway activity implicates low induction of the BECN-1 gene coding for the Beclin-1 protein (Copetti, Bertoli, Dalla, Demarchi, & Schneider, 2009).

Isolation of the contents of the DM extract resulted in fractions F1, F2, and F3, from which F2 showed an increase of around 147 % in the antiproliferative effect ($p<0.05$) (Fig. 2B), an observation that is expected due to the selective extraction of the bioactive compounds. Besides, the DM-F2 LC_{50} value obtained for 22Rv1 was below that for ARPE-19 LC_{50}, suggesting possible bioselectivity. The DM-F2 fraction was selected for further experiments since the American National Cancer Institute considers an extract suitable for further analysis if its LC_{50} value is lower than 30 µg/ml (Momtazi-Borojeni, Behbahani, & Sadeghi-Aliabadi, 2013). The obtained value (27.6 ± 1.8 %) is similar to LC_{50} values reported for HT-29 and Caco-2 human colon cancer cells (28.50 - 31.64 %) when exposed to methanol:water and acetone extracts obtained from Aristotelia chilensis (Céspedes-Acuña et al., 2018). Moreover, LC_{50} were lower than those reported for HT-29 human colon cancer cells after treatment with phenolic-rich extracts of several berries such as black raspberry, cranberry, and strawberries, among others (Seeram et al., 2006).

Based on the significant ($p<0.05$) observed antioxidant capacity from the tested extracts by ABTS and DPPH methods, the effect of the DM-F2 (at its LC_{50}) in the intracellular ROS generation was also evaluated (Fig. 2C). As expected, H2O2 induced the highest ROS production, while no differences ($p<0.05$) were observed between controls (of cisplatin and docetaxel at their respective LC_{50}) and DM-F2. Compared to untreated 22Rv1 cells, DM-F2 increased ($p>0.05$) ROS production up to 55 %.

The search for health food products with value-added benefits has transformed the new food product development (Shinde et al., 2019). The antioxidative potential of *O. vulgaris* ink has not been yet examined, but *in vivo* assays using cuttlefish (Sepia officinalis) ink (1.2 and 2.4 g/kg body weight) administered to healthy and cyclophosphamide-treated (200 mg/kg body weight) Balb/c mice showed significantly ($p<0.05$) reduction of several spleen enzymes associate to antioxidant capacity parameters such as superoxide dismutase activity and malonaldehyde (MDA) content, but higher catalase and reduced glutathione peroxidase activities compared to cyclophosphamide-only treated mice (Zhong et al., 2009). The authors attributed these effects to a synergistic effect from the ink composition such as melanin, proteins, lipids, and glycosaminoglycans, but no association was shown with a specific component.

The antiproliferative and ROS-generation blocking capability that these extracts have on cancerous cell lines is promising since these effects were not observed in non-cancerous cells (Lin, Li, Zamyatnin, Werner, & Bazhin, 2017). Besides, the low ROS production observed in the cells treated with DM-F2 (compared to that observed when exposed to H2O2) is desirable since massive ROS generation can lead to necrotic cell death instead of a pro-apoptotic effect on cancerous cells (Higuchi, 2003). Since the observed ROS levels were comparable to the known anti-carcinogenic drugs, it could be discarded a massive ROS generation leading to the activation of molecular cancer targets aiming to trigger carcinogenesis, metastasis, and further resistance to the anticancer therapy (Ivanova, Zhelev, Aoki, Bakalova, & Higashi, 2016). For instance, ROS in certain cancer cell lines contributes to the up-regulation of mammalian targets reported for rapamycin (mTOR), associated to the malignant transformation of cells such as its involvement in the activation of PI3K protooncogene and the suppression of phosphatase and tensin homolog (PTEN) function and Beclin-1 (Wullschleger, Loewith, & Hall, 2006). ROS are also known autophagy inductors since lysosome clearance of excessive ROS is required,

involving activation of Ca2+-lysosomal channels triggering translocation of a transcription factor for the biosynthesis of autophagic lysosomes (Zhang et al., 2016).

3.3. Structural elucidation of DM-F2

Studies have shown that DM-soluble extracts from organisms are vehicles of moderately polar compounds with biological properties, mainly sterols and terpenes (Fitahia et al., 2015). To identify potential candidates responsible of the observed biological effects in DM-F2, FTIR (Fig. 3A), 13C- and 1H-NMR (Fig. 3B), and ESI/MS (Fig. 3C) analysis were carried out; chemical structures from these analyses are shown in Fig. 3D.

The IR spectrum (Fig. 3A) showed different peaks associated with –OH functional group in the region of 3266-3574 cm-1, which was possible to overlap with the presence of secondary amide at 3386 cm-1. Then, a C-H band was observed at 2925 cm-1, associated with alkane stretching. The signal of one band at 1652 cm-1 confirmed the C=O stretch in the amide group. Furthermore, a signal associated with C-O bond is showed at 1019 cm-1 (Pavia & Lampman, 2009). A summary of these observations can be found in Supplementary Table 2.

Based on the NMR data (Fig. 3B) the first identified compound was cholesterol. From 13C-NMR results, two signals at δ = 140.73 (C1) and 121.69 (C2) ppm representing two C=C bonds were detected. A signal at δ = 71.79 ppm (C3) was also identified, which is characteristic of C-O. Based on 1H-NMR analysis, the signal at δ = 3.54 (d, 1H) suggested C with –OH group, which is characteristic of cholesterol, compared with databases (AIST, 2020). A second elucidated compound (Fig. 3B) was a possibly novel component of the *O. vulgaris* ink extract since no records were found in the available databases. As cholesterol did not exhibit an antiproliferative effect against 22Rv1 cells (LC_{50} > 200 µg/mL), additional compounds in the extracts might be exerting the observed outcomes in the cells. This possible unreported compound, [N-(2-ozoazepan-3-yl) pyrrolidine-2-carboxamide] (OPC) was elucidated as follows: from 13C-NMR analyses, two signals at low field, one at δ = 165.76 (C1) and the other at δ = 162.46 (C2) ppm, were observed, suggesting two amides carbonyl groups. Then, different signals at δ = 52.47 (C3), 47.89 (C4), and 41.85 (C5) ppm that are characteristic of C-N bond were observed. A signal at low-field of 1H-NMR at 7.26 ppm was detected, indicating a N-H bond and confirming an amide group (Pavia & Lampman, 2009). Then, different peaks at δ = 34.02 (C6), 29.70 (C7), 29.46 (C8), 29.12 (C9), and 24.87 (C10) ppm in the 13C-NMR spectrum were also

found, corresponding to C-H bond. The signals of C1, C3, C5, C6, C9, and C10 were associated with caprolactam (cycloheptane with an N-H bond). Based on the available databases, the other signals (C3, C4, C7, and C8) may correspond to a pyrrolidine (a cyclopentane with an N-H bond), bonded to the caprolactam compound by a carboxamide structure (Reich, 2020). Graphics indicating the identified chemical structures are indicated in Figs. 3D and 3E. Both 13C and 1H-NMR spectra of cholesterol and OPC can be found in Supplementary Figure S1.

Fig. 3C shows the ESI-MS analysis, indicating the presence of a compound with a molecular weight of 225.20 (m/z) and their possible isotopes. This information was screened against the NMR analysis (Fig. 3B), which further indicated the presence of OPC.

Until this date, OPC has not been found reported. The natural accumulation of caprolactam derivatives in buckwheat and sunflower achenes has been reported (Kalinová, Tříska, Vrchotová, & Moos, 2014). D'Auria et al. (1997) detected a caprolactam formamide in the n-hexane fraction of New Caledonian sponge (Jaspis carteri) tissue using both 1H- and 13C-NMR analyses. Likewise, the authors used a similar purification approach like the one used in this research, isolating the newly compound by open column chromatography using $CHCl_3$

3.4. Pro-apoptotic and cell morphology changes induced by DM-F2 in 22Rv1 cells

The effect of DM-F2 on apoptosis and cell morphology in 22Rv1 cells is shown in Fig. 4. As observed in the flow cytometry dispersions (Fig. 4A) and their quantification (Fig. 4B), the DM-F2 treatment mainly induced an early apoptosis process, which was higher ($p<0.05$) than that observed in untreated cells or when treated with cisplatin (43.2 ± 0.2 %, 5.8 ± 0.7 %, and 32.2 ± 0.2 %, respectively). The exposure time to DM-F2 (24 h) was selected since it was determined that a 48-h treatment at the same dose (LC_{50}) DM-F2 caused 50 % mortality in the cells (Fig. 2B).

The treatment time (24 h) was selected since the objective of this part of the study was to observe the highest percentage of cells in early apoptosis (FITC-A + / PE-A−).

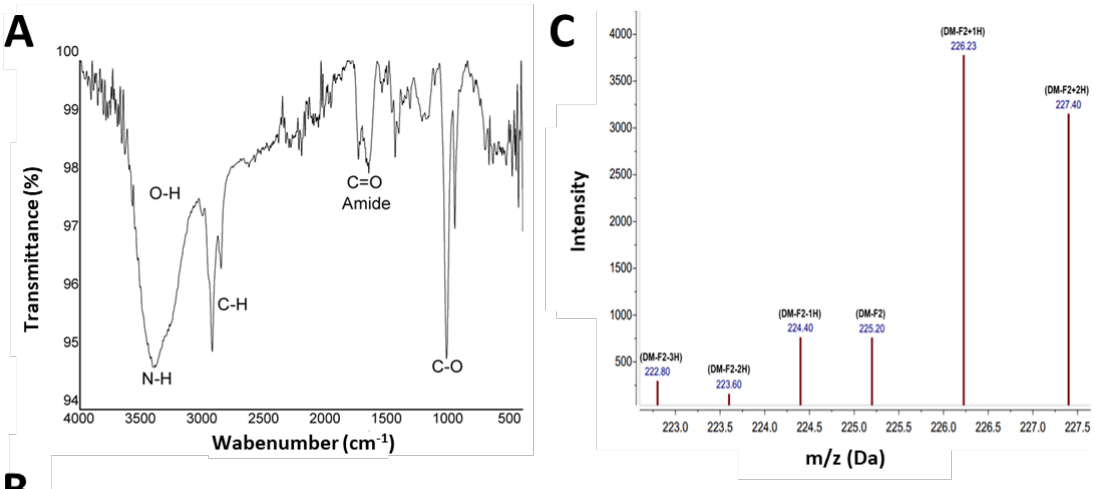

B

Cholesterol (CHOL)			N-(2-ozoazepan-3-yl) pyrrolidine-2-carboxamide (OPC)		
No.	**δ_C**	**δ_H**	**No.**	**δ_C**	**δ_H**
1	140.73	-	-	-	7.26 (s, 1H)
2	121.69	5.35 (d, J = 5.30 Hz, 1H)	1	165.76	-
3	71.79	3.54 (d, J = 29.5 Hz, 1H)	2	162.46	-
4	56.83		3	52.47	4.15 (t, J = 4.6 Hz, 1H)
5	56.13		4	56.07	4.13 (t, J= 4.60 Hz, 1H)
6	50.20		5	47.89	3.56 (dt, J= 4.6, 6.2 Hz, 2H)
7	42.30	2.19 (s, 2H)	6	41.85	3.51 (dt, J= 4.6, 6.2 Hz, 2H)
8	39.76		7	34.02	2.04 (m, J = 6.2 Hz, 2H)
9	39.50		8	29.70	1.82 (m, J= 6.2Hz, 2H)
10	37.24		9	29.28	1.82 (m, J= 6.2Hz, 2H)
11	36.59	-	10	29.12	1.23 (m, J= 6.2 Hz, 2H)
12	36.17		11	24.87	1.23 (m, J=6.2 Hz, 2H)
13	35.77				
14	31.89				
15	31.65				
16	28.21				
17	27.21				
18	24.27				
19	23.81				
20	22.86	0.87 (s, 3H)			
21	22.67	0.86 (s, 3H)			
22	21.07				
23	19.38	1.06 (s, 3H)			
24	18.70	0.92 (s, 3H)			
25	11.84	0.68 (s, 3H)			

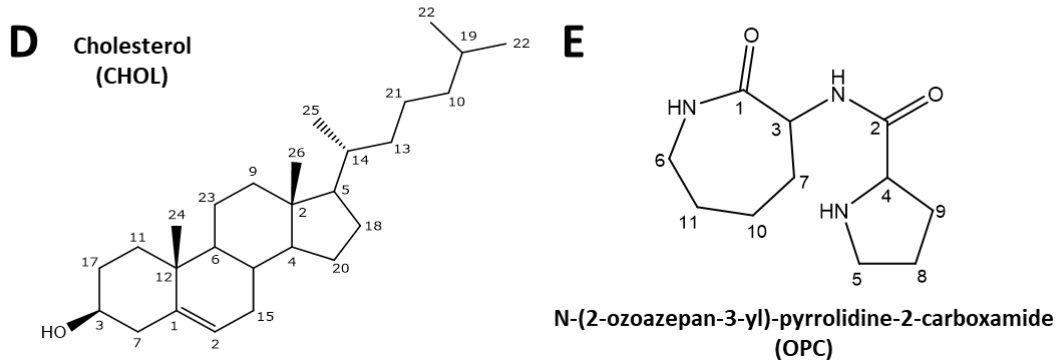

Figure 3. Chemical and structural elucidation of DM-F2 fraction. **(A)** Fourier-transformed infrared spectroscopy (FTIR) analysis; **(B)** Electrospray ionization mass spectrometry (ESI/MS) analysis; **(C)** ^{13}C- and ^{1}H-NMR (nuclear magnetic resonance) analysis; **(D)** Chemical structures of the two main compounds identified by the chemical

and structural analyses (cholesterol and [N-(2-ozoazepan-3-yl)-pyrrolidine-2-carboxamide] (OPC).

δ: chemical shift, **J:** Coupling constant, **d:** doublet, **dd:** a doublet of doublets, **m:** multiplet, **s:** singlet.

The ESI/MS analysis was conducted in the negative mode of OPC.

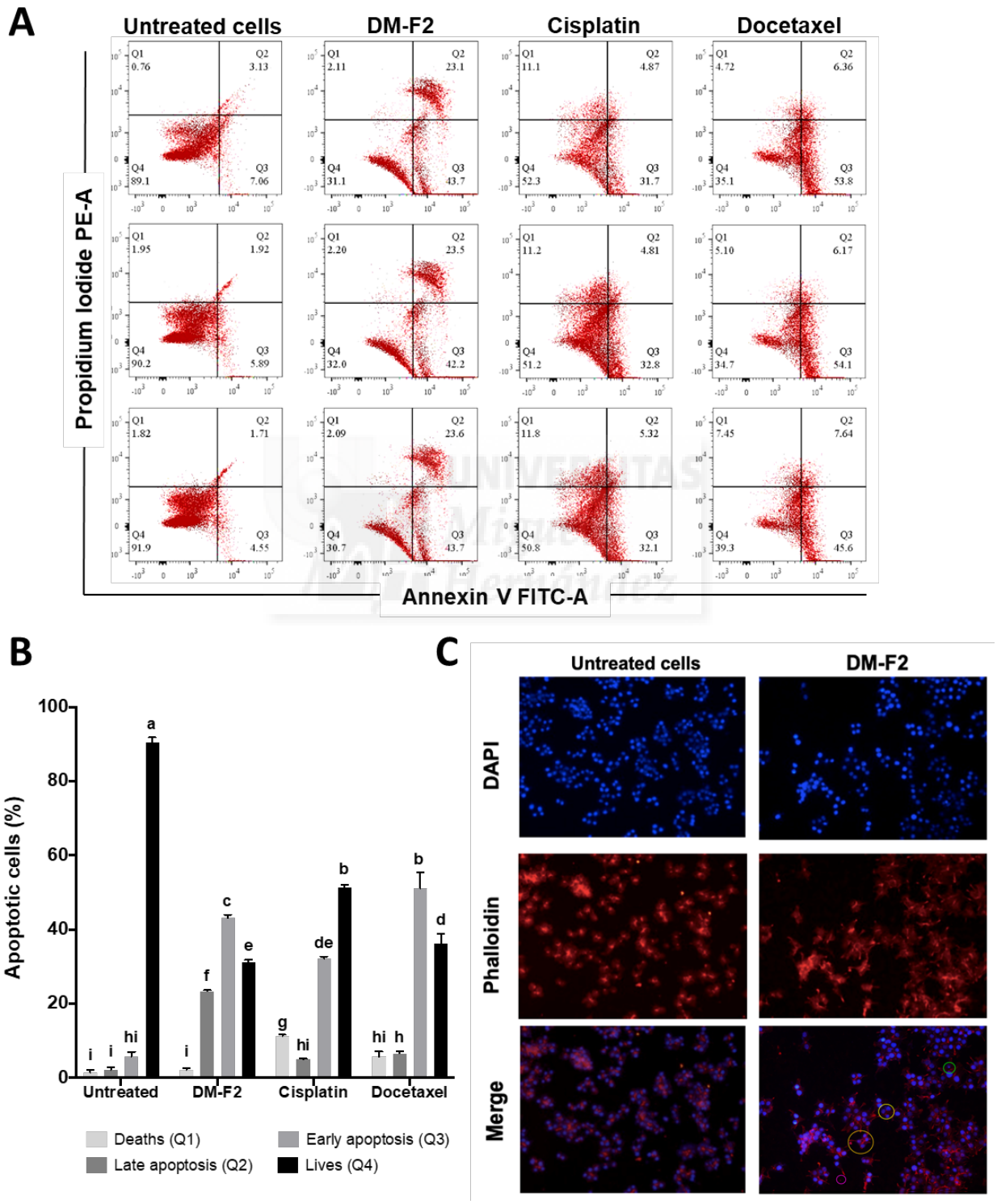

Figure 4. Pro-apoptotic and cell morphology effect of DM-F2 and drug controls in 22Rv1 cells. **(A)** Positive Annexin-V FITC and propidium iodide (PI) cells by flow cytometry; **(B)**

Quantification of apoptotic cells from the flow cytometry analysis; **(C)** Cell morphology changes by DAPI and Phalloidin tetramethylrhodamine staining.

The results from **B** are represented as the means ± S.D. from three independent experiments in triplicates. Different letters express significant differences ($p<0.05$) by Tukey-Kramer's test. **DAPI:** 4'6-diadimino-2-phenylindole dilactate; **DM-F2:** Fraction 2 from dichloromethane extract (DM) of *O. vulgaris* ink.

For **A,** the quadrants (Q1) are death cells (Q1), late apoptosis (Q2), early apoptosis (Q3), and live cells (Q4). The concentrations of DM-F2, cisplatin, and docetaxel corresponded to their LC_{50} (27.6 µg/ml, 1.6 µg/ml, and 9.0 µg/ml, respectively for cisplatin and docetaxel). Hydrogen peroxide (H_2O_2) was used as a positive control of apoptosis.

For **C,** the morphological changes were inspected after 4 h of treatment. Actin cytoskeleton (red) and DNA (blue) were visualized by phalloidin and DAPI staining, respectively. The cell observations were made at 20x. The circles in the figure means: Yellow: chromatin condensation; Orange: blebs; Pink: apoptotic body's; Green: Nuclear fragmentation.

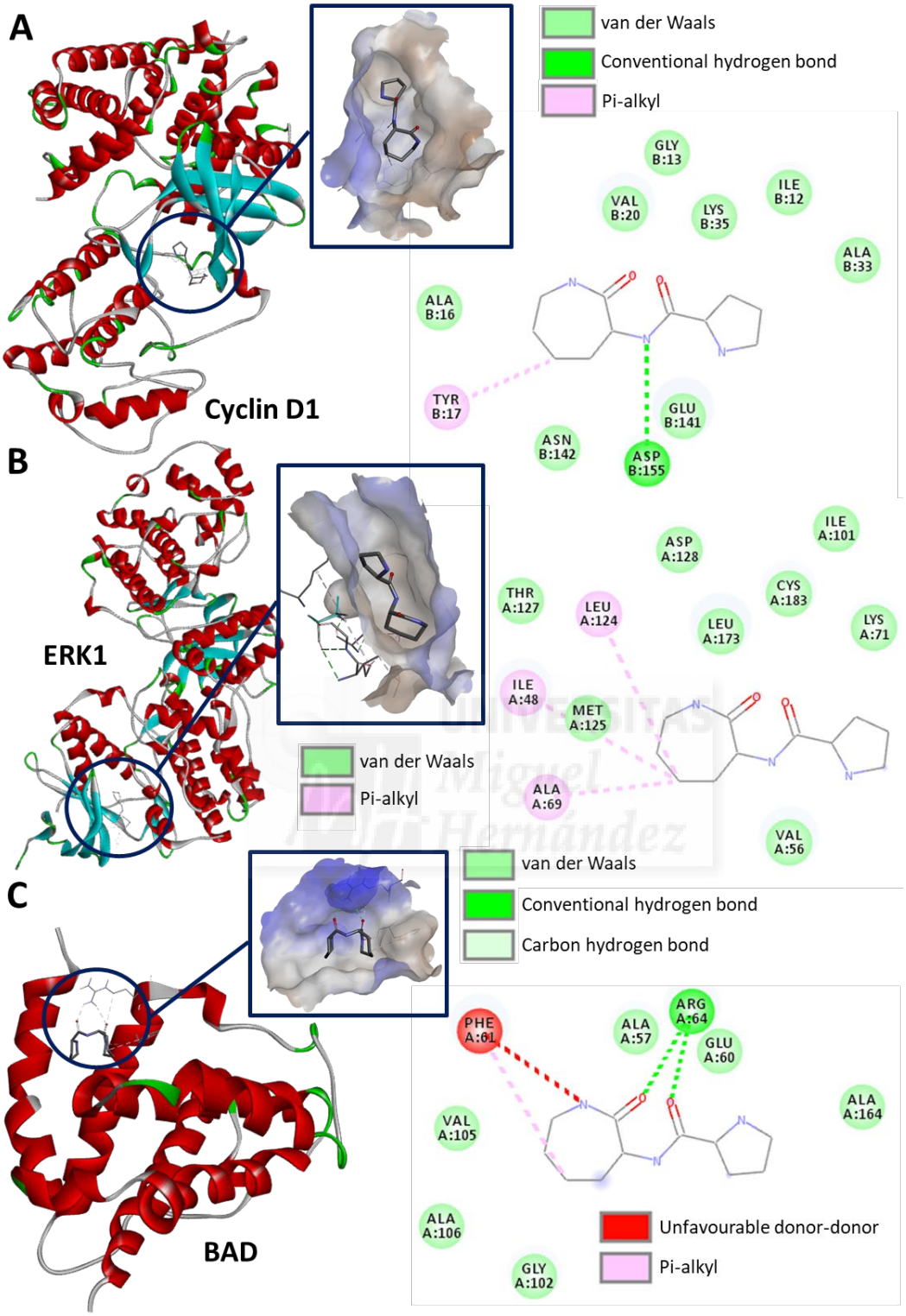

Figure 5. *In silico* analysis with the best potential interactions between N-(2-ozoazepan-3-yl)-pyrrolidine-2-carboxamide (OPC) and selected cancer targets of 22Rv1 cells. Interactions of OPC and **(A)** Cyclin D1; **(B)** ERK1; **(C)** BAD.

The 2D graphic is a representation of the potential chemical interactions and involved amino acids residues from the cancer target proteins.

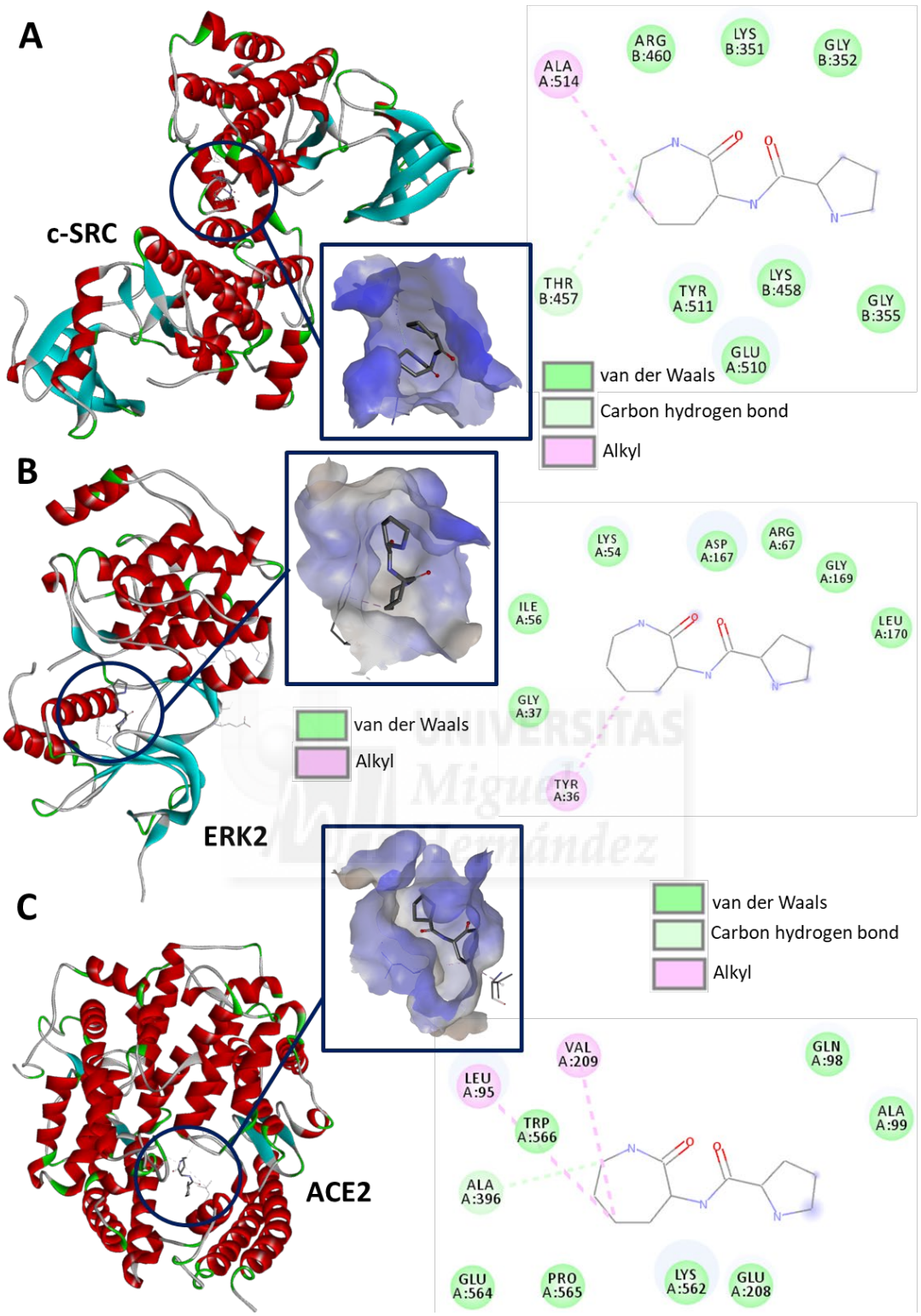

Figure 6. *In silico* analysis with the best potential interactions between N-(2-ozoazepan-3-yl)-pyrrolidine-2-carboxamide (OPC) and additional selected cancer targets of 22Rv1 cells. Interactions of OPC and **(A)** c-SRC; **(B)** ERK2; **(C)** ACE2.

The 2D graphic is a representation of the potential chemical interactions and involved amino acids residues from the cancer target proteins.

Moreover, it is known that only half of the population remains alive after 48 h; at 24 h a larger number of cells exist, which could be verified since only 31 % of dead cells were observed (FITC-A - / PE-A+) after 24 h (Fig. 4B).

To confirm pro-apoptotic processes in the 22Rv1 cells, a fluorescence staining procedure was conducted (Fig. 4C). The DM-F2 induced morphological changes (Supplementary Fig. S2), such as a reduction in pseudopods and increased surface protrusions (pink circles), nuclear segmentations (green circles), and membrane blebs (orange circles). In contrast, untreated cells did not exhibit DNA fragmentation. Despite the lack of information about the new compound found in DM-F2, biological activity from pyrrolidine derivates from marine organisms has been linked to antiproliferative and proapoptotic effects in renal carcinoma cell lines (Morais, Pat, Gobe, Johnson, & Healy, 2006). The significantly increase in pro-apoptotic cells (~4.5-fold) is similar to the effect of Manuka honey from Leptospermum scoparium tree (10-20 mg/mL), which has exhibited values from ~3.50 to ~4.20-fold times in the apoptosis increase from HCT116 human colon cancer cells due to increased p53 and caspase-3 activation, compared to untreated cells (Afrin et al., 2018). The authors also reported cell cycle arrest due to lower G0/G1 and higher S phase transition in the treated cells against the untreated ones. Cyclin E, Cyclin D1, CDK2, and CDK4 mRNA were also modified (significant reduction, $p < 0.05$) following a dose-response type of relationship.

Certain components of mollusks' ink have been associated with the regulation of apoptotic mechanisms. For instance, squid (Sepia esculenta) ink polysaccharides prevented apoptosis on cyclophosphamide-induced apoptosis in Kunming male mice by reducing p38 protein phosphorylation, decreased caspase-3 expression, and increased Bcl-2 protein expression (Gu et al., 2017). The authors also reported the capability of these polysaccharides to avoid pro-autophagy mechanisms *in vivo* on mice Leydig cells after cyclophosphamide treatment, evading the transformation of free microtubule-associated protein 1 light chain 3 (LC3-I) to lipid-bound LC3 (LC3-II), mediating in the encasement of the cellular contents during the autophagic elongation process. Moreover, a decrease of Beclin-1 protein expression was observed due to the polysaccharide treatment. Blockade of the acrolein induced p38 MAPK and PI3K/Akt signals by glycosaminoglycans from the same ink also evaded the autophagic mechanism (Gu et al., 2017b).

Another component of the ink, such as aryl butene derivatives, have exhibited antiproliferative (up to 89 % inhibition) effects on K562 breast cancer cells, related to the presence of a ferrocenyl group and -OH substitution (Arbi et al., 2018) since these groups may potentially take advantage of an hydrophobic environment present in MNK1/2 kinase (MAPK-interacting kinase), limiting oncogene-driven signaling (Sansook et al., 2018).

3.5. In silico molecular docking of OPC and selected cancer targets from 22Rv1 cells

Figures 5 and 6 show the molecular docking analysis between selected cancer targets in 22Rv1 cells and OPC. In consequence, each figure represents binding between OPC and Cyclin D1 (Fig. 5A), ERK1 (Fig. 5B), BAD (Fig. 5C), c-SRC (Fig. 6A), ERK2 (Fig. 6B), and ACE2 (Fig. 6C). These cancer targets were selected considering reported profiling of selected proteins involved in cancer development for the 22Rv1 cell line (Skjøth & Issinger, 2006) and the specific association of each molecule according to the Human Protein Atlas database (Uhlen et al., 2015). The selected molecules also corresponded to the most probable binding conformation between the selected ligand (OPC) and each protein.

Most of the potential bindings found were van der Waals, pi-alkyl, and carbon-hydrogen bond. However, Fig. 5A shows conventional hydrogen-bond, which might explain their higher bonding energy with OPC as indicated in Supplementary Table S3 (-6.70 kcal/mol). ERK1 (Fig. 5B) did not exhibit carbon-hydrogen bonding but presented multiple interactions with several amino acid residues (Supplementary Table S4), aiming to a higher binding affinity with OPC than the other evaluated proteins. BAD protein also showed conventional hydrogen bond, but the presence of an unfavorable donor-donor reduces its binding affinity with OPC, reaching -6.10 kcal/mol at its most probable binding conformation (Supplementary Table S3). Other proteins such as c-SRC (Fig. 6A), ERK2 (Fig. 6B), ACE2 (Fig. 6C) also displayed lower binding energies than Cyclin D1 and ERK1, ranging from -5.60 kcal/mol to -6.10 kcal/mol.

The results from the *in silico* studies suggest the potential action of the OPC molecule in selected cancer targets. For instance, it has been reported that Cyclin D1 inhibition is associated with a disruption in cancer development due to its importance in the cell cycle progression (Alao, 2007). In cancer cells, Cyclin D1 regulates the transition from G1 to

the S phase, actively working with CDK4 and CDK6, which phosphorylate and inactivate the retinoblastoma protein (RB), which coincides with RB function loss in most human cancers (Cress, Engel, & Santiago-Cardona, 2014). There are no reports of the effect of *O. vulgaris* ink in the modulation of the cell cycle, but Huang et al. (2012) informed the impact of sepia oligopeptides (5, 10, and 15 mg/mL, 24 h) decreasing human prostate cancer (PC-3) positive cells from the S phase (~14 %) and G2/M phase (~17 %); moreover, SubG1 (~22 %) and G0/G1 phases (~8 %) also significantly ($p < 0.05$) increased. A further impact of the ink on cell cycle arrest should be explored to deepen in the observed pro-apoptotic mechanisms.

The cyclin D1 function might also be induced by the estrogen receptor alpha (ERα) which physically interacts with c-SRC, activating downstream signaling to regulate in both, transformed and normal cells, processes such as cell proliferation, survival, and metastasis (Ventura et al., 2017). As c-SRC also phosphorylates p27, demonstrated *in vitro* and *in vivo*, cell cycle promotion is alternatively affected since p27 protein also induced cell cycle arrest due to its binding to cyclin E-CDK2 (Chu et al., 2007).

Given the affinity found between OPC and ERK1 and BAD, the potential of this molecule to contribute to a pro-apoptotic mechanism involving the ERK1/2 pathway and the involvement of intrinsic mitochondrial proteins may be suggested (Stecca & Rovida, 2019). Within this pathway, c-SRC modulates MEKK2/3 proteins involved in cell cycle arrest and induces proteins from the intrinsic apoptosis mechanism such as Bad (Barros & Marshall, 2005).

4. Conclusion

The results obtained in this study showed that *Octopus vulgaris*ink extracts might provide health benefits derived from its content in bioactive compounds. The DM-F2 extract showed the most potent antiproliferative, DNA-disruption, and pro-apoptotic effects on 22Rv1 cells. These effects might be attributed to a novel identified compound in DM-F2, N-(2-ozoazepan-3-yl)-pyrrolidine-2-carboxamide (OPC). To our knowledge, this is the first report of these biological effects from *O. vulgaris* ink on 22Rv1 cell line, underlining potential biological effects from an underutilized marine food product.

Nomenclature

Chemical compounds used in this article: ABTS (PubChem CID: 9570474); Dichloromethane (PubChem CID: 6344); DAPI (PubChem CID: 57347489); DPPH (PubChem CID: 2735032); Ethyl acetate (PubChem CID: 8857); Hexane (PubChem CID: 8058); MTT (PubChem CID: 64965); Phalloidin tetramethylrhodamine (PubChem CID: 135119009).

Abbreviations: ABTS: 2,2-azinobis-3-ethylbenzothiazoline sulfonic acid; AcOEt: Ethyl acetate; AFB1: Aflatoxin B1; CDK4, CDK6: Cyclin-dependent kinase 4 and 6; CHOL: Cholesterol; DAPI: 4'6-diadimino-2-phenylindole dilactate; DM: Dichloromethane extract of *O. vulgaris* ink; DM-F2: Fraction 2 (F2) of DM; DPPH: 1,1-diphenil-2-picrylhydrazil; EA: Ethyl acetate extract of *O. vulgaris* ink; ER□: Estrogen receptor alpha; ESI/MS: Electrospray ionization mass spectrometry; ELISA: Enzyme-linked immunosorbent assay; FBS: Fetal bovine serum; FRAP: Ferric ion reducing antioxidant power; Hex: Hexane; HX: Hexane extract of *O. vulgaris* ink; FITC: Fluorescein isothiocyanate; FTIR: Fourier-transformed infrared spectroscopy; LC: Liquid chromatography; LC3-I: Free microtubule-associated protein 1 light chain 3; LC3-II: Lipid-bound LC-3; LC_{50}: Half lethal concentration; MNK1/2 kinase: MAPK-interacting kinase; mTOR: mammalian target of rapamycin; MTT: 3-(4,5-dimethylthiazol-2-yl)-2,5-diphenyltetrazolium bromide; NMR: Nuclear magnetic resonance; OPC: N-(2-ozoazepan-3-yl) pyrrolidine-2-carboxamide; PTEN: Phophatase and tensin homolog; RB: Retinoblastoma protein; ROS: Reactive oxygen species; SDS: Sodium dodecyl sulfate; TLC: Thin-layer chromatography; TE: Trolox equivalents; TPTZ: 2,4,6-tripyridyl-s-triazine; RFU: Relative fluorescence units; WE: Water extract of *O. vulgaris* ink.

References

Afrin, S., Giampieri, F., Gasparrini, M., Forbes-Hernández, T. Y., Cianciosi, D., Reboredo-Rodriguez, P., Amici, A., Quiles, J. L., & Battino, M. (2018). The inhibitory effect of Manuka honey on human colon cancer HCT-116 and LoVo cell growth. Part 1: the suppression of cell proliferation, promotion of apoptosis and arrest of the cell cycle. Food & Function, 9(4), 2145–2157. https://doi.org/10.1039/C8FO00164B

AIST. (2020). Spectral database for organic compounds SDBS. Retrieved from https://search.library.wisc.edu/catalog/9910005236902121

Alao, J. P. (2007). The regulation of cyclin D1 degradation: roles in cancer development and the potential for therapeutic invention. Molecular Cancer, 6(1), 24. https://doi.org/10.1186/1476-4598-6-24

Aqil, F., Zahin, M., El Sayed, K. A., Ahmad, I., Orabi, K. Y., & Arif, J. M. (2011). Antimicrobial, antioxidant, and antimutagenic activities of selected marine natural products and tobacco cembranoids. Drug and Chemical Toxicology, 34(2), 167–179. https://doi.org/10.3109/01480545.2010.494669

Arbi, M. El, Ketata, E., Neifar, A., Mihoubi, W., Gupta, G. K., Pigeon, P., Top, S., Gargouri, A., & Jaouen, G. (2018). Aryl butenes active against K562 cells and lacking tyrosinase inhibitory activity as new leads in the treatment of leukemia. Mini-Reviews in Medicinal Chemistry, 18(15), 1294–1301. https://doi.org/10.2174/1389557517666170208142254

Ayu Shazwani, Z., & Rabeta, M. S. (2020). Enzymatic hydrolysis as an approach to produce alternative protein from cephalopods ink powder: a short review. Food Research, 4(5), 1383–1390. https://doi.org/10.26656/fr.2017.4(5).423

Bade, B. C., & Dela Cruz, C. S. (2020). Lung Cancer 2020. Clinics in Chest Medicine, 41(1), 1–24. https://doi.org/10.1016/j.ccm.2019.10.001

Barros, J. C., & Marshall, C. J. (2005). Activation of either ERK1/2 or ERK5 MAP kinase pathways can lead to disruption of the actin cytoskeleton. Journal of Cell Science, 118(8), 1663–1671. https://doi.org/10.1242/jcs.02308

Benzie, I. F. F., & Strain, J. J. (1996). The ferric reducing ability of plasma (FRAP) as a measure of "antioxidant power": The FRAP assay. Analytical Biochemistry, 239(1), 70–76. https://doi.org/10.1006/ABIO.1996.0292

Besednova, N. N., Zaporozhets, T. S., Kovalev, N. N., Makarenkova, I. D., & Yakovlev, Y. M. (2017). Cephalopods: The potential for their use in medicine. Russian Journal of Marine Biology, 43(2), 101–110. https://doi.org/10.1134/S1063074017020031

Céspedes-Acuña, C. L., Xiao, J., Wei, Z.-J., Chen, L., Bastias, J. M., Avila, J. G., … Kubo, I. (2018). Antioxidant and anti-inflammatory effects of extracts from Maqui berry Aristotelia chilensis in human colon cancer cells. Journal of Berry Research, 8(4), 275–296. https://doi.org/10.3233/JBR-180356

Chen, L., Deng, H., Cui, H., Fang, J., Zuo, Z., Deng, J., Li, Y., Wang, X., & Zhao, L. (2018). Inflammatory responses and inflammation-associated diseases in organs. Oncotarget, 9(6). https://doi.org/10.18632/oncotarget.23208

Chu, I., Sun, J., Arnaout, A., Kahn, H., Hanna, W., Narod, S., Sun, P., Tang, C., Hengst, L., & Slingerland, J. (2007). p27 phosphorylation by Src regulates inhibition of cyclin E-Cdk2. Cell, 128(2), 281–294. https://doi.org/10.1016/j.cell.2006.11.049

Copetti, T., Bertoli, C., Dalla, E., Demarchi, F., & Schneider, C. (2009). p65/RelA modulates BECN1 transcription and autophagy. Molecular and Cellular Biology, 29(10), 2594–2608. https://doi.org/10.1128/MCB.01396-08

Cress, D., Engel, B., & Santiago-Cardona, P. (2014). The retinoblastoma protein: a master tumor suppressor acts as a link between cell cycle and cell adhesion. Cell Health and Cytoskeleton, (7), 1–10. https://doi.org/10.2147/CHC.S28079

Cruz-Ramírez, S.-G., López-Saiz, C.-M., Rosas-Burgos, E.-C., Cinco-Moroyoqui, F.-J., Velázquez, C., Hernández, J., & Burgos-Hernández, A. (2015). Antimutagenic, antiproliferative, and antioxidant effect of extracts obtained from octopus (Paraoctopus limaculatus). Food Science and Technology (Campinas), 35(4), 722–728. https://doi.org/10.1590/1678-457X.0001

Cucinotta, F., & Pieroni, A. (2018). “If you want to get married, you have to collect virdura ”: the vanishing custom of gathering and cooking wild food plants on Vulcano, Aeolian Islands, Sicily. Food, Culture & Society, 21(4), 539–567. https://doi.org/10.1080/15528014.2018.1481263

D’Auria, M. V., Giannini, C., Minale, L., Zampella, A., Debitus, C., & Frostin, M. (1997). Bengamides and related new amino acid derivatives from the new caledonian marine sponge Jaspis carteri. Journal of Natural Products, 60(8), 814–816. https://doi.org/10.1021/np970050q

Derby, C. D. (2014). Cephalopod ink: production, chemistry, functions and applications. Marine Drugs, 12(5), 2700–2730. https://doi.org/10.3390/md12052700

Ebada, S. S., Edrada, R. A., Lin, W., & Proksch, P. (2008). Methods for isolation, purification and structural elucidation of bioactive secondary metabolites from marine invertebrates. Nature Protocols, 3(12), 1820–1831. https://doi.org/10.1038/nprot.2008.182

Fitahia, E. M., Raheriniaina, C. E., Bazin, M. A., Huvelin, J.-M., Logé, C., Ranaivoson, E., & Nazih, H. (2015). Anti-proliferative and pro-apoptotic effect of dichloromethane extract of *Octopus vulgaris*by-products on human breast cancer cell lines. Waste and Biomass Valorization, 6(2), 237–242. https://doi.org/10.1007/s12649-014-9344-1

Fukumoto, L. R. R., & Mazza, G. (2000). Assessing antioxidant and prooxidant activities of phenolic compounds. Journal of Agricultural & Food Chemistry, 48(8), 3597–3604. https://doi.org/10.1021/jf000220w

García-Romo, J., Noguera-Artiaga, L., Carolina Gálvez-Iriqui, A., Samuel Hernández-Zazueta, M., Fernando Valenzuela-Cota, D., Iván González-Vega, R., Plascencia-Jatomea, M., Sandoval-Petris, E., Robles-Sánchez, R. M., Juárez, J., Hernández-Martínez, J., Santacruz-Ortega, C., Burgos-Hernández, A., & Burboa-Zazueta, G. (2020). Antioxidant, antihemolysis, and retinoprotective potentials of bioactive lipidic compounds from wild shrimp (Litopenaeus stylirostris) muscle. CyTA-Journal of Food, 18(1), 153–163. https://doi.org/10.1080/19476337.2020.1719210

Gu, Y.-P., Yang, X.-M., Luo, P., Li, Y.-Q., Tao, Y.-X., Duan, Z.-H., Xiao, W., Zhang, D., & Liu, H.-Z. (2017). Inhibition of acrolein-induced autophagy and apoptosis by a glycosaminoglycan from Sepia esculenta ink in mouse Leydig cells. Carbohydrate Polymers, 163, 270–279. https://doi.org/10.1016/j.carbpol.2017.01.081

Gu, Y. P., Yang, X. M., Duan, Z. H., Luo, P., Shang, J. H., Xiao, W., Tao, Y., Zhang, D., Zhang, Y., & Liu, H. Z. (2017b). Inhibition of chemotherapy-induced apoptosis of testicular cells by squid ink polysaccharide. Experimental and Therapeutic Medicine, 14(6), 5889–5895. https://doi.org/10.3892/etm.2017.5342

Higuchi, Y. (2003). Chromosomal DNA fragmentation in apoptosis and necrosis induced by oxidative stress. Biochemical Pharmacology, 66(8), 1527–1535. https://doi.org/10.1016/S0006-2952(03)00508-2

Huang, F., Yang, Z., Yu, D., Wang, J., Li, R., & Ding, G. (2012). Sepia ink oligopeptide induces apoptosis in prostate cancer cell lines via caspase-3 activation and elevation of Bax/Bcl-2 ratio. Marine Drugs, 10(12), 2153–2165. https://doi.org/10.3390/md10102153

Ivanova, D., Zhelev, Z., Aoki, I., Bakalova, R., & Higashi, T. (2016). Overproduction of reactive oxygen species – obligatory or not for induction of apoptosis by anticancer drugs.

Chinese Journal of Cancer Research, 28(4), 383–396. https://doi.org/10.21147/j.issn.1000-9604.2016.04.01

Kaczara, P., Sarna, T., & Burke, J. M. (2010). Dynamics of H2O2 availability to ARPE-19 cultures in models of oxidative stress. Free Radical Biology and Medicine, 48(8), 1064–1070. https://doi.org/10.1016/j.freeradbiomed.2010.01.022

Kalinová, J. P., Tříska, J., Vrchotová, N., & Moos, M. (2014). Verification of presence of caprolactam in sprouted achenes of Fagopyrum esculentum Moench and its influence on plant phenolic compound content. Food Chemistry, 157, 380–384. https://doi.org/10.1016/j.foodchem.2014.02.049

Lin, S., Li, Y., Zamyatnin, A. A., Werner, J., & Bazhin, A. V. (2017). Reactive oxygen species and colorectal cancer. Journal of Cellular Physiology, 233(7), 5119–5132. https://doi.org/10.1002/jcp.26356

Liu, C., Li, X., Li, Y., Feng, Y., Zhou, S., & Wang, F. (2008). Structural characterisation and antimutagenic activity of a novel polysaccharide isolated from Sepiella maindroni ink. Food Chemistry, 110(4), 807–813. https://doi.org/10.1016/j.foodchem.2008.02.026

Liu, G., Ma, Y. M., Tai, W. Y., Xie, C. M., Li, Y. N., Li, J., & Nan, F. J. (2008). Design, synthesis, and biological evaluation of caprolactam-modified bengamide analogues. ChemMedChem, 3(1), 74–78. https://doi.org/10.1002/cmdc.200700214

Liu, H., Luo, P., Chen, S., & Shang, J. (2011). Effects of squid Ink on growth performance, antioxidant functions and immunity in growing broiler chickens. Asian-Australasian Journal of Animal Sciences, 24(12), 1752–1756. https://doi.org/10.5713/ajas.2011.11128

López-Saiz, C. M., Suárez-Jiménez, G. M., Plascencia-Jatomea, M., & Burgos-Hernández, A. (2013). Shrimp lipids: A source of cancer chemopreventive compounds. Marine Drugs, 11(10), 3926–3950. https://doi.org/10.3390/md11103926

Luzardo-Ocampo, I., Campos-Vega, R., Gonzalez de Mejia, E., & Loarca-Piña, G. (2020). Consumption of a baked corn and bean snack reduced chronic colitis inflammation in CD-1 mice via downregulation of IL-1 receptor, TLR, and TNF-α associated pathways. Food Research International, 132(C), 109097. https://doi.org/10.1016/j.foodres.2020.109097

Maron, D. M., & Ames, B. N. (1983). Revised methods for the Salmonella mutagenicity test. Mutation Research/Environmental Mutagenesis and Related Subjects, 113(3–4), 173–215. https://doi.org/10.1016/0165-1161(83)90010-9

Mimura, T., Maeda, K., Tsujibo, H., Satake, M., & Fujita, T. (1982). Studies on biological activities of melanin from marine animals. II. Purification of melanin from *Octopus vulgaris*Cuvier and its inhibitory activity on gastric juice secretion in rats. Chemical and Pharmaceutical Bulletin, 30(4), 1508–1512. https://doi.org/10.1248/cpb.30.1508

Momtazi-Borojeni, A. A., Behbahani, M., & Sadeghi-Aliabadi, H. (2013). Antiproliferative activity and apoptosis induction of crude extract and fractions of Avicennia marina. Iranian Journal of Basic Medical Sciences, 16(11), 1203–1208. Retrieved from http://www.ncbi.nlm.nih.gov/pubmed/24494074

Morais, C., Pat, B., Gobe, G., Johnson, D. W., & Healy, H. (2006). Pyrrolidine dithiocarbamate exerts anti-proliferative and pro-apoptotic effects in renal cell carcinoma cell lines. Nephrology Dialysis Transplantation, 21(12), 3377–3388. https://doi.org/10.1093/ndt/gfl543

Nair, J. R., Pillai, D., Joseph, S. M., Gomathi, P., Senan, P. V, & Sherief, P. M. (2011). Cephalopod research and bioactive substances. Indian Journal of Geo-Marine Sciences, 40(February), 13–27.

Nayak, M. K., Seo, J., Park, S., & Park, S. Y. (2007). Colorimetric and highly selective “turn-on” fluorescent anion chemosensors with excited state proton transfer. Journal of Photochemistry and Photobiology A: Chemistry, 191(2–3), 228–232. https://doi.org/10.1016/j.jphotochem.2007.04.028

Nenadis, N., Wang, L.-F. F., Tsimidou, M., & Zhang, H.-Y. Y. (2004). Estimation of scavenging activity of phenolic compounds using the ABTS • + assay. Journal of Agricultural and Food Chemistry, 52(15), 4669–4674. https://doi.org/10.1021/jf0400056

Pavia, D. L., & Lampman, G. M. (2009). Introduction to spectroscopy. In Spectroscopy. https://doi.org/10.1887/0750303468/b293c1

Reich, H. J. (2020). NMR chemical shifts of compounds. Retrieved October 17, 2020 from https://www.chem.wisc.edu/areas/reich/nmr/index.htm

Rubaie, Z. M., Idris, M. H., Kamal, A. H. M., & King, W. S. (2012). Diversity of cephalopod from selected division of Sarawak, Malaysia. International Journal on Advanced Science, Engineering and Information Technology, 2(4), 279. https://doi.org/10.18517/ijaseit.2.4.203

Saleem, M. Z., Nisar, M. A., Alshwmi, M., Din, S. R. U., Gamallat, Y., Khan, M., & Ma, T. (2020). Brevilin a inhibits STAT3 signaling and induces ros-dependent apoptosis, mitochondrial stress and endoplasmic reticulum stress in MCF-7 breast cancer cells. OncoTargets and Therapy, 13, 435–450. https://doi.org/10.2147/OTT.S228702

Sansook, S., Lineham, E., Hassell-Hart, S., Tizzard, G. J., Coles, S. J., Spencer, J., & Morley, S. J. (2018). Probing the anticancer action of novel ferrocene analogues of MNK inhibitors. Molecules, 23(9), 2126. https://doi.org/10.3390/molecules23092126

Seeram, N. P., Adams, L. S., Zhang, Y., Lee, R., Sand, D., Scheuller, H. S., & Heber, D. (2006). Blackberry, black raspberry, blueberry, cranberry, red raspberry, and strawberry extracts inhibit growth and stimulate apoptosis of human cancer cells *in vitro*. Journal of Agricultural and Food Chemistry, 54(25), 9329–9339. https://doi.org/10.1021/jf061750g

Senan, P. V, Sherief, P. M., & Nair, J. R. (2013). Anticancer properties of purified fraction C2 of cuttlefish (Sepia pharaonis) ink on cervical cancer cells. Indo American Journal of Pharmaceutical Research, 3(9), 7444–77454.

Shinde, P., Banerjee, P., & Mandhare, A. (2019, April). Marine natural products as source of new drugs: a patent review (2015–2018). Expert Opinion on Therapeutic Patents, Vol. 29, pp. 283–309. https://doi.org/10.1080/13543776.2019.1598972

Skjøth, I., & Issinger, O.-G. (2006). Profiling of signaling molecules in four different human prostate carcinoma cell lines before and after induction of apoptosis. International Journal of Oncology, 28, 217–229. https://doi.org/10.3892/ijo.28.1.217

Stecca, B., & Rovida, E. (2019). Impact of ERK5 on the hallmarks of cancer. International Journal of Molecular Sciences, 20(6), 1426. https://doi.org/10.3390/ijms20061426

Trott, O., & Olson, A. A. J. A. (2010). Autodock vina: improving the speed and accuracy of docking. Journal of Computational Chemistry, 31(2), 455–461. https://doi.org/10.1002/jcc.21334.AutoDock

Uhlen, M., Fagerberg, L., Hallstrom, B. M., Lindskog, C., Oksvold, P., Mardinoglu, A., … Ponten, F. (2015). Tissue-based map of the human proteome. Science, 347(6220), 1260419–1260419. https://doi.org/10.1126/science.1260419

Van Vuuren, R. J., Botes, M., Jurgens, T., Joubert, A. M., & Van Den Bout, I. (2019). Novel sulphamoylated 2-methoxy estradiol derivatives inhibit breast cancer migration by disrupting microtubule turnover and organization. Cancer Cell International, 19(1). https://doi.org/10.1186/s12935-018-0719-4

Vate, N. K., & Benjakul, S. (2016). Effect of the mixtures of squid ink tyrosinase and tannic acid on properties of sardine surimi gel. Journal of Food Science and Technology, 53(1), 411–420. https://doi.org/10.1007/s13197-015-1974-1

Ventura, C., Núñez, M., Gaido, V., Pontillo, C., Miret, N., Randi, A., & Cocca, C. (2017). Hexachlorobenzene alters cell cycle by regulating p27-cyclin E-CDK2 and c-Src-p27 protein complexes. Toxicology Letters, 270, 72–79. https://doi.org/10.1016/j.toxlet.2017.02.013

Vizetto-Duarte, C., Branco, P. C., & Custódio, L. (2020). Marine natural products as a promising source of therapeutic compounds to target cancer stem cells. Current Medicinal Chemistry, 27. https://doi.org/10.2174/0929867327666200320155053

WHO. (2020). Cancer. Retrieved April 7, 2020, from https://www.who.int/health-topics/cancer#tab=tab_1

Wullschleger, S., Loewith, R., & Hall, M. N. (2006). TOR signaling in growth and metabolism. Cell, 124(3), 471–484. https://doi.org/10.1016/j.cell.2006.01.016

Zaharah, F. et al. (2017). Antioxidant and antimicrobial activities of squid ink powder. Food Research, 2(1), 82–88. https://doi.org/10.26656/fr.2017.2(1).225

Zhang, X., Cheng, X., Yu, L., Yang, J., Calvo, R., Patnaik, S., Hu, X., Gao, Q., Yang, M., Lawas, M., Delling, M., Marugan, J., Ferrer., M., & Xu, H. (2016). MCOLN1 is a ROS sensor in lysosomes that regulates autophagy. Nature Communications, 7(1), 12109. https://doi.org/10.1038/ncomms12109

Zhong, J.-P., Wang, G., Shang, J.-H., Pan, J.-Q., Li, K., Huang, Y., & Liu, H.-Z. (2009). Protective effects of squid ink extract towards hemopoietic injuries induced by cyclophosphamide. Marine Drugs, 7(1), 9–18. https://doi.org/10.3390/md7010009

PUBLICACIÓN 2

Bioactive compounds from *Octopus vulgaris* ink extracts exerted antiproliferative and anti-inflammatory effects *in vitro*

Martín S. Hernández-Zazueta, Iván Luzardo-Ocampo, Joel S. García-Romo, Luis Noguera-Artiaga, Ángel A. Carbonell-Barrachina, Pablo Taboada-Antelo, Rocío Campos-Vega, Ema Carina Rosas-Burgos, María G. Burboa-Zazueta, Josafat M. Ezquerra-Brauer, Armando Burgos-Hernández*

Food and Chemica Toicology. 2021. 151: 0278-6915. Doi: 10.1016/j.fct.2021.112119

PUBLICACIÓN 2: TRANSCRIPCIÓN LITERAL

Bioactive compounds from *Octopus vulgaris* ink extracts exerted anti-proliferative and anti-inflammatory effects *in vitro*.

Martín S. Hernández-Zazueta[1], Iván Luzardo-Ocampo[3], Joel S. García-Romo[1], Luis Noguera-Artiaga[4], Ángel A. Carbonell-Barrachina[4], Pablo Taboada-Antelo[5], Rocío Campos-Vega[2], Ema Carina Rosas-Burgos[1], María G. Burboa-Zazueta[6], Josafat M. Ezquerra-Brauer[1], Armando Burgos-Hernández[1]*

1 Departamento de Investigación y Posgrado en Alimentos, Universidad de Sonora, 1658 Hermosillo, Sonora, México.

2 Research and Graduate Program in Food Science, School of Chemistry, Universidad Autónoma de Querétaro, 76010 Querétaro, Qro., Mexico.

3 Instituto de Neurobiología, Universidad Nacional Autónoma de México, 76230, Juriquilla, Qro., Mexico.

4 Escuela Politécnica Superior de Orihuela, Universidad Miguel Hernández de Elche, 03312 Alicante, España.

5 Departamento de Física Aplicada, Universidad de Santiago de Compostela, 15782 Santiago de Compostela, España.

6 Departamento de Medicina y Ciencias de la Salud, Universidad de Sonora, 83000 Hermosillo, Sonora, México.

*Corresponding author at: Departamento de Investigación y Posgrado en Alimentos, Universidad de Sonora, Apartado Postal 1658, 83000 Hermosillo, Sonora, México. Tel.: +526-622-592-208; Fax: +526-622-592-209. E-mail address: armando.burgos@unison.mx

Abbreviations: AGE-RAGE: Advanced glycation end-products receptor for AGE; AMC: Analysis of major components; BCA: Bicinchoninic acid; DAPI: 4'6'-diamidino-2-phenylindole-tetramethylrhodamine B isothiocyanate; DM: Dichloromethane extract from *Octopus vulgaris*ink; DM-F1, F2, F3: Fraction 1, 2, 3 from DM extract; DMEM:

Dulbecco's modified eagle medium; EA: Ethyl acetate extract from *O. vulgaris* ink; FA: Fatty acid; FBS: Fetal bovine serum; FcƐR1: FCƐ receptor 1; FDR: False discovery rate; FITC: Fluorescein isothiocyanate; GC-MS: Gas-chromatography; KEGG: Kyoto Encyclopedia of Genes and Genomes; H2DCFDA: 2',7'-dichlorodihydrofluorescein diacetate; HDFs: Human dermal fibroblasts; HX: Hexane extract from *O. vulgaris* ink; IBD: Inflammatory bowel disease; IC50: Half inhibitory concentration; iNOS: Inducible nitric oxide synthase; JAK-STAT: Janus kinase-signal transducer and activator of transcription; LC-ESI-Q: Liquid chromatography coupled to quantitative electrospray ionization; LPS: Lipopolysaccharides from Escherichia coli O111:B4; MDA: Malonaldehyde; MIC_{80}: 80 % minimal inhibitory concentration; MS: mass spectrometry analysis; MTT: 3-(4,5-dimethylthiazol-2-yl)-2,5-diphenyltetrazolium bromide; ND: Non-detected; NF-kB: Nuclear factor kB; PBMCs: Peripheral blood mononuclear cells; PI3K: Phosphatidylinositol-3-kinase pathway; PLS-DA: Partial least-squares discriminant analysis; RFU: Relative fluorescence units; RI (exp.): Experimental retention index; RI (rep.): Reported retention index; ROS: Reactive oxygen species; RT: Room temperature (25 ± 1 ºC); SDS: Sodium dodecyl sulfate; sICAM-1: Soluble forms of intercellular adhesion molecule 1; SOD: Superoxide dismutase; TH: T-helper cells; TLC: Thin-layer chromatography; TLP: Thin-layer plate; TRAIL: TNF-related apoptosis-inducing signal; VIP: Variable Importance in Projection; WE: Water extract from *O. vulgaris* ink.

Keywords: Octopus (*Octopus vulgaris*); anti-proliferative effect; cytokine modulation; colorrectal cancer; ink; metabolomic analysis.

1. Introduction

Cancers were responsible for more than 18 million dead worldwide, being lung (11.58 %), breast (11.55 %), colorectal (10.23 %), prostate (7.06 %), and stomach (5.72 %) cancers the most common conditions (IARC, 2018). Approximately 25 % of all cancers are associated to inflammatory processes, and an estimated 15 % of cancer deaths are associated with them (Allavena et al., 2008; Coussens and Werb, 2002). Within cancer processes, pro-inflammatory molecules, such as cytokines and chemokines, inducible nitric oxide synthase (iNOS), reactive oxygen species (ROS), and nuclear factor-kappa B (NF-kkB) are upregulated (Sarkar and Fisher, 2006). The systemic inflammatory response is associated with an adverse outcome, but intense immune cell infiltration has

been linked to improved survival due to the recognition of transformed malignant cells and restriction of tumor growth (Tuomisto et al., 2019).

The conventional treatments such as chemotherapy and radiotherapy have been extensively used in the majority of cases with locally advanced or systemic metastasis, with no major improvements in their prognosis (Sun et al., 2020). In the case of chemotherapy, the drugs used act blocking specific points of the cell cycle, affecting both active mitotic cancer cells and the proliferation of normal non-cancerous-fast growing cells (bone marrow, hair follicles, or cells from the digestive system), resulting in side effects (Mitchison, 2012). The development of cancer is highly associated with risk factors such as lifestyle choices and the diet (Mysuru Shivanna and Urooj, 2016). Therefore, targeting anti-inflammatory bioactive compounds from natural products has emerged as an integrative approach of the cancer condition (Ammendola et al., 2020). Secondary metabolites from the wide variety of marine fauna a flora could be a natural source of compounds with unlimited biological properties (Barzkar et al., 2019; Malve, 2016), some of them with beneficial effects over the treatment and prevention of cancer (Khalifa et al., 2019). Marine products have exhibited regulation of tumor autophagy via PI3K/Akt/mTOR, p53, and up-regulation of activated c-Jun N-terminal kinase (JNK) signaling (Wargasetia and Widodo, 2019). On the other hand, cephalopod ink has shown potential as an anticancer agent *in vitro* in several cancer lines, but its specificity on certain cancer cells has not been fully explored (Fahmy and Soliman, 2013; Naraoka et al., 2000). Even more, few reports have assessed the anti-inflammatory properties of the ink or its relationship with the development of cancer (Derby, 2014). However, there are reports regarding the antimicrobial potential of peptides (OctoPartenopin) from *O. vulgaris*' suckers, evidenced in the inhibition of known microorganisms such as *S. aureus, P. aeruginosa,* and *C. albicans* (Maselli et al., 2020) and the antimicrobial activity of specific cell types like hemocytes, also exhibiting high inhibition activity against *B. cereus, L. monocytogenes,* and *S. aureus,* among other bacterial strains (Troncone et al., 2015).

Our research group previously reported the antioxidant, antimutagenic, cytoprotective, anti-proliferative, and pro-apoptotic effects in selected human cancer cell lines (A549, HeLa, and 22Rv1), but no anti-inflammatory mechanisms nor their effects on colorectal cells was explored (Hernández-Zazueta et al., 2021). Thus, the present study aimed to evaluate the anti-proliferative and anti-inflammatory effect from *Octopus vulgaris*ink

extracts *in vitro* using selected human cancer cell lines (HCT116, HT-29, and MDA-MB-231), human peripheral blood mononuclear cells (PBMCs), and a murine cell line (RAW 264.7). Human retinal pigmented epithelial cells (ARPE-19) were used as a control for cytotoxicity based on previous research using these cells as healthy control (Lord et al., 2019; Weng et al., 2017).

2. Materials and methods

2.1. Preparation of *O. vulgaris* ink extracts and fractions

The ink from *O. vulgaris* sacs was extracted as reported by Ebada, Edrada, Lin, & Proksch (2008). Briefly, 1.30 Kg of octopus wastes was collected, from which 20 sacs were obtained as discard material from the octopus. For this, the collected animals were placed alive on an ice bed, anesthetized with sprayed $MgCl_2$, and killed by decapitation across the edge of the mantle. The mantle was then opened along the ventral surface, and the proximal end of the ink sac was taken from the tissue, whereas the duct end of the sac was cut with scissors, avoiding ink leakage (Madaras et al., 2010). The sacs were carefully washed with distilled water (Moustafa and Awaad, 2016), and the ink was removed. The animals' collection was carried out following the guidelines for humane handling, care, treatment, and transportation of animals from the Animal Welfare Act from the United States Department of Agriculture (USDA). The euthanization was conducted as indicated by the National Institute of Health (NIH) Guide for Care and Use of Laboratory Animals. This research was approved by the Bioethics Committee of the University of Sonora (CBI-UNISON 1/2017).

Afterwards, 15 mL of the ink were homogenized with HPLC-grade water (1:1 ratio), and freeze-dried (Labconco Corp., Kansas City, MO, US). Four extracts were prepared from the resulting freeze-dried mixture: water (WE), hexane (HX), ethyl acetate (EA), and dichloromethane (DM) extracts. Since the DM extracts exhibited the highest anti-proliferative potential after the initial screening with the cancel cells, purified DM fractions were generated. For this, the DM extract was dissolved in ethyl acetate and fractioned in silica gel columns (3.5 cm × 60 cm, 60-120 mesh silica gel, Sigma-Aldrich). The elution was conducted using hexane: ethyl acetate (99:1) as a mobile phase, producing 25 mL-fractions that were collected. A total of 38 fractions were obtained, and those with similar contents (monitored by thin-layer chromatography, TLC) were mixed to obtain the F1, F2, and F3 fractions from DM. For the semipreparative TLC DM fractions were applied onto a silica (F_{254}, 0.040-0.043 mm, Merck, Kenilworth, NJ, US)

pre-coated TLC plate and developed under a 95:5 hexane:ethyl acetate (v/v) mobile phase (Liu et al., 2008). The TLC plate was UV-monitored to determine the composition of the eluted fractions. The fractions were evaporated under vacuum and dried with nitrogen.

2.2. Analysis of volatile compounds of DM and DM-F2 extracts by gas chromatography/mass spectrometry (GC-MS)

The analysis of volatile compounds of the bioactive fraction DM and DM-F2 was determined by gas chromatography coupled to mass spectrometry (GC-MS) (Noguera-Artiaga et al., 2019) using a Shimadzu GC-17A coupled by a Shimadzu QP-5050 mass detector system (Shimadzu Corporation, Kyoto, Japan). The GC-MS was equipped with an SLB-5ms Capillary GC Column (30 m × 0.25 mm, 0.25 μm, Supelco Inc, Sigma-Aldrich). Helium was used as carrier gas at a flow rate of 0.6 mL/min in a splitless mode. The oven temperature started at 80 °C and, after 5 min of stabilization, was increased by 2 °C/min up to 220 °C. After 5 min of stabilization, the temperature was increased by 25 °C/min up to 300 °C, and it was held for 1.80 min. Detector and injector temperatures were 300 and 230 °C, respectively. The compounds were identified using 3 analytical methods: retention indexes, GC-MS retention indexes, and mass spectra (NIST05 and WILEY229 spectral libraries' collection). The identification was considered tentative when it was based on only mass spectral data. Results were expressed as a percentage of the total area represented by each one of the compounds.

2.3. Untargeted metabolomic analysis

A global and untargeted metabolomic analysis was conducted for the identified metabolites from DM and DM-F2 using GC-MS. (Gertsman and Barshop, 2018) All data were normalized using the MetaboAnalyst 3.0 software. Analysis of major components (AMC) was used to observe the patterns of metabolites from each sample. A partial least square discriminant analysis (PLS-DA) was used to rank each metabolite from the samples according to the number of components and variables of each model (Lê Cao et al., 2011). The variable importance in projection (VIP) scores was obtained for classifying the importance of each metabolite based on its discrimination rule of importance (VIP ≥ 2) (RoyChoudhury et al., 2017).

2.4. Cell culture

The human colorectal carcinoma HCT116 (ATCC® CCL-247™), colorectal adenocarcinoma HT-29 (ATCC® HTB-28™), mammary gland/breast adenocarcinoma

MDA-MB-231 (ATCC® HTB-26™) and murine macrophages RAW 264.7 (ATCC® TIB-71™) were acquired from American Type Culture Collection (Manassas, VA, US.). The cells were cultured under proper conditions (37 ºC, humidified 5 % CO_2 atmosphere) as indicated by the manufacturer.

2.5. MTT Assay

The Cell Proliferation Kit I [3-(4,5-dimethylthiazol-2-yl)-2,5-diphenyltetrazolium bromide, MTT] Colorimetric assay (ROCHE, Basel, Switzerland) was used to evaluate the anti-proliferative effect of the extracts obtained of octopus's ink. The cells (1×10^4 cells/well) were seeded in 96-well plates for 24 h. After medium removal, DMSO-dissolved extracts and diluted in 10 % fetal bovine serum-Dulbecco's modified eagle medium (DMEM) (Sigma-Aldrich, St. Louis, MO, US) were added to wells (100 µL) at various concentrations (25, 50, 100, 200 µg/ml) and incubated (48 h, 37 ºC). Before the last 24 h of the cell culture, 10 µL of MTT stock solution was added to each well, and after 4 h was added 100 µL of sodium dodecyl sulfate (SDS) solution. After 12 h incubation, plates were read at 570 nm and a reference wavelength of 650 nm. Results were adjusted to a mathematical-biological model provided by NCSS statistical package and were expressed as half lethal concentration (LC_{50}) (µg/mL). These values were calculated for cancer cells, RAW 264.7, and ARPE-19 cells.

2.6. Fluorescence staining for DNA and cell membrane by DAPI and phalloidin

Structural and morphological changes in HCT116 cells, derived from the presence of DM-F2, was evaluated using the phalloidin and 4',6'-diamidino-2-phenylindole-tetramethylrhodamine B isothiocyanate (DAPI) dilactate staining (Van Vuuren, Botes, Jurgens, Joubert, & Van Den Bout, 2019). Briefly, HCT116 cells (1×10^4 cells/well) were seeded in 96-wells microtitration plates (24 h). After incubation, cells were treated with the DM-F2 extract (LC_{50}: 52.64 µg/mL) for 48 h. Cells were then fixed with 3.7 % formaldehyde in PBS and permeabilized with 0.2 % Triton X-100 in PBS for 15 min. Afterward, cells were stained either with phalloidin (Sigma-Aldrich) or DAPI (Sigma-Aldrich) in order to visualize F-actin or the nuclear material through DNA, respectively. The microtitration plates were mounted and visualized on an inverted epifluorescence microscope (Leica DMi8, Leica Microsystems, Wetzlar, Germany).

2.7. Measurement of nitrites production

RAW 264.7 cells (2.5×10^4 cells/well) were seeded in 96-wells microtitration plates for 24 h. Then, the medium was removed, the cells were treated with LPS (1 µg/mL) and the

extracts (HX, EA, DM, WE, DM-F1, DM-F2, and DM-F3; 25-200 µg/mL) for 24 h. After incubation, 100 µL of the cell supernatants were mixed with 100 µL of Griess reagent [0.1% N-(1-naphthyl)-ethylenediamine and 1 % sulfanilamide in 5 % H_3PO_4] and incubated in the dark (10 min, RT: 25 ± 1 ºC). The total production of nitrite was calculated based on the absorbance at 540 nm measured in the sample using a microtitration plate absorbance reader and contrasted to a standard curve of $NaNO_2$; results were expressed as half inhibitory concentration (IC_{50}, µg/mL) using LPS-induced RAW 264.7 cells as the positive control, and untreated cells as the negative control. The IC_{50} values were calculated in the NCSS statistical software.

2.8. Measurement of intracellular reactive oxygen species (ROS) levels

Intracellular ROS levels were measured by the 2,7-dichlorodihydrofluorescein diacetate (H_2DCFDA) assay. RAW 264.7 (2×10^4 cells/well) were seeded in 96-wells microtitration plates and incubated (24 h). After a medium replacement step, cells were incubated either with lipopolysaccharides (LPS) from *E. coli* O111:B4 (Sigma-Aldrich) (1 µg/mL) dissolved in DMEM, or in the presence of a testing fraction (HX, EA, DM, WE, DM-F1, DM-F2, and DM-F3; 25-200 µg/mL) for 22 h. Then, cells were washed twice (PBS 100 µL, pH 7.4) and incubated with 5 µL of 20 µM 2',7'-dichlorodihydrofluorescein diacetate (H_2DCFDA, Thermo Fisher, Waltham, MA, US) in the darkness (30 min, room temperature: 25 ± 1 ºC). Fluorescence was measured at an excitation/emission wavelengths of 485/530 nm in a fluorescence plate reader. The results were expressed in IC_{50} (µg/mL).

2.9. Inflammatory Cytokines Array

The effect of DM-F2 in the modulation of cytokines associated to inflammatory processes was assessed using the Mouse Cytokine Antibody Array Panel A (ARY0016, R&D Systems, Minneapolis, MN, US). RAW 264.7 cells (1×10^6) were seeded in Petri dishes (60 mm) and allowed to grow and attach for 48 h. The cells were then treated either with LPS (1 µg / ml) of LPS+DM (IC_{50} NO: 87.33 µg/mL) in fetal bovine serum (FBS)-free medium for 24 h. After the treatments, the cells were lysed (Halt™ Protease Inhibitor, Thermo Fisher Scientific, Waltham, MA, US) for 30 min at 4 ºC, and protein concentration was measured by bicinchoninic acid (BCA) assay (Pierce™ BCA Protein Assay, Thermo Fisher Scientific) to standardize all the treatments. The protein lysates were then assayed in the kit, following the manufacturer's instructions. The results were

obtained using a ChemiDoc XRS+ cell imaging system (BioRad Corp, Hercules, CA, US). The relative cytokine expression against the control was visualized using the ImageQuant TL 8.1. software (General Electrics, GE Healthcare, Chicago, Illinois). The data were expressed as a fold change against the control (LPS-challenged RAW 264.7 cells). The protein network for an *in silico* analysis of the modulated cytokines was generated using the STRING® platform (von Mering et al., 2007) and edited in the Cytoscape® software. Data generated by the STRING analysis, including the enrichment Kyoto Encyclopedia of Genes and Genomes (KEGG) pathways and Enrichment Process, were normalized using the protein false discovery rate (FDR) values.

2.10. Analysis of IL-4 and NF-kB cell expression by flow cytometry

The impact of DM-F2 on the modulation of IL-4 and NF-kB was measured by flow cytometry using isolated mononuclear cells of human peripheral blood mononuclear cells (PBMCs) (Chávez-Sánchez et al., 2010). For this, PBMCs were isolated by a gradient of density using Ficoll-Paque PLUS (GE Healthcare), and the blood was diluted with PBS (1:2). Then, the top eluent was centrifuged (450 × g, 30 min) with Ficoll-Paque, and the cells were then placed in a sterile test tube, washed with 100 µL of PBS, re-suspended in the culture medium, and counted. Before applying treatments, the cells were examined before and after activation with LPS for 24 h. Then, the cells (1×10^6 cells/well) were treated either with LPS or DM-F2 and fluorescent markers for human IL-4 (Cat. 500806, BioLegend, San Diego, CA, US) and fluorescein isothiocyanate (FITC) anti-human IL-4 clone (MP4 25D2, BioLegend) were added. Nuclear factor-kB (NF-kB) was also evaluated after a 15 mM pre-treatment of cells with NF-kB antibody (Cat. B5681, Sigma-Aldrich) for 30 min. Fluorescence expressed in relative fluorescence units (RFU) was measured in a BD FACSVerse^{TM} flow cytometer (BD Biosciences, NY, US) after 10000 events analyzed.

2.11. *In silico* evaluation of interactions between DM metabolites and cytokines

The 3D structures of selected ligands for the *in silico* interaction were downloaded from PubChem database: 4-methylcaprolactam (PubChem CID: 19242), myristic acid (PubChem CID: 11005), hexadecanoic acid (PubChem CID: 985), hexadecanal (PubChem CID: 984), heptadecanal (PubChem CID: 71552), and octadecanal (PubChem CID: 12553). For the protein receptors, 3D structures of NF-kB (1LE5) and IL-2 (4YUE) were downloaded from the Protein databank. The other proteins (IL-1α, IL-1β, IL-3, IL-

4, IL-7, IL-16, CCL17, and IL-27) were modeled in SwissModel based on their FASTA sequences from Uniprot® (P01582, P10749, Q5SX77, P07750, Q544C8, O54824, F6R5P4, and Q8K3I6, respectively). The best 3D structure based on their identity percentage was selected (**Supplementary Table S1**). The docking procedure done by Luna-Vital, Weiss, & Gonzalez de Mejia (2017) was followed. The best binding sites were predicted in MetaPocket 2.0 online utility (Zhang, Li, Lin, Schroeder, & Huang, 2011), and the docking calculations were conducted in AutoDock tools (Trott and Olson, 2010). The best docking conformation were graphed in Discovery Studio Visualizer v. 19.1.0.18287 software (Dassault Systèmes, Vélizy-Villacoublay, France).

2.12. Statistical Analysis

Unless indicated, all data were expressed as the means ± SD of three independent experiments in triplicates. An analysis of variance (ANOVA) was conducted, followed by a *post-hoc* Tukey-Kramer's test ($p<0.05$). All the analyses were done using the SPSS Statistics software.

3. Results

3.1. Anti-proliferative effect of *O. vulgaris* ink extracts and DM-fractions on cancer cells lines

Among the octopus ink extracts, DM exhibited the highest anti-proliferative activity in colorectal adenocarcinoma cell lines (HT-29 and HCT116) (**Table 1**) but did not show an inhibitory effect under 100 µg/ml in human breast adenocarcinoma cell line (MDA-MB-231). Since DM displayed the best biological effect on the HCT116 cell line, fractions were isolated (DM-F1, DM-F2, and DM-F3) and evaluated on the same cell line. None of the fractions were cytotoxic on the ARPE-19 cell line (LC_{50} > 200 µg/mL), but only the DM-F2 fraction exhibited a remarkable anti-proliferative effect, showing a lower ($p<0.05$) LC_{50} than DM (19.72 ± 0.18 % lower). Both cisplatin and docetaxel were used as positive controls of anti-proliferative effect. Considering that the DM extract showed its highest anti-proliferative effect on HCT116 cells, its fractions were only assayed against such cell line.

Table 1. Anti-proliferative potential of *O. vulgaris* ink extracts, dichloromethane soluble fractions (DM-F1, DM-F2, and DM-F3), and drug controls on human cell lines at 48 h of incubation.

Extracts	Non-cancerous cell (LC_{50}, µg/ml)	Cancerous cells (LC_{50}, µg/ml)		
	ARPE-19	HCT116	MDA-MB-231	HT-29
HX	> 200 ^{Aa}	> 200 ^{Aa}	> 200 ^{Aa}	> 200 ^{Aa}
EA	> 200 ^{Aa}	75.7 ± 4.8 ^{Cb}	143.6 ± 4.6 ^{Bb}	85.6 ± 3.5 ^{Cc}
DM	192.7 ± 20.8 ^{Aa}	65.6 ± 3.9 ^{Db}	108.6 ± 5.1 ^{Bc}	81.6 ± 5.0 ^{Cc}
WE	> 200 ^{Aa}	> 200 ^{Aa}	> 200 ^{Aa}	> 200 ^{Aa}
DM-F1	> 100 ^{Bd}	> 200 ^{Aa}	-	-
DM-F2	> 100 ^{Ad}	52.6 ± 3.0 ^{Bc}	-	-
DM-F3	> 100 ^{Bd}	> 200 ^{Aa}	-	-
Cisplatin	137.9 ± 6.5 ^{Bb}	7.4 ± 0.7 ^{De}	152.1 ± 4.7 ^{Ab}	103.9 ± 0.6 ^{Cb}
Docetaxel	110.3 ± 4.5 ^{Ac}	11.0 ± 2.5 ^{Bd}	9.0 ± 1.3 ^{Bd}	2.4 ± 0.0 ^{Cd}

The values are expressed as the means ± from three different experiments, in triplicates. Different lower-case letters by columns indicate significant differences ($p<0.05$) between treatments, for each cell line, by Tukey-Kramer's test. Different upper-case letters by row are significantly different ($p<0.05$), between cell lines and for each treatment, by Tukey-Kramer's test. **DM:** Dichloromethane extract; **DM-F1, F2, F3:** Purified fractions from the DM extract; **EA:** Ethyl acetate extract; **HX:** Hexane extract; **WE:** Water extract.

3.2. Impact of DM-F2 extract on the morphological changes on HCT116 cells by DAPI and phalloidin staining

Compared to the negative control (untreated HCT116 cells), the 4 h exposition to DM-F2 induced morphological changes associated to cell death, such as the appearance of surface protrusions and membrane blebs, reduced pseudopods, and increased nuclear segmentation in HCT116 cells (**Fig. 1**).

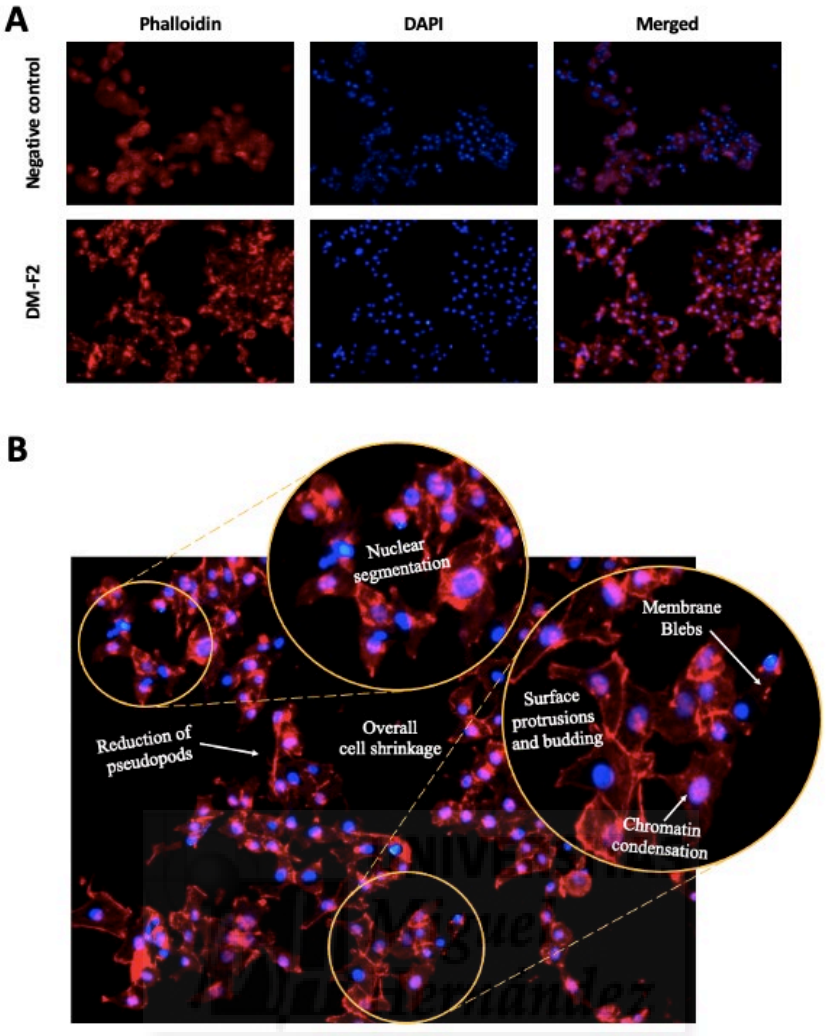

Fig. 1. (A) Effect of DM-F2 on the morphology of HCT116 cells after staining with DAPI and phalloidin; **(B)** Morphological changes associated to apoptotic cell death.

DAPI: 4'6-diadimino-2-phenylindole dilactate; **DM-F2:** Fraction 2 from dichloromethane extract (DM) of *O. vulgaris* ink.

3.3. Effect of *O. vulgaris* ink extracts on the cell viability, nitrites, and intracellular reactive oxygen species (ROS) inhibition on RAW 264.7 macrophages.

RAW 264.7 cells were treated with various concentrations of the *O. vulgaris* extracts and DM soluble fractions for 24 h and the cell viability was determined by the metabolic reduction of tetrazolium salt to a formazan dye (MTT assay) (**Table 2**). Except for EA, none of the extracts were cytotoxic (LC_{50} > 100 µg/mL). DM, DM-F2, and EA exhibited the lowest IC_{50} values for the inhibition of nitrites and ROS production. DM-F1, DM-F2, HX, and WE did not exhibit inhibitory potential against the same parameters. Outstandingly, DM-F2 IC_{50} values for the inhibition of nitrites and ROS production was significantly ($p<0.05$) lower than DM (51.72 ±

1.07 and 23.67 ± 6.22 % lower, respectively). Since DM-F2 was not cytotoxic, reductions of NO and ROS are linked to anti-inflammatory mechanisms rather than reductions in the cell viability.

Table 2. Effect of *O. vulgaris* ink extracts and dichloromethane soluble fractions on the production of nitrites, reactive oxygen species production (ROS), and cell viability of RAW 264.7 cells.

Extracts	RAW 264.7 (µg/ml)		
	IC_{50} Nitrites	IC_{50} ROS	LC_{50} Cell viability
HX	195.0 ± 5.8 [a]	> 200 [a]	> 200 [a]
EA	47.8 ± 4.7 [d]	52.8 ± 4.7 [d]	67.7 ± 4.7 [c]
DM	61.9 ± 4.5 [c]	87.3 ± 1.9 [c]	100.9 ± 4.4 [b]
WE	> 200 [a]	> 200 [a]	> 200 [a]
DM-F1	> 200 [b]	> 200 [b]	> 200 [b]
DM-F2	29.9 ± 2.8 [e]	66.7 ± 6.9 [d]	> 200 [b]
DM-F3	> 200 [b]	> 200 [b]	> 200 [b]

The values are expressed as the means ± from three different experiments, in triplicates. Different letters within columns indicate significant differences ($p<0.05$) by Tukey-Kramer's test. Cells were exposed to 24 h-treatment. **DM:** Dichloromethane extract; **DM-F1, DM-F2, DM-F3:** DM fractions; **EA:** Ethyl acetate extract; **HX:** Hexane extract; **ROS:** Intracellular reactive oxygen species; **WE:** Water extract.

3.4. Untargeted metabolomic analysis of volatile compounds from DM and DM-F2

For the untargeted metabolomic analysis of the most biologically active components of the extracts (DM and DM-F2) (**Fig. 2**), the generated heatmap (**Fig. 2A**) clustered the samples into two different groups, being hexadecanoic acid, myristic acid, and 1-tetradecanol the most abundant compounds in the DM extract, while octadecanol, 1-(15-methyl-1-oxohexadecyl) pyrrolidine, and 9-octadecenamide were the most abundant compounds in the DM-F2 extract.

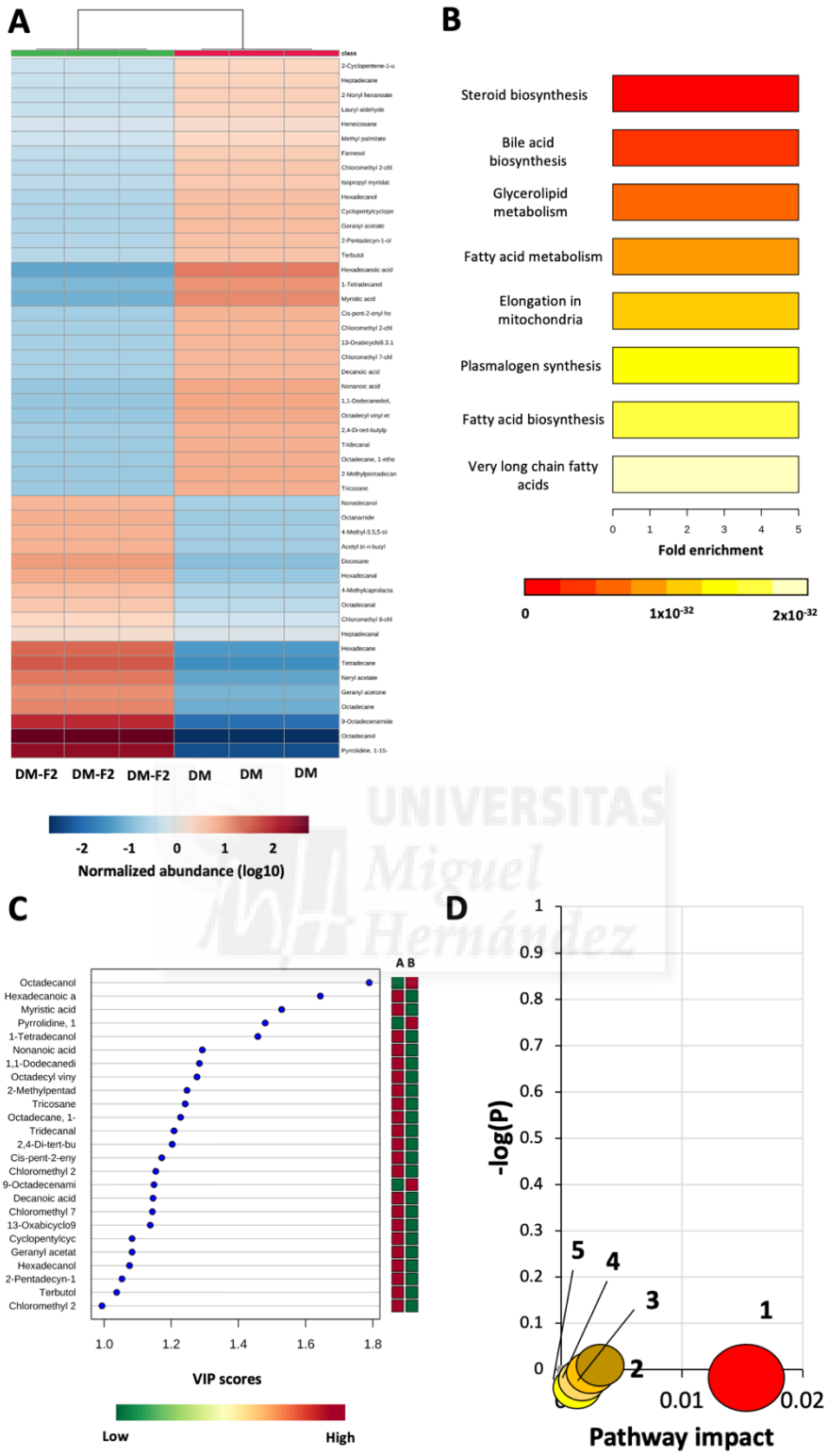

Figure 2. Untargeted metabolomic analysis of DM and DM-F2 extracts. **(A)** Heatmap clustering for the identified volatile compounds from DM and DM-F2; **(B)** Enrichment pathways analysis; **(C)** VIP scores from the partial least squares (PLS) analysis; **(D)** Pathways impact from the metabolomic arrangement of compounds.

For Fig. 2C, A: DM and B: DM-F2. For Fig. 2D, **1:** Fatty acid biosynthesis; **2:** fatty acid elongation; **3:** fatty acid degradation; **4:** N-glycan biosynthesis; **5:** biosynthesis of unsaturated fatty acids.

The predicted involvement of these compounds in selected metabolic pathways from the KEGG database (**Figure 2B**) showed that most of them are related to very long-chain fatty acids, fatty acids biosynthesis, plasmalogen synthesis, and elongation in mitochondria pathways. The analysis of variable in importance (VIP) scores for all the identified compounds by GC-MS (**Figure 2C**) from DM (A) and DM-F2 (B) highlighted octadecanol, hexadecanoic acid, myristic acid, and 1-(15-methyl-1-oxohexadecyl) pyrrolidine as the compounds with the highest VIP values (~1.4-1.8). Enrichment analysis of the compounds for the predictive involvement in potential metabolic pathways associated all of them to fatty acids pathways such as the biosynthesis of unsaturated fatty acids, N-glycan biosynthesis, fatty acid degradation, and fatty acid elongation (**Figure 2D**). The metabolomic analysis was conducted based on the identified metabolites from DM (**Supplementary Table S1**) and DM-F2 (**Supplementary Table S2**).

3.5. Effect of DM-F2 on the modulation of cytokines produced by RAW 264.7

Out of 40 cytokines, 8 were differentially up-regulated (>1.5 fold) (CCL17, IL-16, IL-7, IL-4, IL-3, IL-1β, IL-1α, and G-CSF) (**Fig. 3A**). The functional relationship of these cytokines based on fusion evidence, neighborhood evidence, and the existing databases after the bioinformatics analysis (STRING®) (**Fig. 3B**) indicated that most cytokines are involved in the cytokine-cytokine receptor interaction, inflammatory bowel disease (IBD), the Janus kinase-signal transducer and activator of transcription (JAK-STAT) pathway, maturation and differentiation of immune cells, IL-17, and the phosphatidylinositol-3-kinase (PI3K/Akt) pathway (**Fig. 3C**). As a result of this involvement, the modulated cytokines suggest the capability of octopus ink to target the regulation of signaling receptor activity, response to stimulus, the immune response, and cytokine production (**Fig. 3D**). Outstandingly, the DM-F2 extract increased the expression of the anti-inflammatory cytokine IL-4 and decreased the expression of the nuclear factor kB (%) on PBMCs (52.61 ± 0.10 % and -54.47 ± 2.75 %, respectively) **(Fig. 3E**).

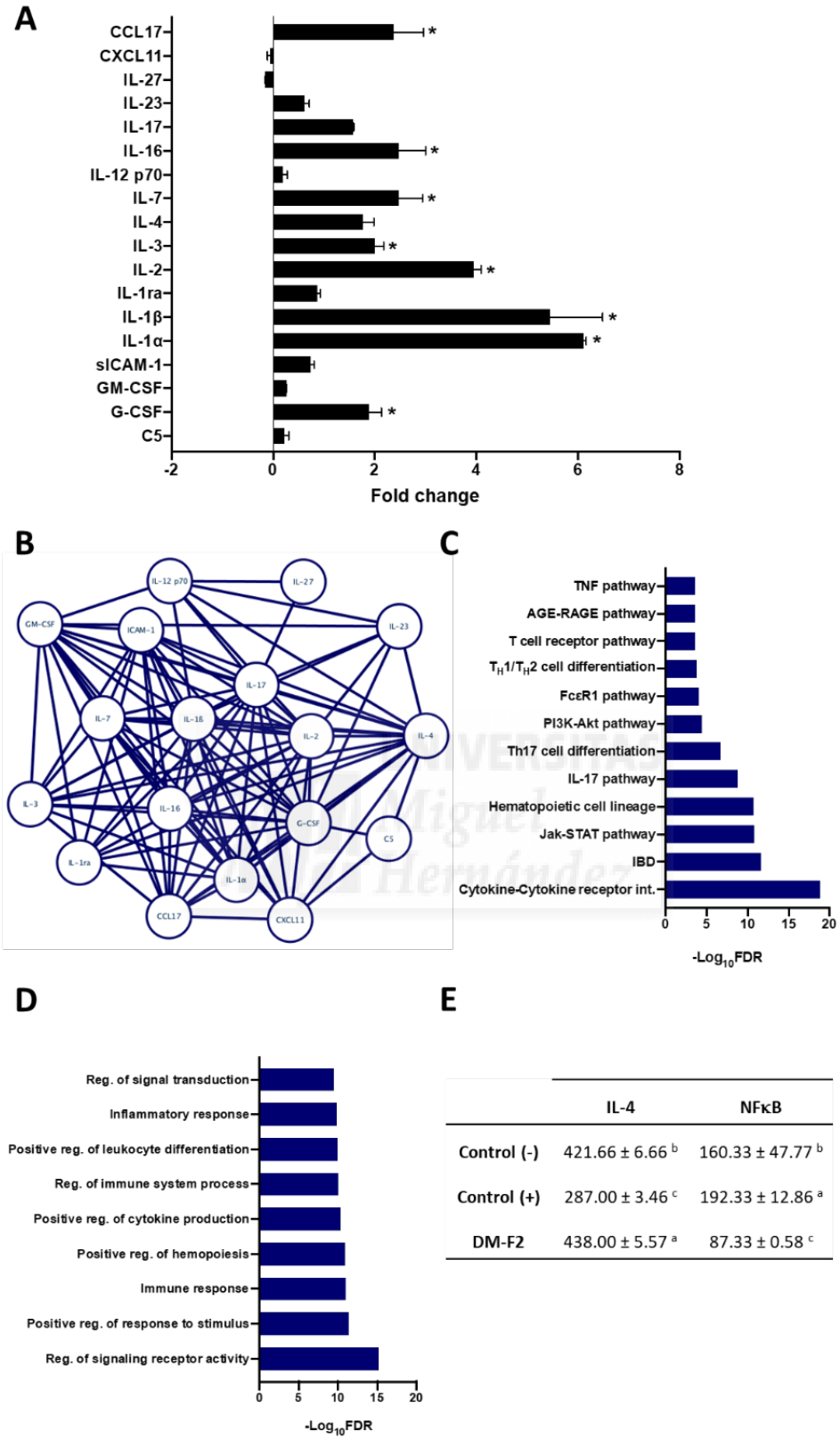

	IL-4	NFκB
Control (-)	421.66 ± 6.66 [b]	160.33 ± 47.77 [b]
Control (+)	287.00 ± 3.46 [c]	192.33 ± 12.86 [a]
DM-F2	438.00 ± 5.57 [a]	87.33 ± 0.58 [c]

Figure 3. Expression and association of cytokines involved in the inflammatory process mediated by the DM-F2 on LPS-stimulated RAW 264.7 macrophages and PBMCs. **(A)** Effect of DM-F2 on cytokine expression; **(B)** Functional associations of cytokines; **(C)** KEGG pathways associated with the differentially expressed cytokines; **(D)** Biological processes related to the modulation of

the cytokines; **(E)** Regulation of anti-inflammatory (IL-4) and pro-inflammatory cytokines (NF-kB) analyzed by flow cytometry on PBMCs cells.

The cytokines data (Fig. 3A) are expressed as fold change relative to negative control (LPS-stimulated RAW 264.7) and corresponded to the average of two independent experiments. Asterisks (*) corresponded to significant fold-change. Lines in the cytokines network (Fig. 3B) represent the proteins cytokines interaction. Values from flow cytometry analysis are the means ± SD of three independent experiments in triplicates (Fig. 3E). Different letters indicate significant differences ($p<0.05$) by Tukey-Kramer's least significant difference test. The negative control corresponded to untreated PBMCs, while the positive control are LPS-stimulated PBMCs cells (LPS: 1 μg/mL). **AGE-RAGE:** Advanced glycation end-products-Receptor for AGE; **DM-F2:** Fraction 2 from dichloromethane extract; **FDR:** False discovery rate; **T_H:** T-helper cells; **Fcε R1:** FCε receptor 1; **sICAM-1:** Soluble forms of intercellular adhesion molecule 1; **GM-CSF:** Granulocyte-macrophage colony-stimulator factor; **G-CSF:** Granulocyte colony-stimulator factor; **JAK-STAT:** Janus kinase-signal transducer and activator of transcription; **IBD:** Inflammatory bowel disease; **PI3K-Akt:** Phosphatidylinositol-3-kinase.

3.6. *In silico* interactions of DM compounds and cytokines

Conventional hydrogen bond and pi-alkyl bonding interactions were shared among all the interactions, but the highest affinity was found for IL-1α (**Fig 4A**) (-5.6 kcal/mol, **Table S1**), while the lowest was IL-1β (**Fig. 4B**) (-4.1 kcal/mol, **Table S1**).

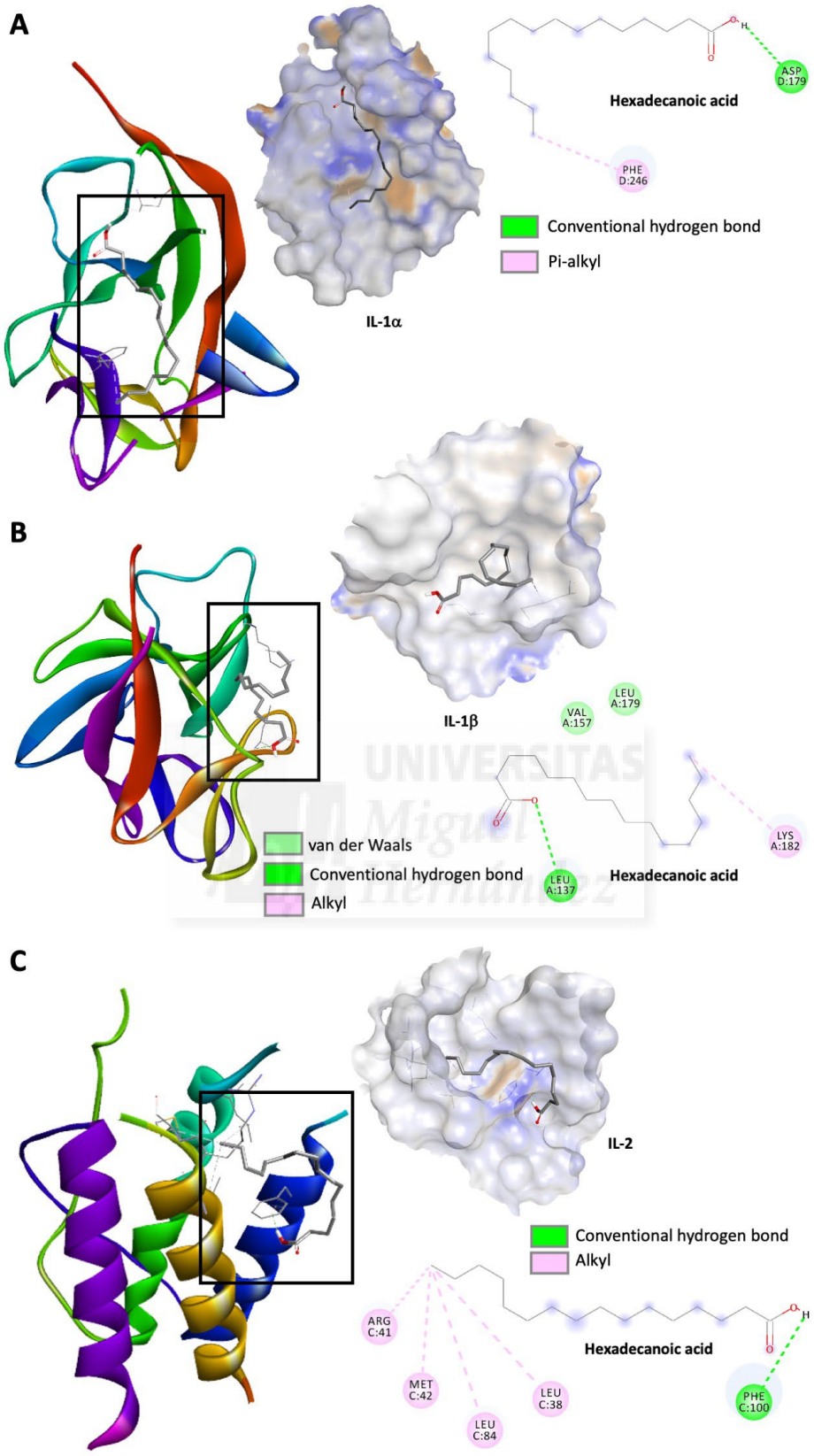

Figure 4. Best *in silico* interactions between hexadecanoic acid and selected proteins modulated by DM extract: **(A)** IL-1α, **(B)** IL-1β, and **(C)** IL-2.

The results show the best docking poses between each selected protein and hexadecanoic acid as indicated by AutoDock Vina. Images were generated with BioVia Discovery software.

Unlike the interactions shown in **Figure 4,** a higher diversity of bonding interactions was found between the selected proteins such as pi-sigma (**Figure 5A**) and carbon-hydrogen bond (**Figure 5B**), but alkyl and pi-alkyl were common among the three depicted interactions. As shown in **Table S1,** interactions with IL-1α were those with the highest binding affinity (-5.8 kcal/mol) and IL-2 the lowest (-4.6 kcal/mol).

The affinity interactions from hexadecanoic acid and 1-(15-methyl-oxohexadecyl) were selected since it exhibits the highest binding affinity energy (**Table S1**) among all the assayed compounds, which were considered from the VIP scores analysis (**Figure 2C**).

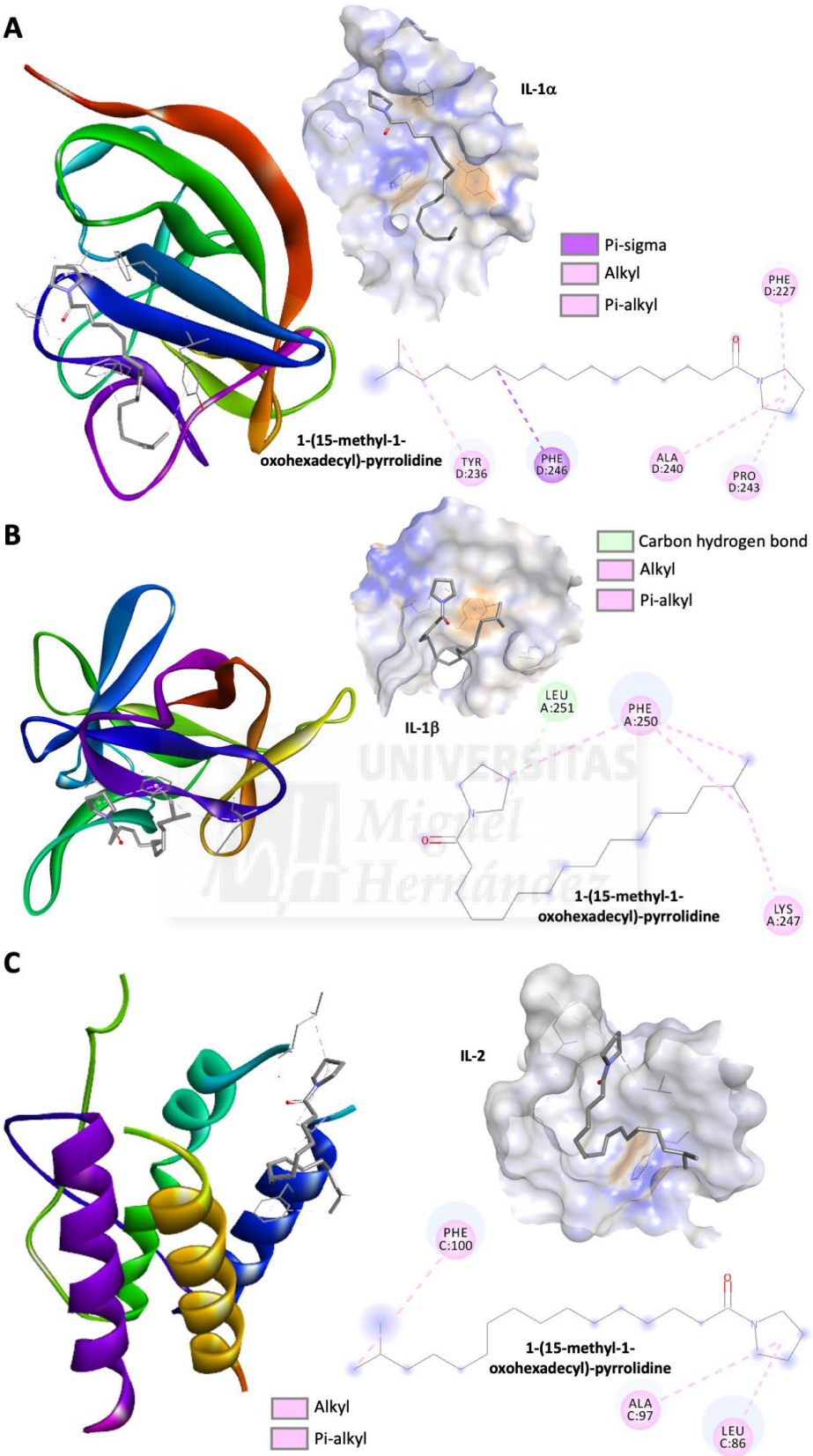

Figure 5. Best *in silico* interactions between 1-(15-methyl-1-oxohexadecyl)-pyrrolidine and selected proteins modulated by DM extract: **(A)** IL-1α, **(B)** IL-1β, and **(C)** IL-2.

The results show the best docking poses between each selected protein and hexadecanoic acid as indicated by AutoDock Vina. Images were generated with BioVia Discovery software.

4. Discussion

It has been well established that pro-inflammatory factors could trigger the development of cancer-associated conditions (Lichtenstern et al., 2020). In consequence, natural anti-inflammatory compounds might deliver an appropriate anti-cancer response, without the observed adverse effects produced by traditional chemical compounds used in the cancer treatment (Taylor et al., 2019). As a potential source of anti-inflammatory compounds with selective anti-proliferative effect, biologically active molecules from *O. vulgaris* ink might valorize this underutilized natural product that is scarcely used in certain food preparations around the world. Despite this potential, most research is focused on cuttlefish ink, thus research exploring the health-derive benefit from octopus is still underdeveloped (Derby, 2014), although some works have focused on octopus' antimicrobial peptides. For example, some researchers have reported the antimicrobial potential of peptides from the posterior salivary glands of *O. vulgaris* (Almeida et al., 2020). The authors informed about several peptide sequences identified by LC-MS/MS, most of them from known venom families such as serine proteases, metalloproteases, and serine proteases inhibitors, that were associated *in silico* with systemic anti-inflammatory responses and antimicrobial effects. Moreover, an *O. vulgaris*' suckers aqueous extract (1 mg/mL) showed inhibition of *S. aureus, P. aeruginosa,* and *C.* albicans (80 % minimal inhibitory concentration, MIC_{80}: 50-150 μM for 4 identified peptidic sequences) effect associated to peptides identified by nano liquid chromatography coupled to quantitative electrospray ionization and mass spectrometry analysis (LC-ESI-Q-Orbitrap MS/MS) (Maselli et al., 2020). The observed antibacterial activity is not only associated to *O. vulgaris* components but also to hemocytes (hemoblast-like cells, hyalinocytes, and granulocytes) carrying out demonstrated antibacterial activity mainly against *S. aureus, L. monocytogenes, B. cereus, Salmonella* spp., and *P. aeruginosa* (bactericidal activity: ~60-90 %) (Troncone et al., 2015).

Regarding other cephalopods, Zhong et al. (2009) assessed the antioxidant potential of *Sepia officinalis* ink *in vivo* using Balb/c mice, finding a significant ($p<0.05$) reduction of antioxidant enzymes' activities such as catalase, glutathione peroxidase, superoxide dismutase, and malonaldehyde. The authors attributed this effect due to the synergistic effects of some ink's components such as melanin, proteins, lipids, and glycosaminoglycans. In another study, Girija et al. (2012) reported the antibacterial activity of the hexane extract from Indian squid (*Loligo duvauceli*) ink on *E. coli* and *K.*

pneumoniae bacterial strains. The same authors also reported a novel protein isolated from the melanin-free ink fraction (Lolduvin-S), also exhibiting inhibitory effects against gram-positive bacterial and pathogenic yeasts Girija et al. (2011).

The standardization of the ink obtention from marine products is a crucial process to extract high quality ink without affecting the chemical structures and its concentrations in the ink. For instance, it has been reported that depending on the collection method, certain components such as L-3,4-dihydroxyphenyl-alanine can be found, while epinephrine or selected proteins could be damaged (Madaras et al., 2010). Therefore, in this research a reported procedure was used to obtain ink extracts using several solvents based on the ability of each one to extract selected compounds. These extracts were initially screened for their anti-proliferative potential on representative cancer cell lines from highly deathly cancer conditions (Bray et al., 2018). Despite the absence of reports depicting the anti-proliferative potential of *O. vulgaris* ink, several reports can be found underlining the anti-proliferative activity from cuttlefish ink. Soufi-Kechaou et al. (2017) reported the antitumoral activity of isolated and purified peptides from *O. vulgaris* and *Sepia officinalis* ink, reporting a significant decrease of IGR 39 (melanoma cells) adhesion ($p<0.05$) for *O. vulgaris* ink isolates than its counterparts from *S. officinalis.* However, *S. officinalis* isolates (10-30 mg/mL) exhibited a higher inhibition of cell migration than *O. vulgaris,* suggesting major anti-metastatic dissemination. More recently, our research group underlined the anti-proliferative potential of *O. vulgaris*' ink fractions, where the same DM fraction showed the highest inhibitory effects against 22Rv1 prostate carcinoma cells (LC_{50}: 68.2 µg/mL) (Hernández-Zazueta et al., 2021). The obtention of several DM fractions indicated that DM-F2 was the most biologically active, inducing 22Rv1 apoptosis (transition to late and early apoptosis) and increasing reactive oxygen species (ROS) production, compared to the untreated cells.

For other cephalopods, it has been reported that *Sepia esculenta* ink exhibits antitumor activity *in vivo* against Meth-A fibrosarcoma from BALB/c mice and its peptidoglycan-containing fraction also showed this activity (Guo-fang et al., 2011). Russo et al. (2003) reported an LC_{50} of 81 µg/ml in Caco-2 colorectal adenocarcinoma cells from the melanin-free ink extract of *Sepia officinalis,* which was attributed to its tyrosinase activity causing oxidative damage to DNA, lipids, or proteins, inactivating vital cell functions and inducing caspase-3 mediated apoptosis.

The anti-proliferative effect of cisplatin relies on its ability to enhance the TNF-related apoptosis-inducing ligand (TRAIL). However, it has shown limited effect against A549 and MDA-MB-231 cancer cell lines due to the need of TRAIL synchronization with additional signaling complexes or the need for specific death receptors (DR4 and DR5) to transmit the pro-apoptotic signal (Gasparian et al., 2017). Docetaxel has demonstrated capability to disrupt the microtubule network that blocks cell cycles in the late G2 and M phases and has been mainly used to treat breast and prostate cancer (Sohail et al., 2018). The further examination by DAPI and Phalloidin of the DM-F2 effects on HCT116 confirmed its enhanced capability to cause apoptosis-inducing modifications such as chromatin fragmentation (pyknosis) and cytoskeleton breakdown. (Coleman et al., 2001; Yuan et al., 2007). No reports of *in vitro* structural changes induced by *O. vulgaris* ink extracts were found, but oligopeptides isolated from *Sepia esculenta* ink have been observed to cause a significant increase in the fluorescence of human A549 lung cancer cells, as examined by DAPI/FITC staining (Zhang et al., 2017). These effects were in line with the inhibition of proliferation and apoptosis induction in the same cell line.

The production of nitrites has been classically linked as an indirect measurement of nitric oxide production, a key mediator of the pro-inflammatory response, and mediator of the redox modification of protein and other biomolecules (Freeman et al., 2017). The high reactivity of NO molecule with oxygen, superoxide, and hydrogen peroxide target the intracellular production of ROS, which also contributes to inflammation and potentially pro-carcinogenic cell damage (DNA damage and mutations) (Brüne et al., 2003; Lonkar and Dedon, 2011). There are no reports on the NO and ROS modulation by *O. vulgaris* ink, but few studies have reported promising effects from squid ink. For instance, polysaccharides isolated from *Sepia esculenta* ink inhibited ROS production (~55 %) in H_2O_2-treated human dermal fibroblasts (HDFs) (200 μM) and regulated HDFs oxidative stress by reducing malonaldehyde (MDA), superoxide dismutase (SOD), and glutathione peroxidase activity, compared to a H_2O_2 control (Chen et al., 2020). Another polysaccharide extract from *S. esculenta* decreased plasmatic ROS, SOD, and MDA levels from cyclophosphamide-treated male Kunming mice (6 weeks age) (Gu et al., 2017).

Fatty acids (FA) are a major class of compounds that can be found in the ink of marine animals such as squids, cuttlefish, and octopus; thus, the metabolomic analysis naturally associated most DM and DM-F2 compounds to FA biosynthesis (**Fig. 2B**) (Derby, 2014).

Hence, the results obtained from **Fig. 2C** classified several FA as metabolites, fitting within the partial-least-squares model, allowing the discrimination of other metabolites with VIP ≥ 2 (Herrera-Cazares et al., 2019; Luzardo-Ocampo et al., 2020). Among the involved pathways, fatty acid biosynthesis reached the major impact, while the other pathways were classified with the same impact (**Fig. 2D**).

The potential anti-inflammatory and anti-proliferative activity from some of these fatty acids has been reported (Santos et al., 2013; Wang et al., 2009). Hexadecanoic or palmitic acid has been previously identified as one of the most abundant saturated fatty acids from crustaceans such as caramote prawn (*Penaeus kerathurus*) and mantis shrimp (*Squilla mantis*), reaching up to 50-60 % (Balzano et al., 2017). Besides, this fatty acid has been found in erythrocytes from fish consumers, partially associated to a lower risk of breast cancer (Kuriki et al., 2007). Octadecanol is a volatile oil that has been identified as a potential metabolite associated with reduced local inflammation in LPS-challenged isolated mouse peritoneal macrophages, showing a decrease in the production of nitrites, TNF-α, and inducible nitric oxide synthase (iNOS) (Li et al., 2013).

There are no reports about the biological activity of 1-(15-methyl-1-oxohexadecyl) pyrrolidine. 9-octadecenamide is an oleamide that has been identified in *Sepia pharaonis* ink extracts and biologically acts as a bioactive lipid signaling molecule in several organisms. (Ebenezer et al., 2020). Moreover, a potent anti-inflammatory activity *in vitro* in LPS-activated BV2 murine microglial cell line has been reported for 9-octadecenamide, decreasing nitrite concentrations and PGE_2 production by blocking iNOS and COX-2 expression, both converging in inhibiting NF-kB DNA binding and transcription (Oh et al., 2010)**.**

Due to their modulation of pro-inflammatory pathways, bioactive compounds from natural food sources have shown promising effects as co-adjuvants for cancer treatment. The JAK-STAT pathway is an essential cellular regulatory pathway that involves multiple proteins, whereas their regulation offers a valuable opportunity to disrupt cell proliferation, regulate the transduction of extracellular signals, and control inflammation (Groner and von Manstein, 2017). As observed by the cytokine regulation, most bioactive compounds of the ink act as signal transductor regulators, serving as a bridge in the interplay between the inflammation development and the maturation of immune cells. The JAK-STAT pathway is critical in the lymphocyte development, influencing their fate into differentiation to naive T cells or inflammatory T cell lineages (Egwuagu, 2009). These processes are in line with the effect of squid ink on increased TNF-α levels in NK-

cells *in vivo*, suggesting an immuno-stimulatory activity on NK cells and macrophages to inhibit tumor cells (Changlong et al., 1999). Another immuno-regulatory activity from this pathway converge in the production of IL-17 by T_H17 cells, acting in the host defense against bacteria and fungi (Ma et al., 2012). Thus, the potential of the ink components to contribute to the host defense against pathogens can also be suggested.

Joint anti-inflammatory and anti-cancer effects from the ink of marine animals also comprises the regulation of the PI3K-Akt and the mitogen-activated protein kinase (MAPK) pathway, which are common in multiple stages of carcinogenesis, because both participate in a p53-dependent pathway (Pencik et al., 2016). Polysaccharides from *Sepia esculenta* ink, mainly composed of monosaccharides, galactosamine, and arabinose, have exhibited *in vivo* protection against cyclophosphamide-induced cytotoxicity through regulation of apoptosis and autophagy activating the PI3K/Akt and p38 MAPK pathways (Liu, Tao, et al., 2016). On MDA-MB-231 cells, the same polysaccharide extract showed the inhibition of tumor metastasis downregulating MMP-2 and MMP-9 metalloproteases, inhibiting key pro-angiogenic pathways for the cancer survival and spreading (Liu, Xiao, et al., 2016). In another study, *Sepia esculenta* ink polysaccharides induced *in vivo* expression of IL-6, IL-10, and TNF-α on epithelial cells (Zuo et al., 2014). Since these polysaccharides also induced the expression of immunoglobulin A gene (*IgA J* chain gene), IgA contents in the intestinal tracts of the exposed mice were elevated (Lu et al., 2016). The authors hypothesized the ability of ink polysaccharides to mediate among gut microbiota and metabolites, the intestinal epithelial cells, brain-gut axis circuit, and the host metabolism. Consequently, the capability of bioactive compounds from *O. vulgaris* ink to regulate both inflammation and cancer might be involved in the production of the basal level of cytokines to effectively respond to the immune development and the recognition of cancer cells to undergo apoptosis. Since components of the ink are also up-regulating the production of IL-1, IL-2, and IL-4, it could be inferred a potential immunomodulatory activity on potential tumor development or blockade of the cancer maintenance (Setrerrahmane and Xu, 2017).

Overall, low binding energies were found for all of the assayed compounds, suggesting that other metabolites might be involved in the observed beneficial effects from *O. vulgaris* ink extracts. These compounds were selected based on those with the highest overall VIP score for both DM and DM-F2 composition, but only those with the lowest binding energies [hexadecanoic acid and 1-(15-methyl-1-oxohexadecyl) pyrrolidine]

(**Supplementary Table S1**) were chosen for the graphics. As the highest affinity was found for IL-1α, it could be inferred a significant influence of the anti-inflammatory and anti-proliferative compounds on related pathways, which are involved by the controlled activity between selected receptors, the participation of exogenous agents that mediate in the activation of caspase-1 and the inflammasome-derived production of IL-1β (Gabay et al., 2010). Findings indicating the ability of cholesterol crystals to activate the NLRP3 inflammasome in macrophages, inducing lysosomal destabilization by the leakage of cathepsin B into the cytoplasm could also confirm this hypothesis (Rajamäki et al., 2010). Nonetheless, as an anti-inflammatory activity was observed from the reduction of the production of nitrites and intracellular ROS, it could be inferred that this pro-inflammasome activity might be acting at the basal level or this overactivation should not be considered pro-inflammatory stimuli, highlighting the not fully understood dual roles of the inflammasome activation (Kelley et al., 2019).

A summary of the observed anti-inflammatory effects is indicated in **Fig. 6.** The black arrows indicate the influence of DM extract in the production of each cytokine. Bioactive compounds from DM-F2 were involved in several pathways. Increments in the production of IL-2, IL-4, IL-27, and IL-23 were associated with overactivation of the JAK-STAT pathway, while the extract inhibited the assemblage of the NF-kB protein complex by inhibiting the IL-17 associated pathway. Since IL-1α is a result of the inflammasome activation, requiring the first stimulus due to NF-kB, increments in its production might be at basal levels since there are no other stimuli that could initiate its activation, such as calcium or ROS production. Several cytokines involved in the LPS-stimulated TLR4 activation were produced, such as G-CSF, GM-CSF, CXCL11, and IL-12, indicating the capability of the DM-F2 bioactive compounds to collaborate in coordinated recruitment of immune cells to the inflammation sites to locally exert a pro-inflammatory effect at basal levels, as demonstrated by nitric oxide and NF-kB reductions.

The results from this research suggests the potential immuno-modulatory and anti-proliferative dual roles of *O. vulgaris* ink components. *O. vulgaris* ink extracts exerted anti-proliferative effects on two colorectal (HCT116 and HT-29) and breast (MDA-MB-231) cancer cell lines. A purified dichloromethane fraction (DM-F2) from the ink exhibited the highest biological activity contributing to the induction of apoptotic-like morphological changes on HCT116 cells. Besides, this fraction exerted an anti-

inflammatory effect on LPS-stimulated RAW 264.7 cells inducing the reduction of the production of nitrites, ROS, and up-regulating cytokines involved in the JAK-STAT, MAPK, PI3K-Akt, and the canonical NF-kB pathway. The metabolomic analysis suggested that fatty acids and aldehydes from the DM-F2 could be responsible for these effects, potentially binding with inflammation/cancer targets such as IL-1α, IL-1β, and IL-2. This evidence underlines the beneficial anti-inflammatory and anti-proliferative effects from bioactive compounds from underutilized natural food products such as *O. vulgaris* ink.

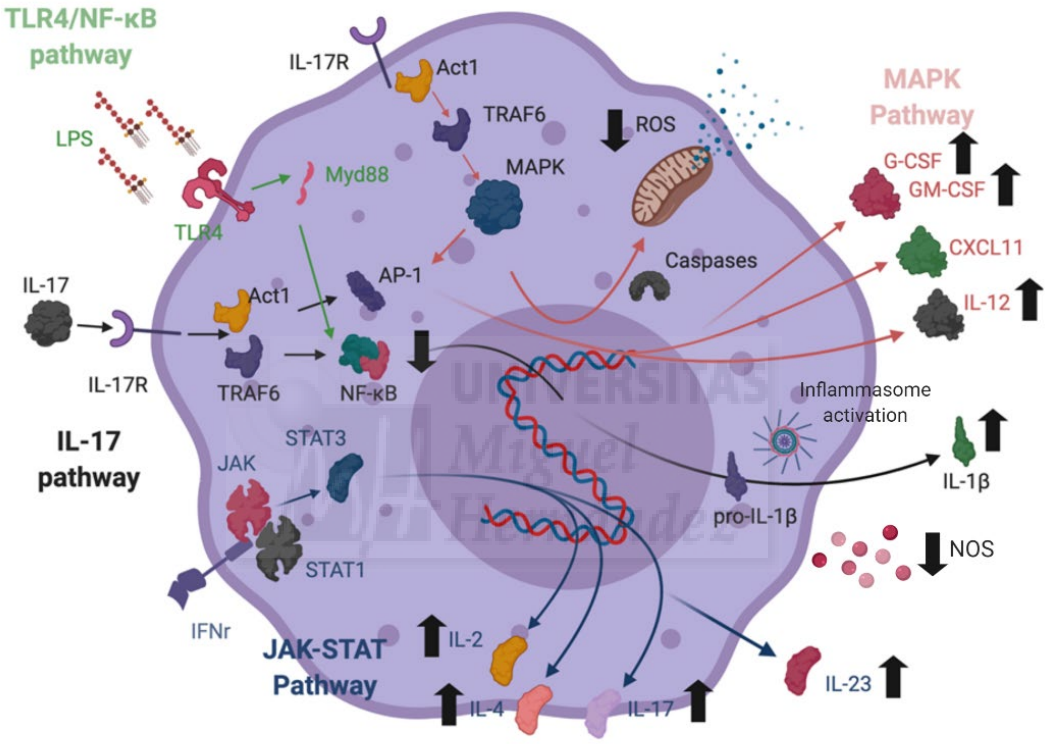

Figure 6. Proposal of the main pro-inflammatory pathways modulated by DM-F2. Graphic was generated with BioRender.com. Black arrows show the direct involvement of DM-F2 in the selected biochemical markers, proteins, and pathways.

References

Allavena, P., Garlanda, C., Borrello, M.G., Sica, A., Mantovani, A., 2008. Pathways connecting inflammation and cancer. Curr. Opin. Genet. Dev. 18, 3–10. https://doi.org/10.1016/j.gde.2008.01.003

Almeida, D., Domínguez-Pérez, D., Matos, A., Agüero-Chapin, G., Osório, H.,

Vasconcelos, V., Campos, A., Antunes, A., 2020. Putative antimicrobial peptides of the posterior salivary glands from the cephalopod *Octopus vulgaris*revealed by exploring a composite protein database. Antibiotics 9, 757. https://doi.org/10.3390/antibiotics9110757

Ammendola, M., Haponska, M., Balik, K., Modrakowska, P., Matulewicz, K., Kazmierski, L., Lis, A., Kozlowska, J., Garcia-Valls, R., Giamberini, M., Bajek, A., Tylkowski, B., 2020. Stability and anti-proliferative properties of biologically active compounds extracted from *Cistus* L. after sterilization treatments. Sci. Rep. 10, 6521. https://doi.org/10.1038/s41598-020-63444-3

Balzano, M., Pacetti, D., Lucci, P., Fiorini, D., Frega, N.G., 2017. Bioactive fatty acids in mantis shrimp, crab and caramote prawn: Their content and distribution among the main lipid classes. J. Food Compos. Anal. 59, 88–94. https://doi.org/10.1016/j.jfca.2017.01.013

Barzkar, Tamadoni Jahromi, Poorsaheli, Vianello, 2019. Metabolites from marine microorganisms, micro, and macroalgae: immense scope for pharmacology. Mar. Drugs 17, 464. https://doi.org/10.3390/md17080464

Bray, F., Ferlay, J., Soerjomataram, I., 2018. Global Cancer Statistics 2018 : GLOBOCAN estimates of incidence and mortality worldwide for 36 cancers in 185 countries. CA Cancer J Clin. 00, 1–31. https://doi.org/10.3322/caac.21492.

Brüne, B., Zhou, J., Von Knethen, A., 2003. Nitric oxide, oxidative stress, and apoptosis. Kidney Int. Suppl. 63, S22–S24. https://doi.org/10.1046/j.1523-1755.63.s84.6.x

Changlong, L., Shen, H., Beixing, L., 1999. The immuno-stimulating activations of squid ink and its extracts. Chinese J. Mar. Drugs 18, 32–34.

Chávez-Sánchez, L., Chávez-Rueda, K., Legorreta-Haquet, M., Zenteno, E., Ledesma-Soto, Y., Montoya-Díaz, E., Tesoro-Cruz, E., Madrid-Miller, A., Blanco-Favela, F., 2010. The activation of CD14, TLR4, and TLR2 by mmLDL induces IL-1β, IL-6, and IL-10 secretion in human monocytes and macrophages. Lipids Health Dis. 9, 117. https://doi.org/10.1186/1476-511X-9-117

Chen, Y., Liu, H., Huang, H., Ma, Y., Wang, R., Hu, Y., Zheng, X., Chen, C., Tang, H., 2020. Squid ink polysaccharides protect human fibroblast against oxidative stress by regulating NADPH oxidase and connexin43. Front. Pharmacol. 10, 1574.

https://doi.org/10.3389/fphar.2019.01574

Coleman, M.L., Sahai, E.A., Yeo, M., Bosch, M., Dewar, A., Olson, M.F., 2001. Membrane blebbing during apoptosis results from caspase-mediated activation of ROCK I. Nat. Cell Biol. 3, 339–345. https://doi.org/10.1038/35070009

Coussens, L.M., Werb, Z., 2002. Inflammation and cancer. Nature 420, 860–867. https://doi.org/10.1038/nature01322

Derby, C.D., 2014. Cephalopod ink: production, chemistry, functions and applications. Mar. Drugs 12, 2700–30. https://doi.org/10.3390/md12052700

Ebada, S.S., Edrada, R.A., Lin, W., Proksch, P., 2008. Methods for isolation, purification and structural elucidation of bioactive secondary metabolites from marine invertebrates. Nat. Protoc. 3, 1820–1831. https://doi.org/10.1038/nprot.2008.182

Ebenezer, J.L., Gunapriya, R., Ranganathan, K., Ganesh, M.K., 2020. Biologically active compounds in *Sepia pharaonis* fish (Ehrenber, 1831) ink extract from Chennai seacoast isolated by gas chromatography. Drug Invent. Today 13, 90–94.

Egwuagu, C.E., 2009. STAT3 in CD4+ T helper cell differentiation and inflammatory diseases. Cytokine 47, 149–156. https://doi.org/10.1016/j.cyto.2009.07.003

Fahmy, R., Soliman, A.M., 2013. *In vitro* antioxidant, analgesic and cytotoxic activities of *Sepia officinalis* ink and *Coelatura aegyptiaca* extracts. African J. Pharm. Pharmacol. 7, 1512–1522. https://doi.org/10.5897/AJPP2013.3564

Freeman, B.A., Pekarova, M., Rubbo, H., Trostchansky, A., 2017. Electrophilic nitro-fatty acids: nitric oxide and nitrite-derived metabolic and inflammatory signaling mediators, in: Ignarro, L.J., Freeman, B.A. (Eds.), Nitric Oxide. Academic Press - ElSevier, pp. 213–229. https://doi.org/10.1016/B978-0-12-804273-1.00016-8

Gabay, C., Lamacchia, C., Palmer, G., 2010. IL-1 pathways in inflammation and human diseases. Nat. Rev. Rheumatol. 6, 232–241. https://doi.org/10.1038/nrrheum.2010.4

Gasparian, M.E., Bychkov, M.L., Yagolovich, A. V., Kirpichnikov, M.P., Dolgikh, D.A., 2017. The effect of cisplatin on cytotoxicity of anticancer cytokine TRAIL and its receptor-selective mutant variant DR5-B1. Dokl. Biochem. Biophys. 477, 385–388. https://doi.org/10.1134/S1607672917060114

Gertsman, I., Barshop, B.A., 2018. Promises and pitfalls of untargeted metabolomics. J. Inherit. Metab. Dis. 41, 355–366. https://doi.org/10.1007/s10545-017-0130-7

Girija, S., Priyadharshini, J. V., Suba K., P., Hariprasad, G., Raghuraman, R., 2011. Isolation and characterization of Lolduvin-S: A novel antimicrobial protein from the ink of indians squid *Loligo duvauceli*. Int. J. Curr. Res. Rev. 3, 4–14.

Girija, S., Priyadharshini, V., Pandi, S.K., Hariprasad, P., Raguraman, R., 2012. Antibacterial effect of squid ink on ESBL producing strains of *Escherichia coli* and *Klebsiella pneumoniae*. Indian J. Geo-Marine Sci. 41, 338–343.

Groner, B., von Manstein, V., 2017. Jak Stat signaling and cancer: Opportunities, benefits and side effects of targeted inhibition. Mol. Cell. Endocrinol. 451, 1–14. https://doi.org/10.1016/j.mce.2017.05.033

Gu, Y.P., Yang, X.M., Duan, Z.H., Luo, P., Shang, J.H., Xiao, W., Tao, Y.X., Zhang, D.Y., Zhang, Y.B., Liu, H.Z., 2017. Inhibition of chemotherapy-induced apoptosis of testicular cells by squid ink polysaccharide. Exp. Ther. Med. 14, 5889–5895. https://doi.org/10.3892/etm.2017.5342

Guo-fang, D., Fang-fang, H., Zui-su, Y., Di, Y.U., Yong-fang, Y., 2011. Anticancer activity of an oligopeptide isolated from hydrolysates of Sepia Ink. Chin. J. Nat. Med. 9, 151–155. https://doi.org/https://doi.org/10.3724/SP.J.1009.2011.00151

Hernández-Zazueta, M.S., García-Romo, J.S., Noguera-Artiaga, L., Luzardo-Ocampo, I., Carbonell-Barrachina, Á.A., Taboada-Antelo, P., Campos-Vega, R., Rosas-Burgos, E.C., Burboa-Zazueta, M.G., Ezquerra-Brauer, J.M., Martínez-Soto, J.M., Santacruz-Ortega, H. del C., Burgos-Hernández, A., 2021. *Octopus vulgaris*ink extracts exhibit antioxidant, antimutagenic, cytoprotective, anti-proliferative, and proapoptotic effects in selected human cancer cell lines. J. Food Sci. 1750-3841.15591. https://doi.org/10.1111/1750-3841.15591

Herrera-Cazares, L.A., Ramírez-Jiménez, A.K., Wall-Medrano, A., Campos-Vega, R., Loarca-Piña, G., Reyes-Vega, M.L., Vázquez-Landaverde, P.A., Gaytán-Martínez, M., 2019. Untargeted metabolomic evaluation of mango bagasse and mango bagasse based confection under *in vitro* simulated colonic fermentation. J. Funct. Foods 54, 271–280. https://doi.org/10.1016/J.JFF.2019.01.032

IARC, 2018. Estimated number of new cancer cases in 2018 worldwide [WWW

Document]. Cancer Today. URL https://gco.iarc.fr/ (accessed 5.29.20).

Kelley, N., Jeltema, D., Duan, Y., He, Y., 2019. The NLRP3 inflammasome: An overview of mechanisms of activation and regulation. Int. J. Mol. Sci. 20, 3328. https://doi.org/10.3390/ijms20133328

Khalifa, S.A.M., Elias, N., Farag, M.A., Chen, L., Saeed, A., Hegazy, M.E.F., Moustafa, M.S., El-Wahed, A.A., Al-Mousawi, S.M., Musharraf, S.G., Chang, F.R., Iwasaki, A., Suenaga, K., Alajlani, M., Göransson, U., El-Seedi, H.R., 2019. Marine natural products: A source of novel anticancer drugs. Mar. Drugs. https://doi.org/10.3390/md17090491

Kuriki, K., Hirose, K., Wakai, K., Matsuo, K., Ito, H., Suzuki, T., Hiraki, A., Saito, T., Iwata, H., Tatematsu, M., Tajima, K., 2007. Breast cancer risk and erythrocyte compositions of n-3 highly unsaturated fatty acids in Japanese. Int. J. Cancer 121, 377–385. https://doi.org/10.1002/ijc.22682

Lê Cao, K.A., Boitard, S., Besse, P., 2011. Sparse PLS discriminant analysis: Biologically relevant feature selection and graphical displays for multiclass problems. BMC Bioinformatics 12. https://doi.org/10.1186/1471-2105-12-253

Li, W., Fan, Ting, Zhang, Y., Fan, Te, Zhou, P., Niu, X., He, L., 2013. *Houttuynia cordata* Thunb. volatile oil exhibited anti-inflammatory effects *in vivo* and inhibited nitric oxide and Tumor Necrosis Factor-α production in LPS-stimulated mouse peritoneal macrophages *in vitro*. Phyther. Res. 27, 1629–1639. https://doi.org/10.1002/ptr.4905

Lichtenstern, C.R., Ngu, R.K., Shalapour, S., Karin, M., 2020. Immunotherapy, inflammation and colorectal cancer. Cells 9, 618. https://doi.org/10.3390/cells9030618

Liu, C., Li, X., Li, Y., Feng, Y., Zhou, S., Wang, F., 2008. Structural characterisation and antimutagenic activity of a novel polysaccharide isolated from *Sepiella maindroni* ink. Food Chem. 110, 807–813. https://doi.org/10.1016/j.foodchem.2008.02.026

Liu, H.-Z., Tao, Y.-X., Luo, P., Deng, C.-M., Gu, Y.-P., Yang, L., Zhong, J.-P., 2016a. Preventive effects of a novel polysaccharide from *Sepia esculenta* ink on ovarian failure and its action mechanisms in cyclophosphamide-treated mice. J. Agric. Food Chem. 64, 5759–5766. https://doi.org/10.1021/acs.jafc.6b01854

Liu, H.-Z., Xiao, W., Gu, Y.-P., Tao, Y.-X., Zhang, D.-Y., Du, H., Shang, J.-H., 2016b. Polysaccharide from *Sepia esculenta* ink and cisplatin inhibit synergistically proliferation and metastasis of triple-negative breast cancer MDA-MB-231 cells. Iran. J. Basic Med. Sci. 19, 1292–1298. https://doi.org/10.22038/ijbms.2016.7913

Lonkar, P., Dedon, P.C., 2011. Reactive species and DNA damage in chronic inflammation: Reconciling chemical mechanisms and biological fates. Int. J. Cancer. https://doi.org/10.1002/ijc.25815

Lord, R.M., Zegke, M., Henderson, I.R., Pask, C.M., Shepherd, H.J., McGowan, P.C., 2019. β-Ketoiminato Iridium(III) organometallic complexes: selective cytotoxicity towards colorectal cancer cells HCT116 p53 -/-. Chem. - A Eur. J. 25, 495–500. https://doi.org/10.1002/chem.201804901

Lu, S., Zuo, T., Zhang, N., Shi, H., Liu, F., Wu, J., Wang, Y., Xue, C., Tang, Q., 2016. High throughput sequencing analysis reveals amelioration of intestinal dysbiosis by squid ink polysaccharide. J. Funct. Foods 20, 506–515. https://doi.org/10.1016/j.jff.2015.11.017

Luna-Vital, D., Weiss, M., Gonzalez de Mejia, E., 2017. Anthocyanins from purple corn ameliorated Tumor Necrosis Factor-α-induced inflammation and insulin resistance in 3T3-L1 adipocytes via activation of insulin signaling and enhanced GLUT4 translocation. Mol. Nutr. Food Res. 61, 1–13. https://doi.org/10.1002/mnfr.201700362

Luzardo-Ocampo, I., Campos-Vega, R., Gonzalez de Mejia, E., Loarca-Piña, G., 2020. Consumption of a baked corn and bean snack reduced chronic colitis inflammation in CD-1 mice via downregulation of IL-1 receptor, TLR, and TNF-α associated pathways. Food Res. Int. 132, 109097. https://doi.org/10.1016/j.foodres.2020.109097

Ma, C.S., Avery, D.T., Chan, A., Batten, M., Bustamante, J., Boisson-Dupuis, S., Arkwright, P.D., Kreins, A.Y., Averbuch, D., Engelhard, D., Magdorf, K., Kilic, S.S., Minegishi, Y., Nonoyama, S., French, M.A., Choo, S., Smart, J.M., Peake, J., Wong, M., Gray, P., Cook, M.C., Fulcher, D.A., Casanova, J.-L., Deenick, E.K., Tangye, S.G., 2012. Functional STAT3 deficiency compromises the generation of human T follicular helper cells. Blood 119, 3997–4008.

https://doi.org/10.1182/blood-2011-11-392985

Madaras, F., Gerber, J.P., Peddie, F., Kokkinn, M.J., 2010. The effect of sampling methods on the apparent constituents of ink from the squid *Sepioteuthis australis*. J. Chem. Ecol. 36, 1171–1179. https://doi.org/10.1007/s10886-010-9869-0

Malve, H., 2016. Exploring the ocean for new drug developments: Marine pharmacology. J. Pharm. Bioallied Sci. https://doi.org/10.4103/0975-7406.171700

Maselli, V., Galdiero, E., Salzano, A.M., Scaloni, A., Maione, A., Falanga, A., Naviglio, D., Guida, M., Di Cosmo, A., Galdiero, S., 2020. OctoPartenopin: Identification and preliminary characterization of a novel antimicrobial peptide from the suckers of *Octopus vulgaris*. Mar. Drugs 18, 380. https://doi.org/10.3390/md18080380

Mitchison, T.J., 2012. The proliferation rate paradox in antimitotic chemotherapy. Mol. Biol. Cell. https://doi.org/10.1091/mbc.E10-04-0335

Moustafa, A.Y., Awaad, A., 2016. Comparative histopathological and histochemical impacts induced by the posterior salivary gland and ink sac extracts of *Octopus vulgaris*in mice. J. Basic Appl. Zool. 74, 23–36. https://doi.org/10.1016/j.jobaz.2016.04.001

Mysuru Shivanna, L., Urooj, A., 2016. A review on dietary and non-dietary risk factors associated with gastrointestinal cancer. J. Gastrointest. Cancer 47, 247–254. https://doi.org/10.1007/s12029-016-9845-1

Naraoka, T., Chung, H.-S.S., Uchisawa, H., Sasaki, J.I., Matsue, H., 2000. Tyrosinase activity in antitumor compounds of squid ink. Food Sci. Technol. Res. 6, 171–175. https://doi.org/10.3136/fstr.6.171

Noguera-Artiaga, L., Salvador, M.D., Fregapane, G., Collado-González, J., Wojdyło, A., López-Lluch, D., Carbonell-Barrachina, Á.A., 2019. Functional and sensory properties of pistachio nuts as affected by cultivar. J. Sci. Food Agric. 99, 6696–6705. https://doi.org/10.1002/jsfa.9951

Oh, Y.T., Lee, J.Y., Lee, J., Lee, J.H., Kim, J.-E., Ha, J., Kang, I., 2010. Oleamide suppresses lipopolysaccharide-induced expression of iNOS and COX-2 through inhibition of NF-κB activation in BV2 murine microglial cells. Neurosci. Lett. 474, 148–153. https://doi.org/10.1016/j.neulet.2010.03.026

Pencik, J., Pham, H.T.T., Schmoellerl, J., Javaheri, T., Schlederer, M., Culig, Z., Merkel, O., Moriggl, R., Grebien, F., Kenner, L., 2016. JAK-STAT signaling in cancer: from cytokines to non-coding genome. Cytokine 87, 26–36. https://doi.org/10.1016/j.cyto.2016.06.017

Rajamäki, K., Lappalainen, J., Öörni, K., Välimäki, E., Matikainen, S., Kovanen, P.T., Eklund, K.K., 2010. Cholesterol crystals activate the NLRP3 inflammasome in human macrophages: A novel link between cholesterol metabolism and inflammation. PLoS One 5, e11765. https://doi.org/10.1371/journal.pone.0011765

RoyChoudhury, S., More, T.H., Chattopadhyay, R., Lodh, I., Ray, C.D., Bose, G., Sarkar, H.S., Chakravarty, B., Rapole, S., Chaudhury, K., 2017. Polycystic ovary syndrome in Indian women: a mass spectrometry based serum metabolomics approach. Metabolomics 13, 115. https://doi.org/10.1007/s11306-017-1253-4

Russo, G.L., De Nisco, E., Fiore, G., Di Donato, P., D'Ischia, M., Palumbo, A., D'Ischia, M., Palumbo, A., 2003. Toxicity of melanin-free ink of *Sepia officinalis* to transformed cell lines: identification of the active factor as tyrosinase. Biochem. Biophys. Res. Commun. 308, 293–299. https://doi.org/10.1016/S0006-291X(03)01379-2

Santos, S., Oliveira, A., Lopes, C., 2013. Systematic review of saturated fatty acids on inflammation and circulating levels of adipokines. Nutr. Res. 33, 687–695. https://doi.org/10.1016/j.nutres.2013.07.002

Sarkar, D., Fisher, P.B., 2006. Molecular mechanisms of aging-associated inflammation. Cancer Lett. 236, 13–23. https://doi.org/10.1016/j.canlet.2005.04.009

Setrerrahmane, S., Xu, H., 2017. Tumor-related interleukins: old validated targets for new anti-cancer drug development. Mol. Cancer 16, 153. https://doi.org/10.1186/s12943-017-0721-9

Sohail, M.F., Rehman, M., Sarwar, H.S., Naveed, S., Qureshi, O.S., Bukhari, N.I., Hussain, I., Webster, T.J., Shahnaz, G., 2018. Advancements in the oral delivery of Docetaxel: challenges, current state-of-the-art and future trends. Int. J. Nanomedicine Volume 13, 3145–3161. https://doi.org/10.2147/IJN.S164518

Soufi-Kechaou, E., Sariya, I., Bezaa, A., Marrakchi, N., El Ayeb, M., 2017. Antitumoral activity in inks of *Sepia officinalis* and *Octopus vulgaris*(Cephalopoda) from the

northern tunisian coast (central Mediterranean sea). Ann. Ser. Hist. Nat. 27, 125–136. https://doi.org/10.19233/ASHN.2017.15

Sun, L., Zhang, L., Yu, J., Zhang, Y., Pang, X., Ma, C., Shen, M., Ruan, S., Wasan, H.S., Qiu, S., 2020. Clinical efficacy and safety of anti-PD-1/PD-L1 inhibitors for the treatment of advanced or metastatic cancer: a systematic review and meta-analysis. Sci. Rep. 10, 2083. https://doi.org/10.1038/s41598-020-58674-4

Taylor, W.F., Moghadam, S.E., Moridi Farimani, M., N. Ebrahimi, S., Tabefam, M., Jabbarzadeh, E., 2019. A multi-targeting natural compound with growth inhibitory and anti-angiogenic properties re-sensitizes chemotherapy resistant cancer. PLoS One 14, e0218125. https://doi.org/10.1371/journal.pone.0218125

Troncone, L., De Lisa, E., Bertapelle, C., Porcellini, A., Laccetti, P., Polese, G., Di Cosmo, A., 2015. Morphofunctional characterization and antibacterial activity of haemocytes from *Octopus vulgaris*. J. Nat. Hist. 49, 1457–1475. https://doi.org/10.1080/00222933.2013.826830

Trott, O., Olson, A.J.A., 2010. AutoDock Vina: Improving the speed and accuracy of docking with a new scoring function, efficient optimization, and multithreading. J. Comput. Chem. 31, 455–461. https://doi.org/10.1002/jcc.21334

Tuomisto, A.E., Mäkinen, M.J., Väyrynen, J.P., 2019. Systemic inflammation in colorectal cancer: Underlying factors, effects, and prognostic significance. World J. Gastroenterol. 25, 4383–4404. https://doi.org/10.3748/wjg.v25.i31.4383

Van Vuuren, R.J., Botes, M., Jurgens, T., Joubert, A.M., Van Den Bout, I., 2019. Novel sulphamoylated 2-methoxy estradiol derivatives inhibit breast cancer migration by disrupting microtubule turnover and organization. Cancer Cell Int. 19. https://doi.org/10.1186/s12935-018-0719-4

von Mering, C., Jensen, L.J., Kuhn, M., Chaffron, S., Doerks, T., Kruger, B., Snel, B., Bork, P., Krüger, B., Snel, B., Bork, P., 2007. STRING 7 - Recent developments in the integration and prediction of protein interactions. Nucleic Acids Res. 35, 358–362. https://doi.org/10.1093/nar/gkl825

Wang, S., Wu, D., Lamon-Fava, S., Matthan, N.R., Honda, K.L., Lichtenstein, A.H., 2009. *In vitro* fatty acid enrichment of macrophages alters inflammatory response and net cholesterol accumulation. Br. J. Nutr. 102, 497.

https://doi.org/10.1017/S0007114509231758

Wargasetia, T.L., Widodo, N., 2019. The link of marine products with autophagy-associated cell death in cancer cell. Curr. Pharmacol. Reports 5, 35–42. https://doi.org/10.1007/s40495-019-00167-8

Weng, S., Mao, L., Gong, Y., Sun, T., Gu, Q., 2017. Role of quercetin in protecting ARPE-19 cells against H2O2-induced injury via nuclear factor erythroid 2 like 2 pathway activation and endoplasmic reticulum stress inhibition. Mol. Med. Rep. 16, 3461–3468. https://doi.org/10.3892/mmr.2017.6964

Yuan, B.Z., Jefferson, A.M., Millecchia, L., Popescu, N.C., Reynolds, S.H., 2007. Morphological changes and nuclear translocation of DLC1 tumor suppressor protein precede apoptosis in human non-small cell lung carcinoma cells. Exp. Cell Res. 313, 3868–3880. https://doi.org/10.1016/j.yexcr.2007.08.009

Zhang, Z., Li, Y., Lin, B., Schroeder, M., Huang, B., 2011. Identification of cavities on protein surface using multiple computational approaches for drug binding site prediction. Bioinformatics 27, 2083–2088. https://doi.org/10.1093/bioinformatics/btr331

Zhang, Z., Sun, L., Zhou, G., Xie, P., Ye, J., 2017. Sepia ink oligopeptide induces apoptosis and growth inhibition in human lung cancer cells. Oncotarget 8, 23202–23212. https://doi.org/10.18632/oncotarget.15539

Zhong, J.-P., Wang, G., Shang, J.-H., Pan, J.-Q., Li, K., Huang, Y., Liu, H.-Z., 2009. Protective effects of squid ink extract towards hemopoietic injuries induced by cyclophosphamine. Mar. Drugs 7, 9–18. https://doi.org/10.3390/md7010009

Zuo, T., Cao, L., Sun, X., Li, X., Wu, J., Lu, S., Xue, C., Tang, Q., 2014. Dietary squid ink polysaccharide could enhance SIgA secretion in chemotherapeutic mice. Food Funct. 5, 3189–3196. https://doi.org/10.1039/C4FO00569D

PUBLICACIÓN 3

N-(2-ozoazepan-3-yl)-pyrrolidine-2-carboxamide, a novel *Octopus vulgaris* ink-derived metabolite, exhibits a pro-apoptotic effect on A549 cancer cell line and inhibits pro-inflammatory markers

Martín Samuel Hernández-Zazueta, Joel Said García-Romo, Ivan Luzardo-Ocampo, Ángel Antonio Carbonell-Barrachina, Pablo Taboada-Antelo, Ema Carina Rosas-Burgos, Josafat Marina Ezquerra-Brauer, Juan Manuel Martínez-Soto, Maria del Carmen Candia-Plata, Hisila del Carmen Santacruz-Ortega, Armando Burgos-Hernández*

Food and Chemica Toicology. 2023. 177: 0278-6915. Doi: 10.1016/j.fct.2023.113829

PUBLICACIÓN 3: TRANSCRIPCIÓN LITERAL

N-(2-ozoazepan-3-yl)-pyrrolidine-2-carboxamide, a novel *Octopus vulgaris* ink-derived metabolite, exhibits a pro-apoptotic effect on A549 cancer cell line and inhibits pro-inflammatory markers

Martín Samuel Hernández-Zazueta[1], Joel Said García-Romo[1], Ivan Luzardo-Ocampo[2], Ángel Antonio Carbonell-Barrachina[3], Pablo Taboada-Antelo[4], Ema Carina Rosas-Burgos[1], Josafat Marina Ezquerra-Brauer[1], Juan Manuel Martínez-Soto[5], Maria del Carmen Candia-Plata[5], Hisila del Carmen Santacruz-Ortega[6], Armando Burgos-Hernández[1*]

[1] Departamento de Investigación y Posgrado en Alimentos, Universidad de Sonora, 83000 Hermosillo, Sonora, México.

[2] Research and Graduate Program in Food Science, Universidad Autonoma de Queretaro, 76010 Queretaro, Mexico.

[3] Escuela Politécnica Superior de Orihuela, Universidad Miguel Hernández de Elche, 03312 Alicante, España.

[4] Departamento de Física Aplicada, Universidad de Santiago de Compostela, 15782, Santiago de Compostela, España.

[5] Departamento de Medicina y Ciencias de la Salud, Universidad de Sonora, 83000 Sonora, México.

[6] Departamento de Investigación en Polímeros y Materiales, Universidad de Sonora, 83000, Sonora, México.

* Corresponding author at: Departamento de Investigación y Posgrado en Alimentos, Universidad de Sonora, Apartado Postal 1658, 83000 Hermosillo, Sonora, México. Tel.: +526-622-592-208; Fax: +526-622-592-209. E-mail address: armando.burgos@unison.mx

Abbreviations

ΔG: Gibb's free energy; **ADMET:** Absorption, digestion, metabolism, excretion, and toxicity; **BBB:** Blood-brain-barrier; **COSY2D:** two-dimensional (2D) correlated homonuclear spectroscopy; **DAPI:** 4'6-diadimino-2-phenylindole dilactate**; DAPI:** 4',6'-diadimino-2-phenylindole dilactate; **DCC:** N,N′-dicyclohexylcarbodiimide; **DCFH-DA:** Dichloro-dihydro-fluorescein diacetate; **DCM:** Dichloromethane; **DMEM:** Dulbecco's Modified Eagle Medium; **DMSO:** Dimethyl sulfoxide; **FBS:** Fetal bovine serum; **FITC:** Fluorescein isothiocyanate; **FLEX:** Flexibility; **FTIR:** Fourier-transformed infrared spectroscopy; **HIA:** Human intestinal absorption; **HOB:** Human

oral bioavailability; **IC_{50}:** Half inhibitory concentration; **INSATU:** Saturations; **INSOLU:** Insolubility; **LIPO:** Lipophilicity; **LPS:** Lipopolysaccharide; **MANIO:** (3S)-6,7-bis(hydroxymethyl)-5-methyl-3-phenyl-1H, 3H-pyrrolo[1,2-c]thiazole; **MS:** Microwave synthesizer; **MTT:** 3-(4,5-dimethylthiazol-2-yl)-2,5-diphenyltetrazolium bromide; **NMR:** Nuclear magnetic resonance; **OPC:** N-(2-ozoazepan-3-yl) pyrrolidine-2-carboxamide (ozopromide); **PBMCs:** Peripheral blood mononuclear cells; **PDB:** Protein Databank; **POLAR:** Polarity; **RFU:** Relative fluorescence units; **ROS:** Reactive oxygen species; **RPMI:** Roswell Park Memorial Institute cell culture medium; **SDS:** Sodium dodecyl sulfate; **SIZE:** Molecular weight; **SMILES:** Simplified molecular input line entry specifications; **TPSA:** Topological polar surface area; **WLOGP:** Wildman and Crippen lipophilicity.

Keywords: *Octopus vulgaris,* ozopromide (OPC), anti-inflammatory, cytokines, pro-apoptotic.

1. Introduction

Cancer is the second death cause worldwide (WHO, 2020). Differential analysis of the plethora of factors involved in cancer development has highlighted the diet and lifestyle as some of the most influential since the nutrition regimen could impact the way cancer originates and further develops (Banikazemi et al., 2018). Hence, bioactive molecules isolated from food products, particularly underutilized food wastes, could be a promising strategy in cancer prevention, lowering their environmental impact (Socaci et al., 2017).

Despite the large amount of evidence supporting the use of potential chemopreventive or chemoprotective diets, further research is required since conventional treatments might produce adverse drug effects (Nurgali et al., 2018).

Cephalopods have proven to be a source of bioactive molecules displaying therapeutic effects *in vitro* and *in vivo* (Derby, 2014). Although several body parts of cephalopods can be used to extract biologically active molecules, the ink contains a large amount of macro and micromolecules with anti-inflammatory and anticancer effects. Previous studies conducted by our research group identified a novel compound isolated from *O. vulgaris* ink extracts, N-(2-ozoazepan-3-yl)-pyrrolidine-2-carboxamide, named Ozopromide (OPC) with anti-proliferative and pro-apoptotic activities on selected cancer cell lines [prostate (22Rv1), lung adenocarcinoma (A549), and epithelioid cervix adenocarcinoma (HeLa) cells] (Hernández-Zazueta et al., 2021b), whereas the highest effects were found on A549 cells. Moreover, the OPC-containing *O. vulgaris* extracts displayed anti-inflammatory activity on LPS-stimulated RAW 264.7 cells (Hernández-Zazueta et al., 2021a), highlighting the potential of *O. vulgaris* ink as a food-derived nutraceutical product.

As OPC displayed high *in silico* binding affinity with several cancer, cell cycle, and inflammation markers, OPC could be involved in several mechanisms. Since pure OPC has not been previously examined, this research aimed to assess the pro-apoptotic and pro-inflammatory effects of synthesized OPC on A549 cells. We hypothesized that OPC could be linked to most of the observed biological effects *in vitro* and could be proposed as a food-derived potential chemoprotective molecule for further anticancer activity studies.

2. Material and methods

2.1. Chemical and reagents

2.1.1 Synthesis of N-(2-ozoazepan-3-yl) pyrrolidine-2-carboxamide (OPC, ozopromide)

A solution of dry dichloromethane (DCM) was slowly added to a mixture of 1.74 mM N, N'-dicyclohexylcarbodiimide (DCC), and 1.56 mM L-proline. The obtained solution was kept at 32 ºC for 30 min in a container within a Microwave Synthesizer (MS) (Discover© 2020, CEM Corporation, Matthews, NC, USA). Then, 3.12 mM 3-amino-2-azepanone was slowly added to the 3 mL DCM solution. The resulting mixture was kept on the MS for 60 min at 32 °C and filtered using a Whatman No. 1 filter paper. The filtrate was kept at 4 °C for 24 h. Finally, the solvents were distilled off, and the residue was crystallized (-4 ºC) for urea crystal formation and removed. The distilled solution was kept at room temperature (25 ± 1 ºC) for 24 hrs. A general scheme of the synthesis procedure is presented in **Fig. 1A.**

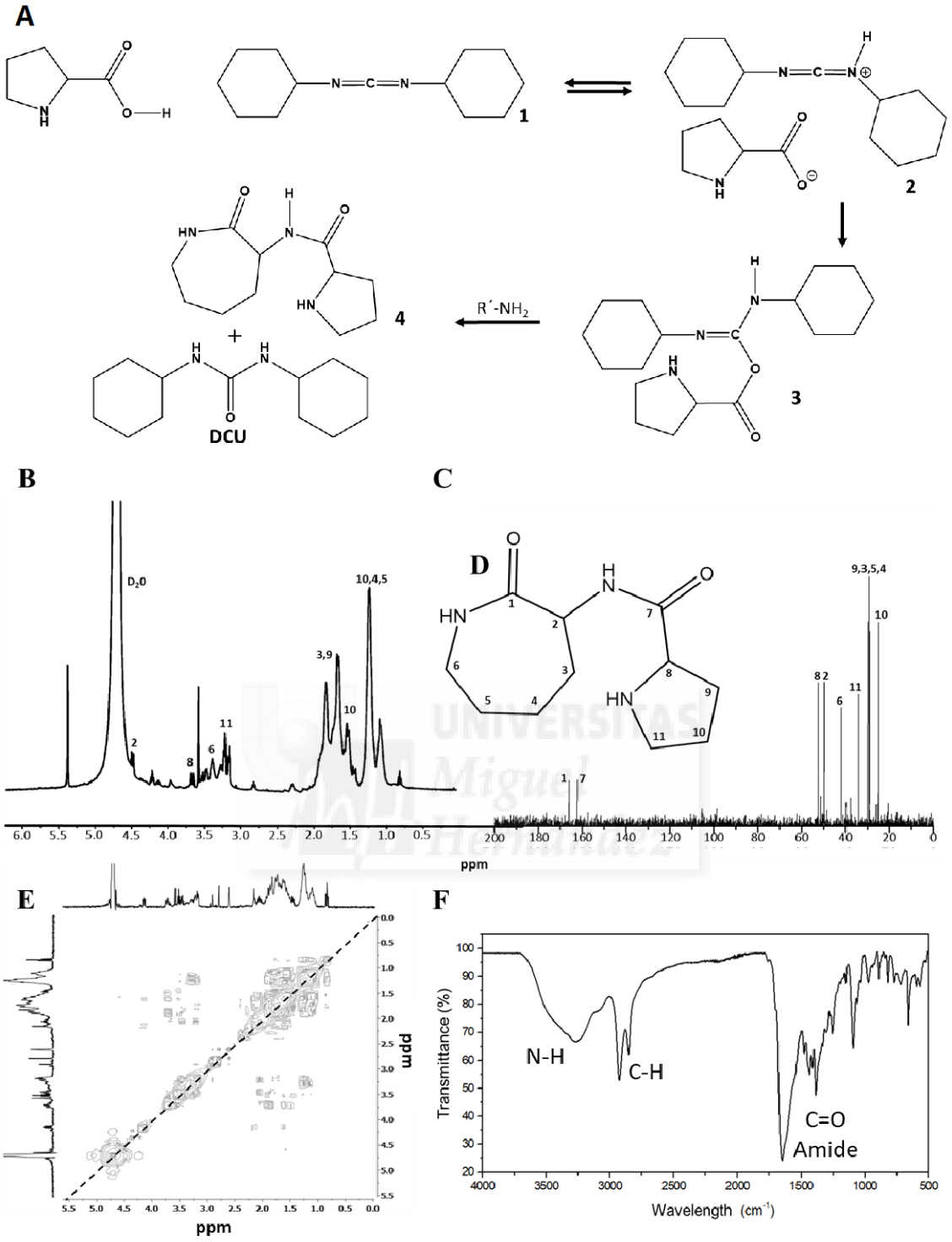

Fig. 1. Overall mechanism of OPC synthesis. **(A)** Synthesis mechanism of Ozopromide [(N-2-ozoazepan-3-yl)-pyrrolidine-2-carboxamide, OPC); **(B)** ^{13}C- and **(C)** ^{1}H-NMR (nuclear magnetic resonance) analyses; and **(D)** chemical structure of the identified OPC. **(E)** Correlated homonuclear spectroscopy (COSY) spectrum (δ 4.6 - 1.5 ppm spectrum portion) obtained by ^{1}H-NMR. **(F)** Fourier-transformed infrared spectroscopy (FTIR) analysis.

δ, chemical shift; J, coupling constant; d, doublet; dd, a doublet of doublets; m, multiplet; s, singlet.

2.2. Structural analysis of ozopromide (OPC)

2.2.1. Fourier-transformed infrared spectroscopy (FTIR)

The obtained OPC mixture was analyzed using a Fourier-transformed infrared spectroscopy FTIR™ Frontier equipment (Perkin Elmer, Waltham, MA, USA) averaging 16 spectra scans (4000 – 400 cm^{-1} range). IR spectra were recorded using potassium bromide pellets.

2.2.2. Nuclear magnetic resonance (NMR) of carbon and proton (^{13}C-NMR and ^{1}H-NMR) and the analysis of two-dimensional correlated mononuclear spectroscopy (COSY-2D)

The AvanceCore 400 MHz NMR equipment (Bruker, Billerica, MA, USA) was employed to analyze the OPC mixture. Approximately 10 µL of the sample was re-suspended in 500 µL $CDCl_3$/tetramethylsilane (internal standard, Sigma-Aldrich, St. Louis, MO, USA) and placed in 5-mm diameter ultra-precision NMR tubes. Carbon (^{13}C-NMR, at 100 MHz) and proton (^{1}H-NMR, at 400 MHz) nuclear magnetic resonance measurements were performed at ppm level to record chemical shifts.

2.3. Evaluation of the cytotoxic potential of OPC

2.3.1. Test cells

Human retinal pigment epithelium ARPE-19 (ATCC® CRL-2302™), lung (carcinoma) A549 (ATCC® CCL-185™), epithelioid cervix adenocarcinoma HeLa (ATCC® CCL-2™), prostate carcinoma 22Rv1 (ATCC® CRL-2505™), human colorectal carcinoma HCT116 (ATCC® CCL-247™), and mammary gland/breast adenocarcinoma MDA-MB-231 (ATCC® HTB-26™) cell lines were acquired from American Type Culture Collection (Manassas, VA, USA). The cells were cultured in RPMI-1640 Medium (Sigma Aldrich, St. Louis, MO, USA) and Dulbecco's modified Eagle's medium (DMEM), supplemented with 15 and 10 % heat-inactivated fetal bovine serum (FBS) (Corning, NY, USA), respectively. The cells were then incubated in a humidified 5 % CO_2 atmosphere at 37 °C.

Human Peripheral Blood Mononuclear Cells (PBMCs) were used to evaluate the OPC impact on inflammation. The extraction and maintenance protocol were conducted following the Declaration of Helsinki (revised in 2013), the ISO 35001 standards (sections 7.7, 8.4-8.7, and 8.10) (ISO, 2019), and the Mexican Official Standards (NMX 15189, sections 5.4.3 and 5.4.4), considering informed consent of the donors and ethical

handling and further disposal of the samples (SEGOB, 2015). Additionally, these tests followed the procedures stablished in the official mexican standard rules NOM-087-ECOL-SSA1-2002. PBMCs were isolated by density gradient from human peripheral blood employing the Ficoll-Paque™ PLUS (GE Healthcare, Otelfingen, Switzerland) reagent. PBS was used to dilute the blood (1:2), layered on a corresponding amount of Ficoll-Paque™ PLUS, and centrifuged at 450× g for 30 min and 25 ºC. Once separated, the cells were relocated into a new tube and washed 3 times using PBS. Subsequently, the cells were re-suspended in RPMI-1640 medium (R7388, Sigma-Aldrich) and incubated at 37 ºC in 5 % CO_2 (VWR 2325 Water-Jacketed CO2 Incubator, PA, USA).

2.3.2. Cytotoxic activity evaluation by the MTT assay

The cytotoxic activity of synthesized OPC was assayed using the colorimetric 3-(4,5-dimethylthiazol)-2-yl)-2,5-diphenyl tetrazolium bromide (MTT) method (Roche, Basel, Switzerland), according to the manufacturer's instructions. OPC was re-suspended in dimethyl sulfoxide (DMSO, 0.25 M) using Dulbecco's Modified Eagle Medium (DMEM) for dilution. Cell culture was performed according to the procedure described by García-Romo et al. (2022), but each of the samples (OPC and cisplatin, dissolved in DMSO) were replaced during the second incubation period. Moreover, the cells were treated with several OPC concentrations (25, 50, 100, 200, and 300 µM) for 24 h. Also, the cytotoxic potential of OPC was determined on peripheral blood mononuclear cells (PBMCs), according to the procedure described by Hernández-Zazueta et al. (2021a).

2.3.3. Morphological assessment on A549 cells

The influence of OPC on structural aspects of A549 cancerous cells was evaluated according to the procedure described by Hernández-Zazueta et al. (2021a), where testing cells were treated with the OPC's half inhibitory concentration (IC_{50}: 111.50 µM) for 24 h.

2.4. Pro-apoptotic effect of ozopromide (OPC) on A549 cells

2.4.1. Pro-apoptotic effect of ozopromide evaluation by flow cytometry

OPC pro-apoptotic activity was assessed employing the eBioscience™ Annexin-V Apoptosis Detection Kit Fluorescein isothiocyanate (FITC) (Cat. No. 88-8005-74, ThermoFisher Scientific, USA) according to manufacturer directions. Untreated, heat-shock subjected (70 ºC, 30 min), cisplatin- (IC_{50}: 111.50 µM), or OPC (IC_{50}: 53.70 µM)-treated stained cells for 24 h were assessed with a BD FACSVerse™ flow cytometer and FACSuite v1 computer program (BD Biosciences, CA, USA) counting 10,000 events,

from which percentages of positive cells were obtained for Annexin V and Propidium Iodide staining in the FITC-A and PE-A channels, respectively. All experiments were done in triplicate.

2.5. Intracellular reactive oxygen species (ROS) levels.

The cells (PBMCs) were cultured in microcentrifuge tubes using RPMI medium supplemented with 5 % FBS under agitation for 24 h under proper conditions (37 ºC and humidified 5 % CO_2 atmosphere). The medium was then discarded and OPC (25, 50, 100, and 200 µM) and LPS from *E. coli* O111:B4 (1 mg/mL, Sigma-Aldrich) were used to treat the cells for 24 h. A basal condition (untreated cells) and LPS-only treated cells were used as a negative and positive control, respectively. Subsequently, a 10 mM 2′,7′-dichloro-dihydro-fluorescein diacetate (DCFH-DA) (cat. D6883, Sigma-Aldrich, SL, MO, USA) solution was added for 15 min in the dark at 25 °C. Finally, the BD FACSVerse equipment and the FACSuite v. 1.0 software (BD Biosciences, CA, USA) were used. Staining was assessed by FITC-A. Data were obtained in relative fluorescence units (RFU) but expressed as percentual relationship against the basal (untreated cells) ROS production.

2.6. Analysis of IL-4, IL-6, IL-8, IL-10 and NF-κB: intracellular cell expression

The effect of OPC (25, 50, 100, and 200 µM) on the modulation of IL-4, IL-6, IL-8, IL-10, and NF-κB, for 24 h, was measured by flow cytometry using LPS-treated (1 mg/mL) isolated PBMCs, following the procedure described by Hernández-Zazueta et al. (2021a). Results were normalized to basal conditions (untreated cells).

2.7. *In silico* analysis of binding affinity between OPC and apoptotic- and inflammation-related protein targets

To investigate how OPC (ligand) might interact with selected targets associated with apoptosis of the A549 cell line, an *in-silico* analysis was performed. On the other hand, the analysis was used to assess the interaction between OPC and the evaluated cytokines. Marvin Sketch was used to draw and 3D-verify the OPC sketching. Cancer-associated molecular targets were obtained from the Protein Databank (PDB) (https://www.rcsb.org/): p53 (PDB ID: 6SL6), c-JUN N-terminal kinase 3 (PDB ID: 1JNK), Bcl-XL (PDB ID: 1R2D), MEK1 (PDB ID: 3DY7), Bcl-2 (PDB ID: 2VM6), and Akt-1 (PDB ID: 3MVH). All other structures and water molecules were deleted using BioVia Discovery software v. 19.1.0.1.18287 (Dassault Systèmes, Vélizy-Villacoublay, France). The selected anti- and pro-inflammatory factors used for the docking

experiments were IL-4 (PBD ID: 1ITM), IL-6 (PDB ID: 1ALU), IL-8 (PDB ID: 5D14), IL-10 (PDB ID: 2H24), and NF-kB (p50/p65 heterodimer, PDB ID: 1VKX). All docking procedures were conducted considering the predicted most probable binding pockets for each protein target, using the DeepSite utility from PlayMolecule (https://playmolecule.org) (Jiménez et al., 2017) (**Supplementary Fig. S1**). Controls were included for each molecule for comparison purposes with the binding affinity found for OPC as follows: (a) IL 6: the IL-6 receptor (IL-6R, PDB ID: 1N26) (Varghese et al., 2002) and a reported IL-6 inhibitor ((4S)-4-[[4-[(2,4-diaminopteridin-6-yl)methylamino]benzoyl]amino]-5-[(2-methylpropan-2-yl)oxy]-5-oxopentanoic acid or $C_{23}H_{28}N_8O_5$, PubChem CID: 122677576) (Shukla et al., 2019); (b) IL-8: the IL-8 receptor (CXCR1, UniProt ID: P25024) and a known IL-8 inhibitor (repertaxin, PubChem CID: 9838712) (Casilli et al., 2005); (c) IL-4: the IL-4 receptor (IL-4R, PDB ID: 3BPN) and an amino nicotinonitrile as IL-4 inhibitor (Quinnell et al., 2020) modeled using MarvinSketch v. 22.20.0 (ChemAxon, Budapest, Hungary); (d) IL-10: the IL-10 receptor (IL-10R, PBD ID: 6X93) and a random molecule (pinonic acid, PubChem CID: 10130) generated in https://www.zuiveringstechnieken.nl/en-gb/random-hydrocarbons, since no IL-10 inhibitors were found; (e) NF-kB: 1,2-oxazine (modeled in MarvinSketch v. 22.20.0, ChemAxon) as NF-kB activator as it has been reported its high affinity in the DNA binding site (Somu et al., 2020); and the natural NF-kB inhibitor (IkBa, UniProt ID: Q9UGJ8); (f) p53: The human apoptosis-stimulating proteins of p53 (hiASPP, PDB ID: Q8WUF) as p53 inhibitor (Braithwaite et al., 2006) and the MANIO molecule ([(3S)-6,7-bis(hydroxymethyl)-5-methyl-3-phenyl-1H, 3H-pyrrolo[1,2-c]thiazole, modeled in MarvinSketch v. 22.20.0) as p53 activator (Ramos et al., 2021); (g) c-Jun: c-FOS (UniProt ID: P01100) as the natural c-Jun protein binding (Halazonetis et al., 1988) and c-Jun inhibitor (anthra[1,9]pyrazol-6(2H)-one, PubChem CID: 8515) (Bogoyevitch and Arthur, 2008); (h) Bcl-X: Bax protein (PDB ID: 6EB6) (Billen et al., 2008) and a selective Bcl-X inhibitor ($C_{35}H_{32}FN_5O_4S_2$: 2-[8-(1,3-benzothiazol-2-ylcarbamoyl)-3,4-dihydroisoquinolin-2(1h)-Yl]-5-(3-{4-[3-(dimethylamino)-prop-1-yn-1-yl]-2-fluorophenoxy}propyl)-1,3-thiazole-4-carboxylic acid, PubChem CID (A1155463): 59447577); (i) MEK: RAF protein (PDB ID: 5P21) (McCubrey et al., 2007) and hypothemycin (PubChem CID: 9929643) as a reported MEK inhibitor (Zhao et al., 1999); (j) Bcl-2: Bax protein as the natural Bcl-2 ligand to prevent mitochondrial cytochrome C release (PDB ID: 6EB6) (Naseri et al., 2015) and a reported Bcl-2 inhibitor ($C_{43}H_{32}N_4O_6$: N-(4-hydroxyphenyl)-3-[6-[(3S)-3-(morpholin-4-ylmethyl)-3,4-dihydro-1H-

isoquinoline-2-carbonyl]-1,3-benzodioxol-5-yl]-N-phenyl-5,6,7,8-tetrahydroindolizine-1-carboxamide; PubChem CID: 71654876) (NCI, 2011; Oh et al., 2021); (k) Akt-1: PDK1 (PDB ID: 3NAX) as an activator protein (Carnero, 2010) and the clinical inhibitor Capivasertib (PubChem CID: 25227436) (Lazaro et al., 2020). All proteins from the UniProt database (https://www.uniprot.org/) were downloaded as their amino acids FASTA sequence and then modeled in SwissModel (https://swissmodel.expasy.org/) to select the most similar reported 3D structure based on protein homology. Molecular dynamics exercises for the NF-kB inhibitor were conducted using the UNRES server v. 29.06.2018 (Czaplewski et al., 2018), highlighting the radius of gyration, potential energy, and fluctuation plots (Barrón-García et al., 2021).

AutoDock Tools was used to perform calculations for interactions between OPC or non-protein ligands and protein targets, adding hydrogen bonds, flexible torsions, and binding energy, which were done according to Luna-Vital, Weiss, & Gonzalez de Mejia (2017). For the protein-protein interactions, the pyDockWEB server was used (Jiménez-García et al., 2013). BioVia Discovery Studio computer program v. 19.1.0.1.18287 (Dassault Systèmes) was employed to construct figures out of the most probable docking conformations.

2.8. *In silico* analysis of absorption, digestion, metabolism, excretion, and toxicity (ADMET) properties

The assessment of the OPC's ADMET properties was conducted as reported in Cuellar-Nuñez et al. (2022). Briefly, the OPC molecule was drawn in the MarvinSketch module from SwissADME (Daina et al., 2017) and converted into the simplified molecular input line entry specifications [SMILES: O=C(NC1CCCCNC1=O)C1CCCN1], which were also used in admetSAR 2.0 software (http://lmmd.ecust.edu.cn/admetsar2/) to obtain physicochemical and ADMET properties. The BOILED-Egg diagram was used to plot a prediction of the gastrointestinal absorption and bran penetration of OPC (Luzardo-Ocampo et al., 2020).

2.9. Statistical analysis

Data were reported as the mean ± SD from at least two independent experiments in triplicates. After an analysis of variance (ANOVA), a *post-hoc* Tukey-Kramer's test was performed to differentiate ($p < 0.05$) treatments. The statistical analyses were carried out using SPSS STATICS (IBM Corp., New York, U.S.) and GraphPad Prism v. 8.0 computer packages.

3. Results

3.1. Synthesis and structural elucidation of N-(2-ozoazepan-3-yl) pyrrolidine-2 carboxamide

To confirm the OPC presence in the resultant mixture from the synthesis procedure, ^{13}C- and ^{1}H-NMR (**Fig. 1B** and **1C**, respectively), COSY2D (**Fig. 1E**), and FTIR (**Fig. 1F**) analyses were conducted. The resulting chemical structures are indicated in **Fig. 1D**.

Signals from ^{13}C-NMR analyses at a low field of δ =165.76 and δ =132.46 ppm confirmed the presence of two amide carbonyl groups that could belong to C1 and C7 (**Fig. 1C**). Signals associated with C-N bond were found at δ = 52.47 (C8), 47.89 (C2), and 41.85 (C6) ppm. The signals at a low field for C11, C10, C9, C8, and C7, corresponding to the C-H bond from the pyrrolidine structure bonded to a carboxamide of the caprolactam group were confirmed as C1, C2, C3, C4, C5, and C6 were identified.

A low field signal (7.26 ppm) was detected (**Fig. 1B**), which is associated with N-H bond, suggesting a carboxamide structure. Based on results from ^{1}H-NMR and two-dimensional (2D) correlated homonuclear spectroscopy (COSY2D) (**Fig. 1C**) analyses, the characteristic signals of OPC were identified. The OPC structure was also recognized from the FTIR spectrum (**Fig. 1F**), where the signal of a band observed at 1625 cm^{-1} confirmed the presence of the C=O bond in the amide group. A band linked to the N-H stretch could also be seen at 3250 cm^{-1} to 3500 cm^{-1} (**Supplementary Table S1**).

3.2. Effect of OPC on the viability of cancer cells and pro-apoptotic process

Fig. 2. shows the impact of OPC and positive controls (cisplatin and docetaxel) on the cancer cells' viability (**Fig. 2A**) and pro-apoptotic processes (**Fig. 2B**), which was later observed by fluorescence microscopy.

A

Compounds	Non-cancerous cell (IC_{50}, µM)	Cancerous cells (IC_{50}, µM)				
	ARPE-19	MDA-MB-231	22Rv1	HeLa	A549	HCT-116
Ozopromide (OPC)	>444.40 [b]	180.00 ± 13.3 [b]	157.0 ± 13.3 [a]	183.10 ± 0.0488 [b]	53.70 ± 4.00 [a]	255.50 ± 0.40 [a]
Cisplatin	307.20 ± 14.90 [a]	179.70 ± 21.20 [c]	4.90 ± 0.90 [a]	170.40 ± 26.5 [c]	111.50 ± 8.60 [c]	24.20 ± 1.90 [a]
Docetaxel	>123.70 [b]	226.00 ± 5.60 [a]	34.70 ± 8.00 [b]	23.90 ± 5.50 [a]	26.00 ± 0.81 [b]	11.50 ± 40.00 [a]

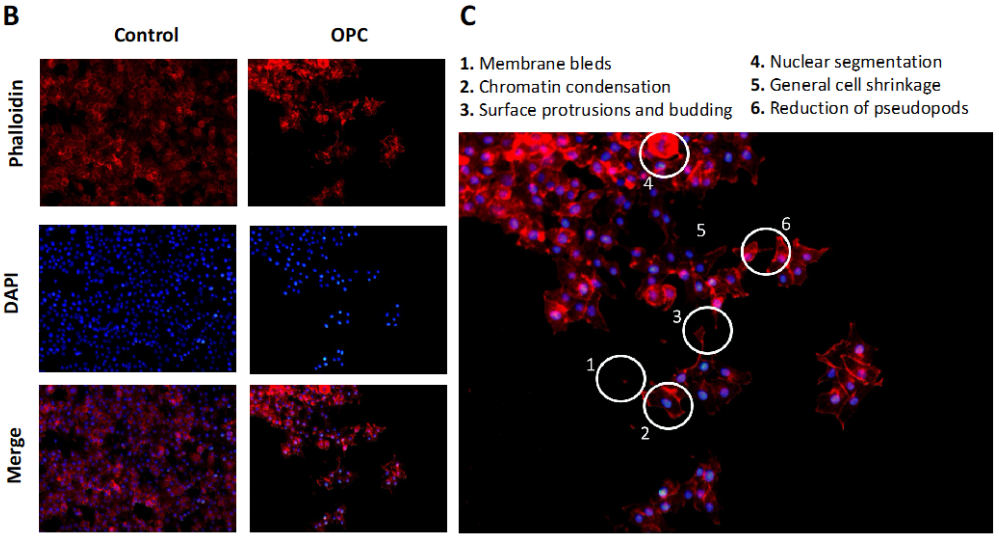

Fig. 2. Cytotoxic and pro-apoptotic effect of OPC on selected cancer cells. **(A)** Impact of ozopromide (OPC) on the cell viability from non-cancerous (ARPE-19) and cancerous (MDA-MB-231, 22Rv1, HeLa, A549, and HCT116) cell lines; **(B)** Cell morphology changes by DAPI and phalloidin tetramethylrhodamine staining. **(C)** Detailed pro-apoptotic features.

The values are the means ± S.D. from at least two independent experiments in triplicates. Different letters express significant differences ($p<0.05$) by Tukey-Kramer's test. For the cytotoxic effect (**A**), measured by the MTT test, the control cells were incubated with DMSO (0.5 mL/100 mL), representing 100% proliferation. All the IC_{50} concentrations were determined using several concentrations of the extracts, fractions, or drug controls (25, 50, 100, 200, and 300 µM) for 24 h. For the morphological experiments (**B** and **C**) the IC_{50} OPC concentration (53.70 µM) of A549 cells was used. **DAPI:** 4'6-diadimino-2-phenylindole dilactate. The morphological changes were inspected after 4 h of treatment. Actin cytoskeleton (red) and DNA (blue) were visualized by phalloidin and DAPI staining. The cell observations were made at 20x.

OPC, cisplatin, or docetaxel did not cause a cytotoxic effect on ARPE-19 cells. Regarding the cancerous cell lines, OPC demonstrated a substantial impact on A549 and 22Rv1 cell lines as the lowest OPC IC_{50} values were observed in these, being these IC_{50} values significantly lower than those of cisplatin but higher than docetaxel values. The fact that the OPC IC_{50} value was lower than cisplatin IC_{50} opens an opportunity to explore the isolation of bioactive molecules from food-derived products such as Octopus ink to target cancer mechanisms without having adverse effects.

To explore how cancerous cell lines were impacted by OP, phalloidin and DAPI staining of OPC-treated A549 cancerous cells was conducted to look for pro-apoptotic effects. Results (**Fig. 2B)** showed that OPC produced the typical markers of an apoptotic mechanism; morphological changes including bulging of the plasmatic membrane, large dynamic membrane blebs (associated with programmed cell death), and chromatin condensation. Besides, general surface protrusions and budding cells were visualized as notorious apoptotic-like morphology since A549 does not typically present it due to its spherical shape. Cell shrinkage, a notorious apoptotic characteristic, was also observed (**Fig. 2C**).

Figure 3 shows the quantification of apoptotic A549 cells with (heat-shock treatment at 70 ºC for 30 min, 111.50 µM cisplatin, and 53.70 µM OPC) or without treatments. The plots (**Fig. 3A**) were quantified (**Fig. 3B**), showing the highest numbers of live cells (Q4) for untreated cells, whereas heat-shock treatment induced the most increased cell death (Q1). OPC generated a higher number of cells at early (Q3) and late (Q2) apoptosis stages than the other treatments, agreeing with a pro-apoptotic mechanism.

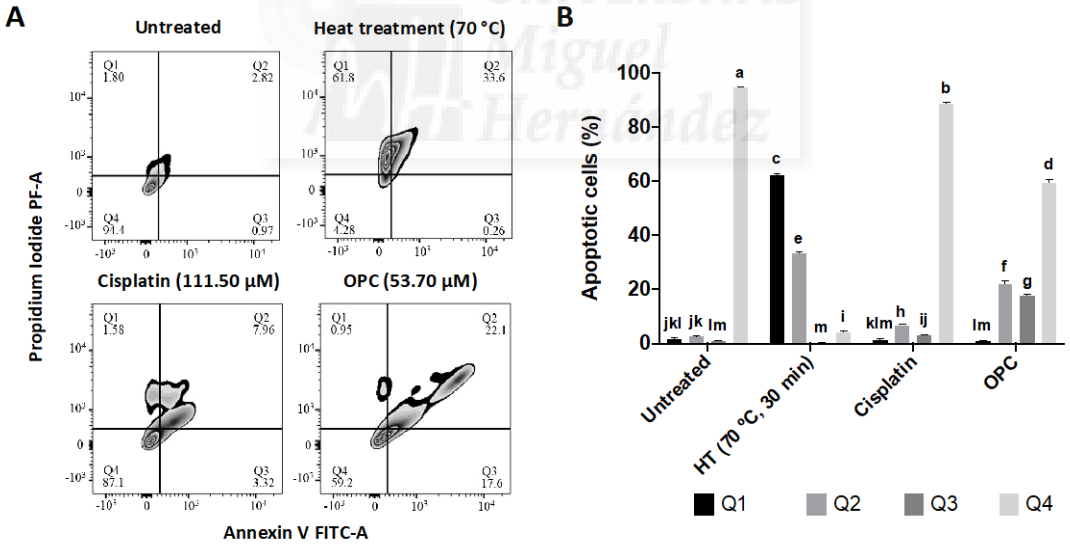

Fig. 3. Pro-apoptotic effect of OPC and controls in A549 cells. **(A)** Propidium iodide (PI) and Annexin V-FITC plot of A549 cells subjected to several treatments. **(B)** Quantification of A549 apoptotic cells (%) from several treatments. The results are represented as the means ± S.D. from at least three independent experiments in triplicates. Different letters express significant differences ($p<0.05$) by Tukey-Kramer's test.; The quadrants indicate death (Q1), late apoptotic (Q2), early apoptotic (Q3), and live cells (Q4). The concentrations of cisplatin and OPC corresponded to their IC_{50} values (111.50 and 53.70 µM, respectively).

3.3. Impact of OPC on ROS generation in LPS-stimulated PBMC cells

Since the anti-inflammatory activity of OPC was previously reported (Hernández-Zazueta et al., 2021), in this work, the impact of OPC against intracellular ROS generation and their quantification in PBMCs cells was studied. **Figure 4** shows that OPC (100 and 200 µM) reduced the relative intracellular ROS accumulation, partly delivering a dose-response phenomenon.

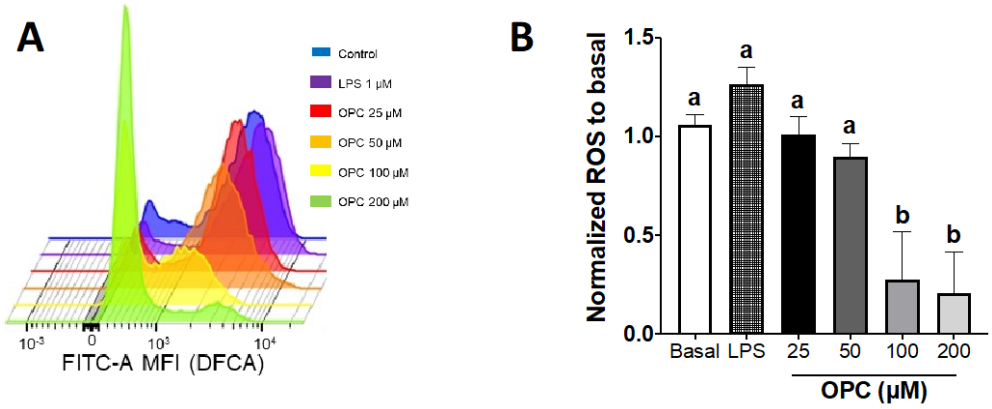

Fig. 4. OPC effect on intracellular reactive oxygen species (ROS) production in PBMCs by flow cytometry analysis. **(A)** Flow cytometry-generated areas from the several OPC concentrations; **(B)** Quantification of relative ROS concentrations from displayed areas, normalized to basal (untreated) cells. The results are represented as the means ± S.D. from three independent experiments in triplicates. Different letters express significant differences ($p<0.05$) by Tukey-Kramer's test. **FITC:** Fluorescein-isothiocyanate; **LPS:** lipopolysaccharide (1 mg/mL).

3.4. Effect of OPC on pro-inflammatory markers on LPS-stimulated PBMC cells.

The way OPC is proposed to impact anti- and pro-inflammatory cytokines on LPS-stimulated PBMCs is shown in **Fig. 5,** along with molecular docking affinity between OPC and the selected cytokines.

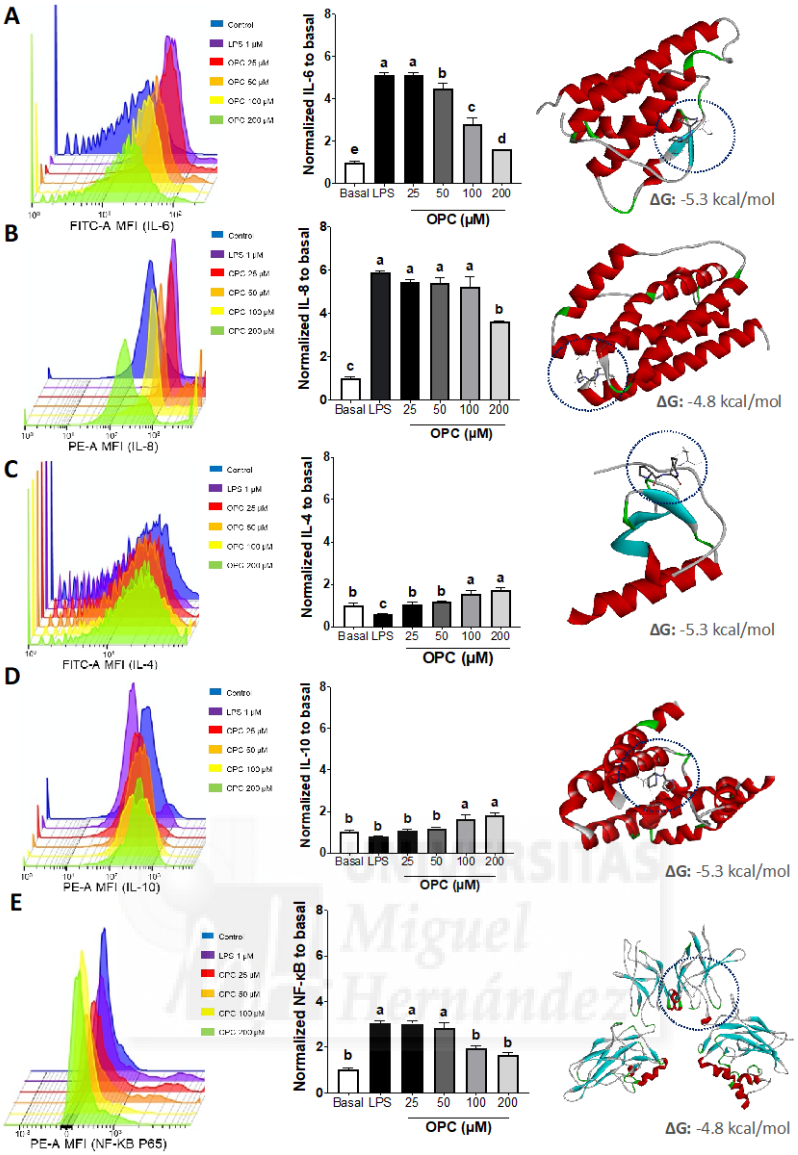

Fig. 5. Impact of OPC in the production of pro- and anti-inflammatory markers, and *in silico* binding affinity, on LPS-stimulated PBMCs cells; **(A)** IL-6; **(B)** IL-8, **(C)** IL-4; **(D)** IL-10; **(E)** NF-kB. The results are represented as the means ± S.D. of normalized relative interleukin expression to the basal cells from three independent experiments in triplicates. Different letters express significant differences ($p<0.05$) by Tukey-Kramer's test. LPS: lipopolysaccharide. Basal cells represent untreated LPS-stimulated PBMCs cells.

An inhibitory effect of OPC over IL-6, with a dose-dependent response, was observed, where 200 mM concentration achieved the strongest IL-6 inhibition (>50 %, compared to LPS-only treated cells). However, only at this concentration was OPC a significantly ($p<0.05$) inhibitor of IL-8 production, in comparison to LPS treatment. On the other hand, a dose-dependent stimulation of OPC over anti-inflammatory cytokines (IL-4 and IL-10) was observed. Results from molecular docking studies suggested a higher affinity of OPC

for IL-6 (-5.3 kcal/mol) and IL-4 (-5.8 kcal/mol), although medium biding energies (-3.0 to -6.0 kcal/mol) were obtained in the simulations. Comparisons between the obtained binding energies and controls for each cytokine (**Supplementary Fig. S2**) indicate that obtained OPC-binding energies are lower than reported receptors or inhibitors for each cytokine. Nonetheless, some of the energies are closer to the inhibitors, since OPC was docked in the most probable binding pocket for each cytokine (**Supplementary Fig. S3**). Remarkably, the lowest expressions of some cytokines (IL-4 and IL-10) (**Fig. 5C, 5D**) could be related to their lowest binding energies, suggesting that the anti-inflammatory activity of OPC could be more associated to the inhibition of pro-inflammatory factors rather than inducing anti-inflammatory cytokines. Moreover, a dose-dependent inhibition of NF-kB expression was found (**Fig. 5E**), but with low affinity to OPC (-4.8 kcal/mol). Particularly for the abovementioned nuclear factor, molecular dynamics testing OPC binding to NF-kB (**Supplementary Fig. S4**) showed that the radius of gyration (**Supplementary Fig. S4A**) ranged from 29 to 32.5. Sill, mostly in the 1000-2000 ps interval the docking maintained a small range. In addition, potential energy was stable between 500 and 2000 ps (**Supplementary Fig. S4B**), and the fluctuations remained low between 0-250 and 400-600 residues (**Supplementary Fig. S4C**), indicating a low conformation change in the atoms within the interaction, suggesting a low OPC influence in NF-kB conformational changes.

3.5. *In silico* molecular docking of OPC and selected cancer targets

Figure 6 shows results from the *in silico* molecular docking interactions between OPC and specific cancer-related molecular targets involved in apoptosis processes such as p53 (**Figure 6A**), c-Jun (**Figure 6B**), Bcl-X (**Figure 6C**), MEK (**Figure 6D**), Bcl-2 (**Figure 6E**), and Akt-1 (**Figure 6F**).

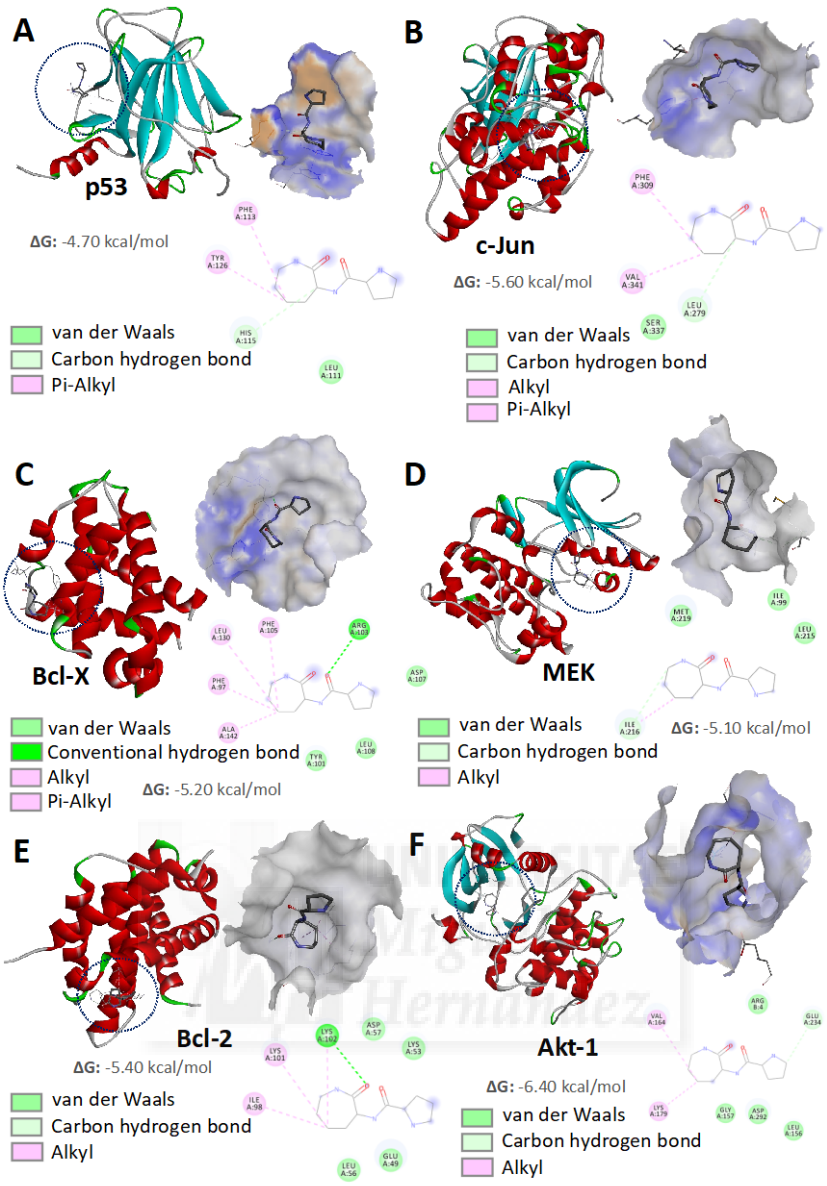

Fig. 6. *In silico* analysis with the best potential interactions between N-(2-ozoazepan-3-yl)-pyrrolidine-2-carboxamide (OPC) and selected cancer targets of A549 cells. Interactions of OCP and **(A)** Cyclin D1; **(B)** ERK1; **(C)** BAD. The 2D graphic represents the potential chemical interactions and involved amino acid residues from the cancer target proteins.

Results from **Supplementary Table S2** showed overall binding energies from -4.70 to -6.40, p53 the lowest and Akt-1 the highest. Van der Waals bonds were common for all the targets, whereas Bcl-X presented conventional hydrogen bonds. Regarding the amino acids involved in the OPC interactions (**Supplementary Table S3**), OPC binding with Bcl-X showed the highest amount of bound amino acids residues (5) and MEK was the lowest (1). OPC displayed a low capability of influencing NF-kB conformation change,

as suggested by molecular docking analyses (**Supplementary Fig. S4**). Representative docking exercises with receptors/activators and inhibitors (controls) for each cancer target (**Supplementary Fig. S5**) showed that, like OPC interactions with cytokines, binding energies between OPC and cancer targets were lower than controls, except for Bcl-X, where OPC displayed higher binding energy (-4.60 and -5.20 kcal/mol for inhibitor and OPC, respectively) (**Supplementary Fig. S6**).

Verification of the ADMET properties for OPC is shown in **Figure 6.** The predicted OPC characteristics within the bioavailability radar (**Figure 6A**) suggested that OPC is highly bioavailable as their properties for lipophilicity (LIPO), molecular weight (SIZE), polarity (POLAR), insolubility (INSOLU), saturations (INSATU), and flexibility (FLEX) fits within the ideal values (**Supplementary Table S4**). Examination of the BOILED-Egg diagram (**Figure 6B),** plotting the atomistic interpretation of the fragmental system of Wildman and Crippen for lipophilicity (WLOGP) and the topological polar surface area (TPSA), suggest an ability of OPC to cross the intestinal barrier but not the blood-brain-barrier (BBB). These results are in accordance with the absorption probability through several methods (**Figure 6C**), such as the human intestinal bioavailability (HIA), the caco-2 cells method, BBB, and human oral bioavailability, showing that, except for the caco-2 method (probability: 0.5362), all other probabilities were high (>0.70). Regarding the OPC properties linked to absorption and digestion (**Figure 6D**), most OPC activities were predicted to inhibit various transporters but could also serve as a substrate for P-glycoproteins and several cytochromes (CYP3A4, CYP2C9, and CYP2D6). Finally, prediction for topical OPC administrations displayed high probability for toxicity (eye corrosion and irritation and skin sensibilization), whereas low probabilities were predicted for the respiratory and reproductive systems (**Figure 6E**).

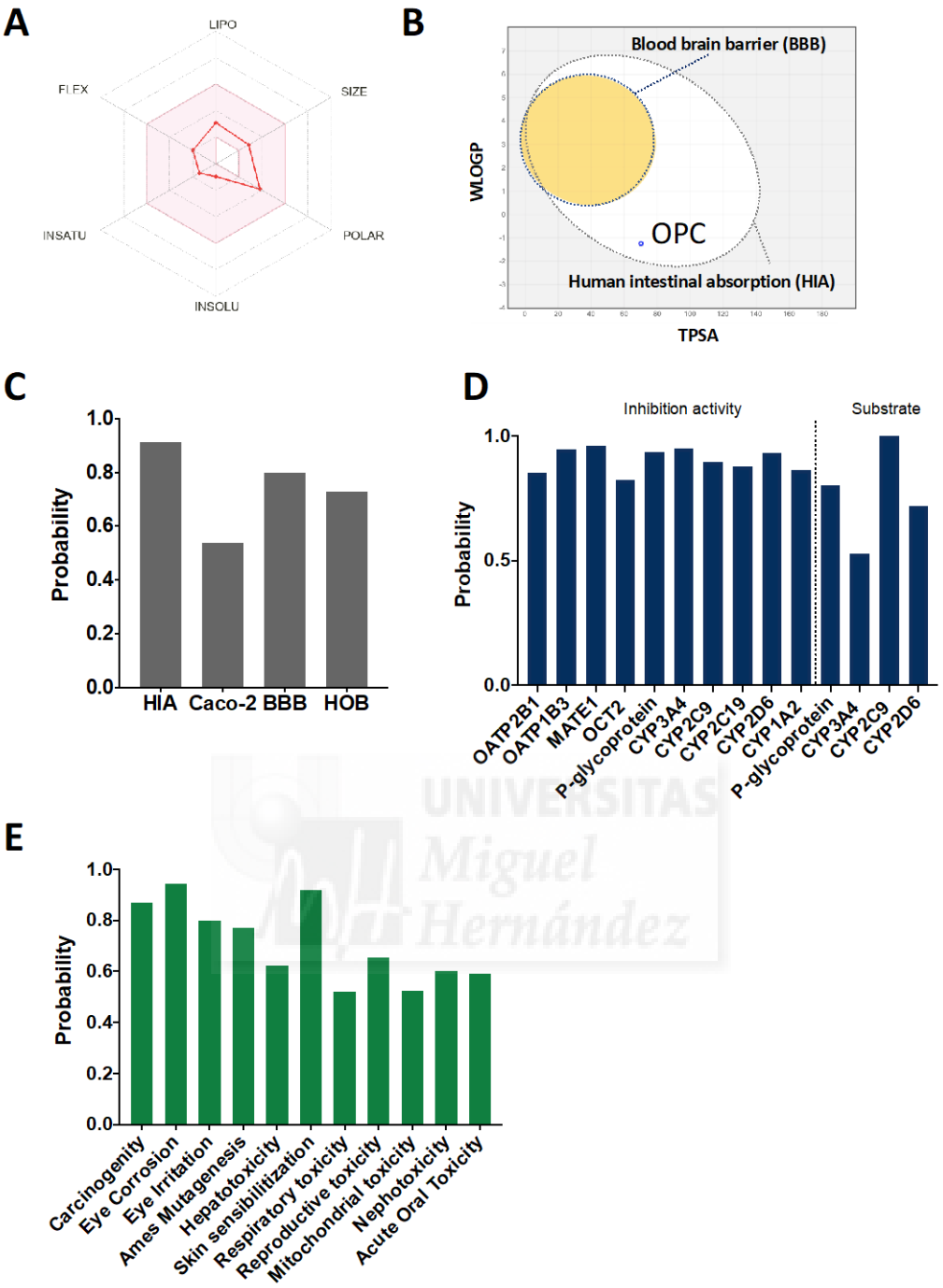

Fig. 6. Predicted absorption, transport, metabolism, excretion, and toxicity (ADMET) properties of OPC *in silico.* **(A)** Bioavailability radar; **(B)** BOILED-Egg diagram; **(C)** Absorption and digestion probability evaluation; **(D)** Potential toxicity evaluation; **(E)** Transport and metabolism probability. **BBB:** Blood-brain-barrier; **FLEX:** Flexibility; **HIA:** Human intestinal absorption; **HOB:** Human oral bioavailability; **INSATU:** Saturations; **INSOLU:** Insolubility; **LIPO:** Lipophilicity; **POLAR:** Polarity; **SIZE:** Molecular weight; **TPSA:** Topological polar surface area; **WLOGP:** Wildman and Crippen lipophilicity.

4. Discussions

Marine by-products are becoming enormously popular as alternative sources of novel food products and value-added components with interesting health benefits, since most of them are currently discarded and represent about 50 - 70 % of the harvest or catch (Ali et al., 2021). Some of the most discarded seafood by-products are the visceral organs, including ink sacs (Shazwani and Rabeta, 2020); the use of these "wastes" might be a significant opportunity to reduce its environmental impact and, at the same time, to obtain from them bioactive molecules that could provide health benefits. Recently, the biological properties of *Octopus vulgaris*ink were evaluated *in vitro* on selected cancerous and non-cancerous cell lines, proposing the recently identified ozopromide (OPC) compound as the bioactive molecule (Hernandez-Zazueta et al., 2021a, 2021b). However, since there are no reports of the biological effects of pure ozopromide, this research was intended to synthesize this molecule and evaluate it in several cancerous and non-cancerous cell lines.

The structural elucidation of the synthesized OPC displayed signals through ^{13}C-NMR analysis that were previously identified in Hernandez-Zazueta et al. (2021b), confirming the presence of the synthesized molecule. Moreover the pyrrolidine bonded to caprolactam group on its carboxamide structure, and observations of the N-H stretch (3250 cm^{-1} to 3500 cm^{-1}) have been previously reported as chemical signatures of carboxamide-like structures (Pavia and Lampman, 2009; Reich, 2020).

Since the antiproliferative effect of the *O. vulgaris* ink was previously reported by our research group on selected cancerous cell lines (HCT116, MDA-MB-231, HT-29, 22Rv1, HeLa, and A549) (Hernandez-Zazueta et al., 2021a, 2021b), OPC was assayed against the same cell lines, displaying a particularly stronger inhibitory activity on the A549 cell line. Despite the absence of reports for OPC, reports on anticancer activities of carboxamides exist. For instance, N-(2-aminophenyl)-2-methylquinone-4-carboxamide and (E)-N-(2-aminophenyl)-2-stirylquinoline-4-carboxamide derivatives were used, at several concentrations (5 and 20 μM), against A549 (cell growth inhibition: 0.55 – 34.1 %), HT-29 (cell growth inhibition: 0.5 - 68.67 %), and HCT-116 (cell growth inhibition: 2.07 - 71.83 %) cells, and this activity was associated to histone deacetylase inhibition, as suggested by several docking studies (ΔG: - 4.80 to - 9.42 kcal/mol) (Omidkhah et al., 2023). Synthetized pyrrolidine carboxamide analogs have shown potential against selected cancerous cell lines such as hepatocellular (HepG2 and Hep3B), lung (A549), and colorectal (HT-29) cancerous cell lines, displaying IC_{50} values ranging between 2.0

and 20.0 mM (Omar et al., 2017). The induction of caspases 3 and 7, after 24 and 48 h of treatment with these compounds, was used to explain the claimed anticancer effect, along with regulation of the cell cycle due to the induction of PKCd cleavage and the transcriptional control of cyclin D1, potentially interfering with G1/S cell cycle arrest (Basu and Pal, 2010). These results are in agreement with those obtained from a previous *in silico* study of the effect of OPC against cyclin D1, showing the lowest binding energies (- 6.70 kcal/mol) compared to other apoptosis-involved proteins such as ERK1 and Bad (Hernández-Zazueta et al., 2021b).

No reports were found regarding OPC effect on A549 cells' apoptosis, but the impact of (2R,4S)-N-(2,5-difluorophenyl)-4-hydroxy-1-(2,2,2-trifluoroacetyl)-pyrrolidine-2-carboxamide on human hepatocellular carcinoma cells showed that, higher early and later apoptosis processes were induced by increasing the concentration (from 0.0 to 62.5 mg/mL) of this compound (Ramezani et al., 2017). The authors suggested a dose-dependent effect based on the capability of the synthesized carboxamide derivative to generate pro-apoptotic effects such as chromatin condensation, cell and nucleus shrinkage, DNA fragmentation, and membrane blebbing. More recently, the same authors showed the impact of the same compound on pro-apoptotic genes linked to caspases 3, 5, 8, and 14, and proposed a mechanism where perforin-granzyme is stimulated to initiate caspase 3 cleavage to induce fragmentation of DNA further, cellular proteins degradation, and apoptotic bodies formation (Ramezani et al., 2019).

The observed decrease in excessive ROS generation caused by OPC could be contributory to alleviate inflammation-derived effects that may further develop into known non-communicable diseases, cancer among them (Brüne et al. 2003; Feng et al. 2001). In fact, high levels of intracellular ROS induce oxidative stress and subsequent inflammatory reactions leading to a variety of cell injuries (Conforti et al., 2009), such as DNA damage and derived mutations (Lonkar and Dedon, 2011).

By means of *in silico* analysis of the interaction of OPC with pro-inflammatory markers, the stability of the interaction of OPC with NF-kB (a known trigger of the canonical inflammatory response) was particularly evaluated. Most of the values resulting from docking studies were within a small range of 1000 - 2000 ps for potential energy (**Supplementary Figure S4**), suggesting a consistent protein size and low denaturation rate (Rho et al., 2019). In addition, the potential energy was stable between 500 and 2000 ps (**Supplementary Fig. S4B**), and the fluctuations remained low between 0 - 250 and

400 - 600 residues (**Supplementary Fig. S4C**), indicating low conformation changes in the atoms participating in the interaction (Meinhold and Smith, 2005; Zhang et al., 2018), indicating a low influence of OPC on NF-kB conformational changes.

Although reports of the participation of OPC in the modulation of cytokines were not found, chemically produced pyrrolidines and carboxamides have been assayed for their anti-inflammatory properties *in vitro* and *in vivo*. A previous examination of the anticancer and anti-inflammatory properties of (2R,4S)-N-(2,5-difluorophenyl)-4-hydroxy-1-(2,2,2-trifluoroacetyl) pyrrolidine-2-carboxamide in HepG2 hepatocellular carcinoma cell line showed a potent inhibition (fold changes: -5.2 to -85.66) of several genes linked to inflammation processes such as receptor superfamilies (*TNFRSF10A, TNFRSF10B, TNFRSF1A*) and a ligand (*TNFSF10*) of the tumor necrosis factor (TNF) (Ramezani et al., 2019). Wilhelm et al. (2014) reported the anti-inflammatory properties *in vivo* of a set of 7-chloroquinoline-1,2,3-triazoyl carboxamides, a series of natural quinoline derivative compounds with reported pharmacological activities. The authors found that several doses of oral-administered 7-chloroquinoline-1,2,3-triazoyl carboxamide (25, 50, and 100 mg/kg) to young rats (21-days old), using acetic acid to induce abdominal inflammation, could reduce abdominal constrictions (> 50 %) compared to control animals. Mechanistic explorations of the effect of synthesized carboxamides on inflammation showed that the intraperitoneal injection of these compounds into male albino rats with carrageenan-induced edema, could reduce its formation up to 50 % (Ugwu et al., 2018). A greater effect was observed after using carboxamides displaying proline-substitutions from the benzene ring, while the presence of electron-withdrawing groups at *para* position of the benzenesulfonamide decreased the anti-inflammatory activity. Results from *in vitro* cyclooxygenase-2 (COX-2) assay showed inhibitions up to 89.20 %, suggesting mechanisms linked to COX-2 reductions.

Wannamaker et al. (2007) reported the anti-inflammatory properties of a pyrrolidine carboxylic acid, following a dose-dependent inhibitory effect on IL-1b, IL-18, nitric oxide, macrophage inflammatory proteins (MIP-1a and MIP-2), and the monocyte chemoattractant protein 1 (MCP-1), in oxazolone-challenged mouse ears, suggesting inhibition of ICE/caspase-1 subfamily members.

At present, reports of *in silico* studies of carboxamides or pyrrolidine-derived molecules on protein targets associated to cancer were not found. However, the *in-silico* analysis of the present study, suggested a potential intrinsic pro-apoptotic process, targeting several

nuclear transcriptional factors that alter cell cycle division and generate DNA damage. Although c-Jun can either act as pro-apoptotic or anti-apoptotic molecule, as c-Jun requires a stimulus that OPC could drive to induce apoptosis and, considering the obtained results, a pro-apoptotic mechanism could be inferred, along with p53 regulation, as this later protein is a c-Jun substrate (Zhao et al., 2015).

As OPC was recently reported (Hernandez-Zazueta et al., 2021a, 2021b), reports regarding their ADMET properties were not found, but favorable probabilities for OPC to be used in oral applications were obtained. Previously mentioned carboxamide derivatives displayed proper intestinal absorption and water solubility when their ADMET properties were predicted (Omidkhah et al., 2023), agreeing with the results obtained in this work.

The fact that the IC_{50} value for OPC was lower than that of cisplatin when applied to A549 cell line and higher for ARPE-19 cell line, promotes the exploration of food-derived products such as octopus' ink, for the search and isolation of bioactive molecules that might target cancer mechanisms with higher specificity for transformed cells. However, most of the biological properties of synthesized compounds tested in vitro, might significantly change in the gastrointestinal environment, as the activity of enzymes and temperature may alter the chemical stability of compounds, their bioaccessibility, bioavailability, and bioactivity (Sánchez-Recillas et al., 2022). Several approaches could be considered for the investigation of OPC delivery: the evaluation of its gastrointestinal performance throughout in vitro digestion methods, the need of protecting OPC through the proper wall material (e.g., encapsulation) to be properly delivered to the small intestine, and the study of OPC effectiveness in *in vivo* models. Conclusions

5. Conclusions

The results from this research suggested the ability of OPC, a novel *O. vulgaris* ink-derived compound, to successfully impact A549 cell viability, inducing both early and late apoptosis. In addition, OPC showed anti-inflammatory activity by reducing ROS production and impacting pro-inflammatory cytokines, which results that were further confirmed by *in silico* studies, demonstrating a medium affinity between OPC and these markers. *In silico* ADMET prediction studies suggested potential less probability of acute toxicities for OPC after oral administration, however, further studies are needed for confirmation. More research is necessary to investigate the effects of OPC using further *in vitro* and *in vivo* cancer and inflammation models.

6. References

Ali, A., Wei, S., Liu, Z., Fan, X., Sun, Q., Xia, Q., Liu, S., Hao, J., Deng, C., 2021. Non-thermal processing technologies for the recovery of bioactive compounds from marine by-products. LWT 147, 111549. https://doi.org/10.1016/j.lwt.2021.111549

Banikazemi, Z., Haji, H.A., Mohammadi, M., Taheripak, G., Iranifar, E., Poursadeghiyan, M., Moridikia, A., Rashidi, B., Taghizadeh, M., Mirzaei, H., 2018. Diet and cancer prevention: Dietary compounds, dietary MicroRNAs, and dietary exosomes. J. Cell. Biochem. 119, 185–196. https://doi.org/10.1002/jcb.26244

Barrón-García, O.Y., Gaytán-Martínez, M., Ramírez-Jiménez, A.K., Luzardo-Ocampo, I., Velazquez, G., Morales-Sánchez, E., 2021. Physicochemical characterization and polyphenol oxidase inactivation of Ataulfo mango pulp pasteurized by conventional and ohmic heating processes. LWT 143, 111113. https://doi.org/10.1016/j.lwt.2021.111113

Basu, A., Pal, D., 2010. Two faces of protein kinase Cδ: The contrasting roles of PKCδ in cell survival and cell death. Sci. World J. 10, 2272–2284. https://doi.org/10.1100/tsw.2010.214

Billen, L.P., Kokoski, C.L., Lovell, J.F., Leber, B., Andrews, D.W., 2008. Bcl-XL inhibits membrane permeabilization by competing with Bax. PLoS Biol. 6, e147. https://doi.org/10.1371/journal.pbio.0060147

Bogoyevitch, M.A., Arthur, P.G., 2008. Inhibitors of c-Jun N-terminal kinases—JuNK no more? Biochim. Biophys. Acta - Proteins Proteomics 1784, 76–93. https://doi.org/10.1016/j.bbapap.2007.09.013

Braithwaite, A.W., Del Sal, G., Lu, X., 2006. Some p53-binding proteins that can function as arbiters of life and death. Cell Death Differ. 13, 984–993. https://doi.org/10.1038/sj.cdd.4401924

Brüne, B., Zhou, J., Von Knethen, A., 2003. Nitric oxide, oxidative stress, and apoptosis. Kidney Int. Suppl. 63, S22–S24. https://doi.org/10.1046/j.1523-1755.63.s84.6.x

Carnero, A., 2010. The PKB/AKT Pathway in Cancer. Curr. Pharm. Des. 16, 34–44. https://doi.org/10.2174/138161210789941865

Casilli, F., Bianchini, A., Gloaguen, I., Biordi, L., Alesse, E., Festuccia, C., Cavalieri, B.,

Strippoli, R., Cervellera, M.N., Bitondo, R. Di, Ferretti, E., Mainiero, F., Bizzarri, C., Colotta, F., Bertini, R., 2005. Inhibition of interleukin-8 (CXCL8/IL-8) responses by repertaxin, a new inhibitor of the chemokine receptors CXCR1 and CXCR2. Biochem. Pharmacol. 69, 385–394. https://doi.org/10.1016/j.bcp.2004.10.007

Conforti, F., Sosa, S., Marrelli, M., Menichini, Federica, Statti, G.A., Uzunov, D., Tubaro, A., Menichini, Francesco, 2009. The protective ability of Mediterranean dietary plants against the oxidative damage: The role of radical oxygen species in inflammation and the polyphenol, flavonoid and sterol contents. Food Chem. 112, 587–594. https://doi.org/10.1016/j.foodchem.2008.06.013

Cuellar-Nuñez, M.L., Luzardo-Ocampo, I., Lee-Martínez, S., Larrauri-Rodríguez, M., Zaldívar-Lelo de Larrea, G., Pérez-Serrano, R.M., Camacho-Calderón, N., 2022. Isothiocyanate-rich extracts from cauliflower (Brassica oleracea var. Botrytis) and radish (Raphanus sativus) inhibited metabolic activity and induced ROS in selected human HCT116 and HT-29 colorectal cancer cells. Int. J. Environ. Res. Public Health 19, 14919. https://doi.org/10.3390/ijerph192214919

Czaplewski, C., Karczyńska, A., Sieradzan, A.K., Liwo, A., 2018. UNRES server for physics-based coarse-grained simulations and prediction of protein structure, dynamics and thermodynamics. Nucleic Acids Res. 46, W304–W309. https://doi.org/10.1093/nar/gky328

Daina, A., Michielin, O., Zoete, V., 2017. SwissADME: a free web tool to evaluate pharmacokinetics, drug-likeness and medicinal chemistry friendliness of small molecules. Sci. Rep. 7, 1–13. https://doi.org/10.1038/srep42717

Derby, C.D., 2014. Cephalopod ink: production, chemistry, functions and applications. Mar. Drugs 12, 2700–30. https://doi.org/10.3390/md12052700

Feng, Q., Kumagai, T., Torii, Y., Nakamura, Y., Osawa, T., Uchida, K., 2001. Anticarcinogenic antioxidants as inhibitors against intracellular oxidative stress. Free Radic. Res. 35, 779–788. https://doi.org/10.1080/10715760100301281

García-Romo, J.-S., Hernández-Zazueta, M.-S., Gálvez-Iriqui, A.-C., Plascencia-Jatomea, M., Burboa-Zazueta, M.-G., Sandoval-Petris, E., Robles-Sánchez, R.-M., Juárez-Onofre, J.-E., Hernández-Martínez, J., Santacruz-Ortega, H. del C., López-

Saiz, C.-M., Burgos-Hernández, A., 2022. Isolation and identification of a new antiproliferative indolocarbazole alkaloid derivative extracted from farmed shrimp (Litopenaeus vannamei) muscle. J. Microbiol. Biotechnol. Food Sci. 11, e2173. https://doi.org/10.55251/jmbfs.2173

Halazonetis, T.D., Georgopoulos, K., Greenberg, M.E., Leder, P., 1988. c-Jun dimerizes with itself and with c-Fos, forming complexes of different DNA binding affinities. Cell 55, 917–924. https://doi.org/10.1016/0092-8674(88)90147-X

Hernández-Zazueta, M.S., Luzardo-Ocampo, I., García-Romo, J.S., Noguera-Artiaga, L., Carbonell-Barrachina, Á.A., Taboada-Antelo, P., Campos-Vega, R., Rosas-Burgos, E.C., Burboa-Zazueta, M.G., Ezquerra-Brauer, J.M., Burgos-Hernández, A., 2021. Bioactive compounds from *Octopus vulgaris*ink extracts exerted anti-proliferative and anti-inflammatory effects *in vitro*. Food Chem. Toxicol. 151, 112119. https://doi.org/10.1016/j.fct.2021.112119

Hernández-Zazueta, M.S., García-Romo, J.S., Noguera-Artiaga, L., Luzardo-Ocampo, I., Carbonell-Barrachina, Á.A., Taboada-Antelo, P., Campos-Vega, R., Rosas-Burgos, E.C., Burboa-Zazueta, M.G., Ezquerra-Brauer, J.M., Martínez-Soto, J.M., Santacruz-Ortega, H. del C., Burgos-Hernández, A., 2021. *Octopus vulgaris*ink extracts exhibit antioxidant, antimutagenic, cytoprotective, antiproliferative, and proapoptotic effects in selected human cancer cell lines. J. Food Sci. 86, 587–601. https://doi.org/10.1111/1750-3841.15591

Jiménez-García, B., Pons, C., Fernández-Recio, J., 2013. pyDockWEB: a web server for rigid-body protein–protein docking using electrostatics and desolvation scoring. Bioinformatics 29, 1698–1699. https://doi.org/10.1093/bioinformatics/btt262

Jiménez, J., Doerr, S., Martínez-Rosell, G., Rose, A.S., De Fabritiis, G., 2017. DeepSite: protein-binding site predictor using 3D-convolutional neural networks. Bioinformatics 33, 3036–3042. https://doi.org/10.1093/bioinformatics/btx350

Lazaro, G., Kostaras, E., Vivanco, I., 2020. Inhibitors in AKTion: ATP-competitive vs allosteric. Biochem. Soc. Trans. 48, 933–943. https://doi.org/10.1042/BST20190777

Lonkar, P., Dedon, P.C., 2011. Reactive species and DNA damage in chronic inflammation: Reconciling chemical mechanisms and biological fates. Int. J. Cancer.

https://doi.org/10.1002/ijc.25815

Luna-Vital, D., Weiss, M., Gonzalez de Mejia, E., 2017. Anthocyanins from purple corn ameliorated Tumor Necrosis Factor-α-induced inflammation and insulin resistance in 3T3-L1 adipocytes via activation of insulin signaling and enhanced GLUT4 translocation. Mol. Nutr. Food Res. 61, 1–13. https://doi.org/10.1002/mnfr.201700362

Luzardo-Ocampo, I., Ramírez-Jiménez, A.K., Cabrera-Ramírez, Á.H., Rodríguez-Castillo, N., Campos-Vega, R., Loarca-Piña, G., Gaytán-Martínez, M., 2020. Impact of cooking and nixtamalization on the bioaccessibility and antioxidant capacity of phenolic compounds from two sorghum varieties. Food Chem. 309, 125684. https://doi.org/https://doi.org/10.1016/j.foodchem.2019.125684

McCubrey, J.A., Steelman, L.S., Chappell, W.H., Abrams, S.L., Wong, E.W.T., Chang, F., Lehmann, B., Terrian, D.M., Milella, M., Tafuri, A., Stivala, F., Libra, M., Basecke, J., Evangelisti, C., Martelli, A.M., Franklin, R.A., 2007. Roles of the Raf/MEK/ERK pathway in cell growth, malignant transformation and drug resistance. Biochim. Biophys. Acta - Mol. Cell Res. 1773, 1263–1284. https://doi.org/10.1016/j.bbamcr.2006.10.001

Meinhold, L., Smith, J.C., 2005. Fluctuations and correlations in crystalline protein dynamics: A simulation analysis of staphylococcal nuclease. Biophys. J. 88, 2554–2563. https://doi.org/10.1529/biophysj.104.056101

Naseri, M.H., Mahdavi, M., Davoodi, J., Tackallou, S.H., Goudarzvand, M., Neishabouri, S.H., 2015. Up regulation of Bax and down regulation of Bcl2 during 3-NC mediated apoptosis in human cancer cells. Cancer Cell Int. 15, 55. https://doi.org/10.1186/s12935-015-0204-2

NCI, 2011. BCl-2 inhibitor BCL201 [WWW Document]. Cancer Drugs Defin. URL https://www.cancer.gov/publications/dictionaries/cancer-drug/def/bcl-2-inhibitor-bcl201 (accessed 11.29.22).

Nurgali, K., Jagoe, R.T., Abalo, R., 2018. Editorial: Adverse effects of cancer chemotherapy: Anything new to improve tolerance and reduce sequelae? Front. Pharmacol. 9. https://doi.org/10.3389/fphar.2018.00245

Oh, K.K., Adnan, M., Cho, D.H., 2021. Drug-repurposing against COVID-19 by

targeting a key signaling pathway: An *in silico* study. Med. Hypotheses 155, 110656. https://doi.org/10.1016/j.mehy.2021.110656

Omar, H.A., Zaher, D.M., Srinivasulu, V., Hersi, F., Tarazi, H., Al-Tel, T.H., 2017. Design, synthesis and biological evaluation of new pyrrolidine carboxamide analogues as potential chemotherapeutic agents for hepatocellular carcinoma. Eur. J. Med. Chem. 139, 804–814. https://doi.org/10.1016/j.ejmech.2017.08.054

Omidkhah, N., Hadizadeh, F., Zarghi, A., Ghodsi, R., 2023. Synthesis, cytotoxicity, Pan-HDAC inhibitory activity and docking study of new N-(2-aminophenyl)-2-methylquinoline-4-carboxamide and (E)-N-(2-aminophenyl)-2-styrylquinoline-4-carboxamide derivatives as anticancer agents. Med. Chem. Res. 32, 506–524. https://doi.org/10.1007/s00044-023-03018-w

Pavia, D.L., Lampman, G.M., 2009. Introduction to spectroscopy, Spectroscopy. Cengage Learning. https://doi.org/10.1887/0750303468/b293c1

Quinnell, S.P., Leifer, B.S., Nestor, S.T., Tan, K., Sheehy, D.F., Ceo, L., Doyle, S.K., Koehler, A.N., Vegas, A.J., 2020. A small-molecule inhibitor to the cytokine interleukin-4. ACS Chem. Biol. 15, 2649–2654. https://doi.org/10.1021/acschembio.0c00615

Ramezani, M.M., Ramezani, M.M., Darehkordi, A., Hassanshahi, G., Mirzaei, M.R., 2019. The New Compound of (2R, 4S)-N-(2, 5-difluorophenyl)-4- hydroxy-1-(2, 2, 2-trifluoroacetyl)-pyrrolidine-2-carboxamide to mediate the expression of some apoptosis genes by the HepG2 cell line. Asian Pacific J. Cancer Prev. 20, 1457–1462. https://doi.org/10.31557/APJCP.2019.20.5.1457

Ramezani, Mahnaz, Ramezani, Mahin, Hassanshahi, G., Mahmoodi, M., Zainodini, N., Darekordi, A., Khanamani Falahati-Pour, S., Mirzaei, M.R., 2017. Does the Novel Class of (2R, 4S)-N-(2, 5-difluorophenyl)-4-hydroxy-1-(2, 2, 2-trifluoroacetyl)-pyrrolidine-2-carboxamide's have any effect on cell viability and apoptosis of human hepatocellular carcinoma cells? Int. J. Cancer Manag. 10. https://doi.org/10.5812/ijcm.8413

Ramos, H., Soares, M.I.L., Silva, J., Raimundo, L., Calheiros, J., Gomes, C., Reis, F., Monteiro, F.A., Nunes, C., Reis, S., Bosco, B., Piazza, S., Domingues, L., Chlapek, P., Vlcek, P., Fabian, P., Rajado, A.T., Carvalho, A.T.P., Veselska, R., Inga, A.,

Pinho e Melo, T.M.V.D., Saraiva, L., 2021. A selective p53 activator and anticancer agent to improve colorectal cancer therapy. Cell Rep. 35, 108982. https://doi.org/10.1016/j.celrep.2021.108982

Reich, H.J., 2020. NMR chemical shifts of compounds [WWW Document]. Struct. Determ. using Spectrosc. methods. URL https://www.chem.wisc.edu/areas/reich/nmr/index.htm

Rho, Y., Kim, J.H., Min, B., Jin, K.S., 2019. Chemically denatured structures of porcine pepsin using small-angle X-ray scattering. Polymers (Basel). 11, 2104. https://doi.org/10.3390/polym11122104

Sánchez-Recillas, E., Campos-Vega, R., Pérez-Ramírez, I.F., Luzardo-Ocampo, I., Cuéllar-Núñez, M.L., Vergara-Castañeda, H.A., 2022. Garambullo (Myrtillocactus geometrizans): effect of *in vitro* gastrointestinal digestion on the bioaccessibility and antioxidant capacity of phytochemicals. Food Funct. 13, 4699–4713. https://doi.org/10.1039/D1FO04392G

Shazwani, A., Rabeta, M.S., 2020. Enzymatic hydrolysis as an approach to produce alternative protein from cephalopods ink powder: a short review. Food Res. 4, 1383–1390. https://doi.org/10.26656/fr.2017.4(5).423

Shukla, P., Khandelwal, R., Sharma, D., Dhar, A., Nayarisseri, A., Singh, S.K., 2019. Virtual screening of IL-6 inhibitors for idiopathic arthritis. Bioinformation 15, 121–130. https://doi.org/10.6026/97320630015121

Socaci, S.A., Farcas, A.C., Vodnar, D.C., Tofana, M., 2017. Food wastes as valuable sources of bioactive molecules, in: Shiomi, N., Waisundara, V. (Eds.), Superfood and Functional Food - The Development of Superfoods and Their Roles as Medicine. InTech, Rijeka, pp. 75–94. https://doi.org/10.5772/66115

Somu, C., Mohan, C.D., Ambekar, S., Dukanya, Rangappa, S., Baburajeev, C., Sukhorukov, A., Mishra, S., Shanmugam, M.K., Chinnathambi, A., Awad Alahmadi, T., Alharbi, S.A., Basappa, Rangappa, K.S., 2020. Identification of a novel 1,2 oxazine that can induce apoptosis by targeting NF-κB in hepatocellular carcinoma cells. Biotechnol. Reports 25, e00438. https://doi.org/10.1016/j.btre.2020.e00438

Ugwu, D.I., Okoro, U.C., Ukoha, P.O., Gupta, A., Okafor, S.N., 2018. Novel anti-

inflammatory and analgesic agents: synthesis, molecular docking and *in vivo* studies. J. Enzyme Inhib. Med. Chem. 33, 405–415. https://doi.org/10.1080/14756366.2018.1426573

Varghese, J.N., Moritz, R.L., Lou, M.-Z., van Donkelaar, A., Ji, H., Ivancic, N., Branson, K.M., Hall, N.E., Simpson, R.J., 2002. Structure of the extracellular domains of the human interleukin-6 receptor α-chain. Proc. Natl. Acad. Sci. 99, 15959–15964. https://doi.org/10.1073/pnas.232432399

Wannamaker, W., Davies, R., Namchuk, M., Pollard, J., Ford, P., Ku, G., Decker, C., Charifson, P., Weber, P., Germann, U.A., Kuida, K., Randle, J.C.R., 2007. (S)-1-((S)-2-{[1-(4-Amino-3-chloro-phenyl)-methanoyl]-amino}-3,3-dimethyl-butanoyl)-pyrrolidine-2-carboxylic acid ((2 R ,3 S)-2-ethoxy-5-oxo-tetrahydro-furan-3-yl)-amide (VX-765), an orally available selective interleukin (IL)-converting enzyme/caspa. J. Pharmacol. Exp. Ther. 321, 509–516. https://doi.org/10.1124/jpet.106.111344

WHO, 2020. Cancer [WWW Document]. Cancer. URL https://www.who.int/health-topics/cancer#tab=tab_1 (accessed 4.7.20).

Wilhelm, E.A., Machado, N.C., Pedroso, A.B., Goldani, B.S., Seus, N., Moura, S., Savegnago, L., Jacob, R.G., Alves, D., 2014. Organocatalytic synthesis and evaluation of 7-chloroquinoline-1,2,3-triazoyl carboxamides as potential antinociceptive, anti-inflammatory and anticonvulsant agent. RSC Adv. 4, 41437–41445. https://doi.org/10.1039/C4RA07002J

Zhang, H., Ma, G., Zhu, Y., Zeng, L., Ahmad, A., Wang, C., Pang, B., Fang, H., Zhao, L., Hao, Q., 2018. Active-site conformational fluctuations promote the enzymatic activity of NDM-1. Antimicrob. Agents Chemother. 62. https://doi.org/10.1128/AAC.01579-18

Zhao, A., Lee, S.H., Moiena, M., Jenkins, R.G., Patrick, D.R., Huber, H.E., Goetz, M.A., Hensens, O.D., Zink, D.L., Vilella, D., Dombrowski, A.W., Lingham, R.B., Huang, L., 1999. Resorcylic acid lactones. Naturally occurring potent and selective inbibitors. J. Antibiot. (Tokyo). 52, 1086–1094. https://doi.org/10.7164/antibiotics.52.1086

Zhao, H.-F., Wang, J., Tony To, S.-S., 2015. The phosphatidylinositol 3-kinase/Akt and

c-Jun N-terminal kinase signaling in cancer: Alliance or contradiction? (Review). Int. J. Oncol. 47, 429–436. https://doi.org/10.3892/ijo.2015.3052

5. RESUMEN RESULTADOS Y DISCUSIÓN

5.1. *Octopus vulgari* sink extracts exhibit antioxidant, antimutagenic, cytoprotective, antiproliferative, and proapoptotic effects in selected human cancer cell lines.

Martin Samuel Hernández-Zazueta, Joel Said García-Romo, Luis Noguera-Artiaga, Iván Luzardo-Ocampo, Ángel Antonio Carbonell-Barrachina, Pablo Taboada-Antelo, Rocio Campos-Vega, Ema Carina Rosas-Burgos, María Guadalupe Burboa-Zazueta, Josafat Marina Ezquerra-Brauer, Juan Manuel Martínez-Soto, Hisila del Carmen, Santacruz-Ortega, and Armando Burgos-Hernández.

Journal of Food Science. 2021. 86(2):587-601.

https://doi.org/10.1111/1750-3841.15591

5.1.1. Objetivo:

Este estudio constituye una primera aproximación al aprovechamiento de la tinta de pulpo *Octopus vulgaris*, un subproducto desaprovechado de la industria pesquera. Esta tinta se revela como una fuente potencial de compuestos diversos con posibles propiedades beneficiosas para la salud humana, particularmente en relación con procesos carcinogénicos e inflamatorios. El proceso incluyó la extracción de diversos compuestos a partir de la tinta utilizando solventes con diferentes polaridades, seguido de su evaluación biológica en líneas celulares humanas de cáncer (22Rv1, HeLa, A549) para determinar sus propiedades antiproliferativas, proapoptóticas, además de la evaluación de sus propiedades antimutagénicas, citoprotectoras, antioxidantes mediante la aplicación de distintas metodologías.

5.1.2. Resumen de Resultados y Discusión:

Dada la creciente preocupación mundial por el cáncer, una enfermedad no transmisible, se emprendió una investigación para explorar el potencial de los productos marinos, como la tinta de *Octopus vulgaris* (OI), como fuentes de compuestos capaces de abordar esta problemática, por lo cual, se evaluaron las propiedades antimutagénicas, citoprotectoras, antiproliferativas, proapoptóticas y antioxidantes de los extractos de OI en líneas celulares humanas de cáncer (22Rv1, HeLa, A549). Se empleó la línea celular ARPE-19 como referencia de células humanas normales para evaluar la citotoxicidad de la tinta.

Los resultados mostraron que el extracto acuoso exhibió la mayor actividad antimutagénica y citoprotectora, mientras que el extracto de diclorometano (DM) mostró la mayor eficacia contra las células 22Rv1. Posteriormente, a través de técnicas cromatográficas, se identificó la DM-F2, que demostró un alto efecto antiproliferativo (LC_{50} = 27.6 µg/mL), modulación de especies reactivas, inducción temprana de apoptosis (42.9%) y disrupción nuclear en las células 22Rv1.

Además, se realizó una elucidación estructural detallada de las fracciones purificadas de DM (F1, F2, F3), lo que condujo a la identificación de un compuesto sin reportes previos en la fracción con mayor actividad antiproliferativa, denominado N-(2-ozoazepan-3-yl)-pirrolidina-2-carboxamida (OPC). Análisis *in silico* predijeron una alta afinidad del OPC con la ciclina D1 (-6.70 kcal/mol), sugiriendo su potencial influencia en el arresto del ciclo celular.

Estos hallazgos resaltan el potencial de productos marinos subutilizados como la tinta de *O. vulgaris* en la promoción de la salud, específicamente en términos de actividad antioxidante y prevención del cáncer. No obstante, se necesitan investigaciones adicionales, tanto *in vitro* como *in vivo*, para esclarecer los mecanismos y beneficios para la salud asociados con el uso de OI.

5.1.3. Resumen de Conclusión:

Los resultados indican que los extractos de tinta de *Octopus vulgaris* (OI) presentan beneficios sustanciales para la salud, demostrando efectos antimutagénicos, citoprotectores, antiproliferativos y proapoptóticos en líneas celulares humanas de cáncer (22Rv1, HeLa, A549).

El análisis estructural identificó un compuesto previamente no descrito, N-(2-ozoazepan-3-yl)-pirrolidina-2-carboxamida (OPC), en el extracto de diclorometano. El análisis *in silico* sugiere una afinidad significativa entre OPC y la Ciclina D1, lo que insinúa su potencial influencia en la inducción del arresto del ciclo celular.

Estos hallazgos resaltan el potencial infrautilizado de la tinta de *Octopus vulgaris* como un recurso natural marino que podría albergar compuestos biológicamente activos con propiedades que promueven la salud, incluyendo propiedades antioxidantes y la prevención del cáncer.

5.2. Bioactive compounds from *Octopus vulgaris* ink extracts exerted antiproliferative and anti-inflammatory effects *in vitro*.

Martin Samuel Hernández-Zazueta, Iván Luzardo-Ocampo, Joel Said García-Romo, Luis Noguera-Artiaga, Ángel Antonio Carbonell-Barrachina, Pablo Taboada-Antelo, Rocío Campos-Vega, Ema Carina Rosas-Burgos, María Guadalupe Burboa-Zazueta, Josafat Marina Ezquerra-Brauer, Armando Burgos-Hernández.

Food and Chemical Toxicology. 2021. 151:0278-6915.
https://doi.org/10.1016/j.fct.2021.112119.

5.1.1. Objetivo:

El presente estudio tuvo como objetivo evaluar los efectos antiproliferativos y antiinflamatorios de los extractos de tinta de *Octopus vulgaris* en células de cáncer humano de colon (HT-29/HCT116) y mama (MDA-MB-231), así como en células de ratón RAW 264.7 estimuladas con el Lipopolisacarido de *E. coli* para medir la expresión de especies reactivas y su posible inibición por efecto de los tratamientos de los extractos y sus fracciones, así como las citocinas y factores que estos modulan relacionadas con la respuesta inflamatoria y su posible relación con el desarrollo de la carcinogénesis.

5.1.2. Resumen de Resultados y Discusión:

El estudio encontró que todos los extractos, excepto el etilacetato, exhibieron efectos antiproliferativos sin ser citotóxicos para las células ARPE-19 y RAW 264.7. Entre las fracciones de diclorometano, DM-F2 mostró el mayor efecto antiproliferativo (LC_{50} = 52.64 µg/mL), induciendo alteraciones morfológicas proapoptóticas en las células HCT116. En las células RAW 264.7, DM-F2 mostró la mayor reducción de nitritos y la regulación al alza de citocinas clave de las vías JAK-STAT, PI3K-Akt e IL-17. El análisis metabolómico de DM-F2 resaltó el ácido hexadecanoico y la 1-(15-metil-1-oxohexadecil)-pirrolidina como los metabolitos más relevantes. Estos compuestos también mostraron una alta afinidad de unión *in silico* (-4.6 a -5.8 kcal/mol) a IL-1α, IL-1β e IL-2. El estudio sugiere que los extractos de tinta de *Octopus vulgaris* podrían ser una fuente de compuestos bioactivos que ofrecen beneficios para la salud relacionadas con las enfermedades crónico-degenerativas como el cáncer, y el ambiente inflamatorio que podría predisponer a la carcinogénesis.

5.1.3. Resumen de Conclusión:

Los extractos de tinta de *Octopus vulgaris*, un producto marino generalmente desechado, contienen compuestos bioactivos con potenciales beneficios para la salud, como ejemplo el extracto de diclorometano (DM) y su fracción DM-F2, donde estos demostraron un potencial efecto antiproliferativo en células de cáncer de colon y mama humanas, sin ser citotóxicos para las células normales.

La fracción DM-F2 indujo la muerte celular apoptótica en las células HCT116, evidenciada por cambios morfológicos y fragmentación del ADN.

Al mismo tiempo, la fracción DM-F2 exhibió actividad antiinflamatoria en las células RAW 264.7 estimuladas con LPS, al reducir la producción de óxido nítrico y modular la expresión de citocinas.

El análisis metabolómico de DM-F2 reveló la presencia de ácido hexadecanoico y 1-(15-metil-1-oxohexadecil)-pirrolidina como los metabolitos más importantes, los cuales mostraron una alta afinidad de unión a receptores de interleucinas *in silico.*

Se sugiere que los compuestos identificados en la fracción DM-F2, podrían ser responsables del efecto inmunomodulador conjunto y antiproliferativo del extracto de tinta, por lo cual se proponen futuros estudios para confirmar su mecanismo de acción y su potencial terapéutico.

5.3. N-(2-ozoazepan-3-yl)-pyrrolidine-2-carboxamide, a novel *Octopus vulgaris* ink-derived metabolite, exhibits a pro-apoptotic effect on A549 cancer cell line and inhibits pro-inflammatory markers

Martin Samuel Hernández-Zazueta, Joel Said García-Romo, Ivan Luzardo-Ocampo, Ángel Antonio Carbonell-Barrachina, Pablo Taboada-Antelo, Ema Carina Rosas-Burgos, Josafat Marina Ezquerra-Brauer, Juan Manuel Martínez-Soto, Maria del Carmen Candia-Plata, Hisila del Carmen Santacruz-Ortega, Armando Burgos-Hernández

Food and Chemical Toxicology. 2023. 177: 0278-6915.
https://doi.org/10.1016/j.fct.2023.113829.

5.1.1. Objetivo:

El objetivo del estudio fue sintetizar y caracterizar N-(2-ozoazepan-3-yl)-pyrrolidine-2-carboxamide (OPC), un nuevo metabolito derivado de la tinta de *Octopus vulgaris*, y evaluar sus efectos antiproliferativos y antiinflamatorios en diferentes modelos celulares. Se utilizaron técnicas de síntesis orgánica, espectroscopía y cromatografía para obtener y purificar OPC, y determinar su estructura mediante análisis de RMN y MS para posteriormente evaluar el efecto antiproliferativo/proapoptótico sobre líneas celulares tumorales humanas.

5.1.2. Resumen de Resultados y Discusión:

Tras la síntesis química, la caracterización estructural de OPC se confirmó mediante análisis de COSY-2D, FTIR, y C-/H-NMR. OPC demostró efectos inhibitorios en el crecimiento de células cancerosas humanas de mama (MDA-MB-231), próstata (22Rv1), cuello uterino (HeLa), y pulmón (A549), siendo el efecto más pronunciado en estas últimas, con un IC_{50} de 53.70 µM. Además, OPC indujo apoptosis en las células A549, manifestando características morfológicas asociadas y una mayor afinidad por las proteínas Akt-1 y Bcl-2, reconocidas por sus roles en la supervivencia celular y apoptosis.

Estos hallazgos destacan a los productos alimenticios marinos como fuentes de moléculas bioactivas con potencial para ser estudiadas para posibles usos terapéuticos, como la tinta, que pueden albergar metabolitos bioactivos con beneficios para la salud. Además, OPC redujo la acumulación intracelular de especies reactivas del oxígeno (ROS) en células PBMC estimuladas con LPS y ejerció un efecto inhibitorio sobre las citoquinas

proinflamatorias IL-6 e IL-8, mientras que estimuló dosis-dependientemente las citoquinas antiinflamatorias IL-4 e IL-10.

Los análisis *in silico* y el diagrama BOILED-Egg sugieren una alta biodisponibilidad de OPC y su capacidad para cruzar la barrera intestinal, aunque no la barrera hematoencefálica (BBB). Las pruebas *in silico* tamien revelaron posibles interacciones con proteínas relacionadas con el cáncer y la inflamación, mostrando una alta afinidad por IL-6 e IL-4, así como una inhibición dependiente de la dosis de NF-kB, aunque con baja afinidad.

Los resultados de los acoplamientos moleculares *in silico* entre OPC y objetivos moleculares relacionados con procesos apoptóticos, como p53, c-Jun, Bcl-X, MEK, Bcl-2 y Akt-1, resultaron variados. Las pruebas de dinámica molecular para el inhibidor NF-kB indicaron que OPC tiene una capacidad limitada para influir en los cambios conformacionales de NF-kB.

Las propiedades ADMET de OPC señalan su alta biodisponibilidad, aunque se predice que podría afectar a varios transportadores y actuar como sustrato para P-glicoproteínas y diversos citocromos (CYP3A4, CYP2C9 y CYP2D6). La administración tópica de OPC presenta una alta probabilidad de toxicidad, como corrosión e irritación ocular y sensibilización cutánea, aunque las probabilidades son bajas para los sistemas respiratorio y reproductivo.

A pesar de estos prometedores resultados, se requiere investigación adicional para explorar por completo el potencial terapéutico de OPC y compuestos afines.

5.1.3. Resumen de Conclusión:

El compuesto ozopromide (OPC), una innovadora molécula derivada de la tinta de *Octopus vulgaris*, exhibe una acción pro-apoptótica en la línea celular de cáncer de pulmón A549, conllevando a la activación de la caspasa-3 y la fragmentación del ADN. Además, el OPC demostró su capacidad para inhibir la expresión de marcadores pro-inflamatorios, tales como el factor nuclear kappa B (NF-κB), el factor de necrosis tumoral alfa (TNF-α) y la interleucina 6 (IL-6), en células estimuladas con lipopolisacárido (LPS). Este compuesto OPC no presentó toxicidad hacia las células normales de fibroblastos humanos (HDFa), lo que apunta hacia un perfil de seguridad favorable. En conjunto, los

hallazgos sugieren que el OPC podría considerarse para futuros estudios como un potencial agente terapéutico prometedor en el tratamiento del cáncer de pulmón y enfermedades inflamatorias, sin embargo, son necesarias mas investigaciones que ayuden por completo a elucidar su mecanismo de acción.

6. DISCUSIÓN GENERAL

6. Discusión general

En el contexto del aumento global de la incidencia de cáncer, una patología no transmisible de gran relevancia clínica y social, se ha intensificado la búsqueda de nuevos agentes terapéuticos derivados de recursos naturales. Entre estos, los productos marinos ofrecen un vasto repertorio de compuestos bioactivos con potencial terapéutico aún por explotar. En particular, la tinta de *Octopus vulgaris* (OI), reconocida por su rica composición en metabolitos secundarios, emerge como un candidato prometedor para la obtención de dichos agentes. Este estudio se enfocó en la exploración exhaustiva de las propiedades antiinflamatorias, antimutagénicas, citoprotectoras, antioxidantes, así como antiproliferativas y proapoptóticas de los extractos de OI en diversas líneas celulares humanas de cáncer, incluyendo HCT-116 (colon) 22Rv1 (próstata), HeLa (cervical) y A549 (pulmonar). Como contraparte, se utilizó la línea celular ARPE-19, correspondiente a epitelio de retina pigmentado de humano, como control de referencia para la evaluación de la citotoxicidad, asegurando así una perspectiva comparativa sobre la selectividad y seguridad de los extractos de tinta en células normales frente a células cancerígenas. Esta aproximación metodológica permitió no solo identificar compuestos con actividad antiproliferativa específica sino también valorar el margen terapéutico de dichos extractos, aspecto crítico para el desarrollo futuro de intervenciones oncológicas basadas en componentes naturales.

Propiedades Antioxidantes y Antimutagénicas: Coadyuvantes en la Prevención de la Carcinogénesis

Los estudios iniciales revelaron que los extractos de tinta de OI manifiestan una potente capacidad antioxidante y antimutagénica, atribuible a su rico perfil de compuestos fenólicos y otros metabolitos secundarios. Esta actividad quimiopreventiva se postula como un mecanismo crucial en la mitigación del estrés oxidativo y la protección del material genético contra las alteraciones mutagénicas. La actividad antioxidante de los extractos de OI puede atribuirse a su capacidad para modular el estrés oxidativo a nivel celular, principalmente a través de la scavenging de especies reactivas de oxígeno (ERO) y la activación de sistemas enzimáticos endógenos de defensa antioxidante, como las superóxido dismutasas (SOD), catalasas (CAT) y peroxidasas. Este efecto protector reduce el potencial de daño al ADN y previene la iniciación de cascadas pro-mutagénicas, a través de la inhibición de la formación de aductos de ADN y la promoción de mecanismos de reparación del ADN. Este mecanismo subraya la importancia de las vías

de señalización antioxidante mediadas por Nrf2, un factor de transcripción clave que regula la expresión de genes antioxidantes y detoxificantes. En conclusión, se sugiere que estos compuestos bioactivos actúan como agentes secuestrantes de radicales libres y moduladores de las vías de señalización celular involucradas en las respuestas antioxidantes endógenas, lo cual es esencial para prevenir la iniciación y promoción tumoral.

Efectos Anti-proliferativos: Inducción de Apoptosis y Alteración del Ciclo Celular

Subsecuentemente, la investigación centrada en la fracción DM-F2 destacó su potencial para inhibir significativamente la proliferación de células tumorales mediante la inducción de procesos apoptóticos y la alteración del ciclo celular. Los hallazgos indican que determinados metabolitos presentes en la tinta podrían interactuar con componentes clave de la maquinaria celular, incluyendo la regulación a la baja de proteínas reguladoras del ciclo celular y la activación de cascadas pro-apoptóticas, evidenciando una acción antineoplásica específica y selectiva. Estos compuestos han demostrado inducir un arresto del ciclo celular en las fases G0/G1 y G2/M, disminuyendo la expresión de ciclinas y quinasas dependientes de ciclinas (CDKs), fundamentales para la progresión del ciclo celular. Paralelamente, se observa una inducción de la apoptosis mediada por la vía intrínseca, con un incremento en la relación Bax/Bcl-2, la liberación de citocromo c de la mitocondria y la activación de caspasas iniciadoras y ejecutoras, lo que culmina en la fragmentación del ADN y la muerte celular programada. Estos efectos son evidencia de la manipulación de vías como la vía de PI3K/Akt y MAPK, cruciales en la supervivencia y proliferación celular. Estos mecanismos subrayan la relevancia que los componentes de la tinta de OI podrían tener en el control del crecimiento tumoral y su potencial aplicación como adyuvantes en la terapia anticancerígena.

Actividad Antiinflamatoria: Modulación del Microambiente Tumoral

La exploración de los efectos antiinflamatorios y pro-apoptóticos del metabolito OPC demostraron su potencial para modular el microambiente tumoral, mitigando la generación de especies reactivas de oxígeno y la expresión de citoquinas proinflamatorias en células A549. Estos resultados se apoyan en análisis *in silico* que corroboran la interacción de OPC con proteínas relacionadas con la apoptosis y la inflamación, sugiriendo una influencia directa sobre la regulación de la muerte celular programada y la respuesta inflamatoria.

De la misma manera, OPC ha demostrado tener un potencial para ejercer un efecto antiinflamatorio notable, inhibiendo la producción de mediadores proinflamatorios como las interleucinas IL-6 e IL-8 y reduciendo la actividad de NF-κB, un factor de transcripción central en la respuesta inflamatoria. Este efecto podría ser el resultado de la interacción de OPC con sitios de unión específicos en estas proteínas, alterando su configuración y función. La modulación de NF-κB, junto con la reducción en la generación de especies reactivas de oxígeno, sugiere una influencia directa sobre la inflamación crónica, que es un factor contribuyente reconocido en la progresión del cáncer y la metástasis. Tal modulación del microambiente tumoral por parte de OPC resalta la importancia de la vía de señalización NF-κB y otras moléculas clave en la promoción del proceso inflamatorio asociado al cáncer, ofreciendo un enfoque terapéutico prometedor para el tratamiento de neoplasias mediante la alteración del nicho tumoral.

Integración y Perspectivas Futuras

La integración de los hallazgos de estos estudios resalta la compleja interacción entre los efectos antioxidantes, anti-proliferativos y antiinflamatorios de los compuestos derivados de la tinta de OI sugiriendo un enfoque multifacético para la posible prevención y tratamiento del cáncer. El efecto observado entre estas actividades biológicas sugiere un enfoque prometedor para estrategias terapéuticas innovadoras con compuestos naturales, sin embargo, es necesaria la implementación de estudios para confirmar si es resultado de sinergia, adición o potenciación de dichos compuestos. Futuras investigaciones deberán centrarse en la elucidación de los mecanismos moleculares específicos subyacentes a estas actividades, la optimización de la biodisponibilidad y la eficacia terapéutica de estos compuestos en modelos preclínicos y clínicos, así como en la evaluación de su seguridad y perfil toxicológico. Este enfoque integrador no solo ofrece una mayor comprensión de las propiedades bioactivas de la tinta de OI sino que también puede promover el desarrollo de nuevos agentes quimioterapéuticos y antiinflamatorios derivados de fuentes marinas.

7. CONCLUSIONES GENERALES E INVESTIGACIONES FUTURAS

7.1 CONCLUSIONES GENERALES

- Los extractos de tinta de *Octopus vulgaris* albergan compuestos con actividad biológica, lo que sugiere su potencial para aportar beneficios a la salud humana.

- El extracto acuoso de la tinta de pulpo exhibe propiedades antioxidantes y antimutagénicas.

- El extracto soluble en diclorometano muestra la mayor actividad antiproliferativa, aunque no afecta la línea celular ARPE-19.

- La subfracción DM-F2 posee efectos antiproliferativos, proapoptóticos y causa alteraciones en el ADN de las células 22Rv1, sin afectar la proliferación de células no cancerosas (ARPE-19).

- La fracción DM-F2 contiene principalmente colesterol y el compuesto N-(2-ozoazepan-3-il)-pirrolidin-2-carboxamida (OPC), previamente no reportado.

- El análisis *in silico* indica que el OPC muestra afinidad de unión con las proteínas ciclina D1, ERK1 y BAD, sugiriendo su participación en un proceso proapoptótico mediante la detención del ciclo celular (apoptosis intrínseca).

- El OPC, derivado de la tinta de *O. vulgaris*, tiene el potencial de impactar de manera efectiva la proliferación de células cancerígenas de pulmón A549, induciendo tanto apoptosis temprana como tardía.

- El OPC presenta potencial antiinflamatorio al reducir la producción de ROS e influir en la producción de citoquinas proinflamatorias como IL-6 e IL-8, resultados respaldados por análisis *in silico* que demuestran una alta afinidad entre el OPC y estos marcadores.

7.2 GENERAL CONCLUSIONS

- *Octopus vulgaris* ink extracts contain biologically active compounds, suggesting their potential to be a source of health benefits to humans.

-The aqueous ink extract exhibits antioxidant and antimutagenic properties.

-The dichloromethane-soluble extract displays the most potent antiproliferative activity, although it does not affect the ARPE-19 cell line.

-The DM-F2 subfraction possesses antiproliferative and proapoptotic effects and induces DNA alterations in 22Rv1 cells, without affecting non-cancerous cell proliferation (ARPE-19).

-The DM-F2 fraction primarily contains cholesterol and the previously unreported compound N-(2-ozoazepan-3-yl)-pyrrolidine-2-carboxamide (OPC).

-*In silico* analysis indicates that OPC exhibits binding affinity with proteins such as cyclin D1, ERK1, and BAD, suggesting its possible involvement in a proapoptotic process through cell cycle arrest (intrinsic apoptosis).

-OPC, derived from *Octopus vulgaris* ink, has the potential to effectively influence the proliferation of A549 lung cancer cells, inducing both early and late-stage apoptosis.

-OPC demonstrates anti-inflammatory potential by reducing ROS production and influencing the production of proinflammatory cytokines like IL-6 and IL-8, with *in silico* analysis supporting a strong affinity between OPC and these markers.

7.3 INVESTIGACIONES FUTURAS

- Realizar ensayos bioquímicos adicionales para confirmar el mecanismo de acción del OPC.

- Realizar estudios de biología molecular para identificar las proteínas moduladas en el proceso de activación de la apoptosis en células cancerígenas, tanto por la vía intrínseca como extrínseca.

- Ampliar la investigación a ensayos *in vivo* para evaluar el OPC como potencial agente terapéutico anticancerígeno en modelos animales.

7.4 FUTURE RESEARCHES

-Conduct additional biochemical assays to confirm OPC's mechanism of action.

-Undertake molecular biology studies to identify the proteins modulated in the apoptosis activation process in cancer cells, both through the intrinsic and extrinsic pathways.

-Expand research to *in vivo* experiments to assess OPC's potential as a possible anticancer therapeutic agent in animal models.

8. REFERENCIAS

8. REFERENCIAS

- **A**

ACS (2018) *Aprenda sobre el cáncer | Recursos sobre el cáncer | Sociedad Americana Contra El Cáncer*. Available at: https://www.cancer.org/es/cancer.html (Accessed: 16 May 2020).

ACS (2018) *Factores de riesgo del cáncer colorrectal*. Available at: https://www.cancer.org/es/cancer/cancer-de-colon-o-recto/causas-riesgos-prevencion/factores-de-riesgo.html (Accessed: 25 May 2021).

ACS (2018) *Quimioterapia para el cáncer colorrectal*. Available at: https://www.cancer.org/es/cancer/cancer-de-colon-o-recto/tratamiento/quimioterapia.html (Accessed: 1 June 2020).

Aggarwal, B. B. (2003) 'Signalling pathways of the TNF superfamily: a double-edged sword', *Nature Reviews Immunology*, 3(9), pp. 745–756. doi: 10.1038/nri1184.

Alberts, B. *et al.* (2008) *Molecular biology of the cell*. doi: 0815341059.

Allavena, P. *et al.* (2008) 'Pathways connecting inflammation and cancer', *Current Opinion in Genetics and Development*, 18(1), pp. 3–10. doi: 10.1016/j.gde.2008.01.003.

- **B**

Benzie, I. F. F., & Strain, J. J. (1996). The ferric reducing ability of plasma (FRAP) as a measure of "antioxidant power": The FRAP assay. Analytical Biochemistry, 239(1), 70–76. https://doi.org/10.1006/ABIO.1996.0292

Besednova, N. N., Zaporozhets, T. S., Kovalev, N. N., Makarenkova, I. D., & Yakovlev, Y. M. (2017). Cephalopods: The potential for their use in medicine. Russian Journal of Marine Biology, 43(2), 101–110. https://doi.org/10.1134/S1063074017020031

Bogdan, C. (2001) 'Nitric oxide and the immune response', *Nature Immunology*, 2(10), pp. 907–916. doi: 10.1038/ni1001-907.

Braekman, J. C. and Daloze, D. (1986) 'Chemical defence in sponges', *Pure and Applied Chemistry*. De Gruyter, 58(3), pp. 357–364. doi: 10.1351/pac198658030357.

- **C**

Chávez-Sánchez, L., Chávez-Rueda, K., Legorreta-Haquet, M., Zenteno, E., Ledesma-Soto, Y., Montoya-Díaz, E., Tesoro-Cruz, E., Madrid-Miller, A., Blanco-Favela, F., 2010. The activation of CD14, TLR4, and TLR2 by mmLDL induces IL-1β, IL-6, and IL-10 secretion in human monocytes and macrophages. Lipids Health Dis. 9, 117. https://doi.org/10.1186/1476-511X-9-117

Coussens, L. M. and Werb, Z. (2002) 'Inflammation and cancer', *Nature*, 420(6917), pp. 860–867. doi: 10.1038/nature01322.

Cruz-Ramírez, S. G. *et al.* (2015) 'Isolation and identification of an antimutagenic phthalate derivative compound from octopus (Paraoctopus limaculatus)', *Tropical Journal of Pharmaceutical Research*, 14(7), pp. 1257–1264. doi: 10.4314/tjpr.v14i7.19.

Cuellar-Nuñez, M.L., Luzardo-Ocampo, I., Lee-Martínez, S., Larrauri-Rodríguez, M., Zaldívar-Lelo de Larrea, G., Pérez-Serrano, R.M., Camacho-Calderón, N., 2022. Isothiocyanate-rich extracts from cauliflower (Brassica oleracea var. Botrytis) and radish (Raphanus sativus) inhibited metabolic activity and induced ROS in selected human HCT116 and HT-29 colorectal cancer cells. Int. J. Environ. Res. Public Health 19, 14919. https://doi.org/10.3390/ijerph192214919.

- **D**

Deniau, A.-L. *et al.* (2010) 'Multiple Beneficial Health Effects of Natural Alkylglycerols from Shark Liver Oil', *Marine Drugs*. Molecular Diversity Preservation International, 8(7), pp. 2175–2184. doi: 10.3390/md8072175.

Derby, C. D. (2014) 'Cephalopod ink: Production, chemistry, functions and applications', *Marine Drugs*, 12(5), pp. 2700–2730. doi: 10.3390/md12052700.

- **E**

Ebada, S. S., Edrada, R. A., Lin, W., & Proksch, P. (2008). Methods for isolation, purification and structural elucidation of bioactive secondary metabolites from marine invertebrates. Nature Protocols, 3(12), 1820–1831. https://doi.org/10.1038/nprot.2008.182

- **F**

Fahmy, R. (2013) '*In vitro* antioxidant, analgesic and cytotoxic activities of Sepia officinalis ink and Coelatura aegyptiaca extracts', *African Journal of Pharmacy and Pharmacology*, 7(22), pp. 1512–1522. doi: 10.5897/AJPP2013.3564.

Figueroa-Hernández, J. L. *et al.* (2005) 'Plant products with anti-cancer properties employed in the treatment of bowel cancer: literature review 1985 and 2004.', *Proceedings of the Western Pharmacology Society*, 48, pp. 77–83. Available at: http://www.ncbi.nlm.nih.gov/pubmed/16416667 (Accessed: 15 May 2018).

Fuentes-pananá, E., Camorlinga-ponce, M. and Maldonado-bernal, C. (2009) 'Infección , inflamación y cáncer gástrico', 51(5), pp. 427–433.

Fukumoto, L. R. R., & Mazza, G. (2000). Assessing antioxidant and prooxidant activities of phenolic compounds. Journal of Agricultural & Food Chemistry, 48(8), 3597–3604. https://doi.org/10.1021/jf000220w

- **G**

Gertsman, I., Barshop, B.A., 2018. Promises and pitfalls of untargeted metabolomics. J. Inherit. Metab. Dis. 41, 355–366. https://doi.org/10.1007/s10545-017-0130-7

Gross, H. and König, G. M. (2006) 'Terpenoids from Marine Organisms: Unique Structures and their Pharmacological Potential', *Phytochemistry Reviews*. Springer Netherlands, 5(1), pp. 115–141. doi: 10.1007/s11101-005-5464-3.

Guadagni, F. *et al.* (2007) 'Non-steroidal anti-inflammatory drugs in cancer prevention and therapy', *Anticancer Res*, 27(5A), pp. 3147–3162. Available at: http://www.ncbi.nlm.nih.gov/pubmed/17970056.

- **I**

Imai, S. *et al.* (1994) 'Gastric carcinoma: monoclonal epithelial malignant cells expressing Epstein-Barr virus latent infection protein.', *Proceedings of the National Academy of Sciences of the United States of America*, 91(19), pp. 9131–5. Available at: http://www.ncbi.nlm.nih.gov/pubmed/8090780 (Accessed: 18 May 2018).

- **K**

Komen, S. G. (2010) 'La quimioterapia y los efectos secundarios'. Available at:

https://ww5.komen.org/uploadedFiles/Content_Binaries/translate/KOMEED082000-SP.pdf (Accessed: 18 May 2018).

Kusters, J. G., van Vliet, A. H. M. and Kuipers, E. J. (2006) 'Pathogenesis of Helicobacter pylori Infection', *Clinical Microbiology Reviews*, 19(3), pp. 449–490. doi: 10.1128/CMR.00054-05.

- **L**

Lê Cao, K.A., Boitard, S., Besse, P., 2011. Sparse PLS discriminant analysis: Biologically relevant feature selection and graphical displays for multiclass problems. BMC Bioinformatics 12. https://doi.org/10.1186/1471-2105-12-253

Lewis, J. S. *et al.* (2000) 'Expression of vascular endothelial growth factor by macrophages is up-regulated in poorly vascularized areas of breast carcinomas', *The Journal of Pathology*. Wiley-Blackwell, 192(2), pp. 150–158. doi: 10.1002/1096-9896(2000)9999:9999<::AID-PATH687>3.0.CO;2-G.

Lirk, P., Hoffmann, G. and Rieder, J. (2002) 'Inducible Nitric Oxide Synthase - Time for Reappraisal', *Current Drug Target -Inflammation & Allergy*, 1(1), pp. 89–108. doi: 10.2174/1568010023344913.

Liu, C. *et al.* (2008) 'Structural characterisation and antimutagenic activity of a novel polysaccharide isolated from Sepiella maindroni ink', *Food Chemistry*, 110(4), pp. 807–813. doi: 10.1016/j.foodchem.2008.02.026.

Lodish, H. *et al.* (2008) 'Molecular cell biology'.

Luna-Vital, D., Weiss, M., Gonzalez de Mejia, E., 2017. Anthocyanins from purple corn ameliorated Tumor Necrosis Factor-α-induced inflammation and insulin resistance in 3T3-L1 adipocytes via activation of insulin signaling and enhanced GLUT4 translocation. Mol. Nutr. Food Res. 61, 1–13. https://doi.org/10.1002/mnfr.201700362

Luzardo-Ocampo, I., Campos-Vega, R., Gonzalez de Mejia, E., Loarca-Piña, G., 2020. Consumption of a baked corn and bean snack reduced chronic colitis inflammation in CD-1 mice via downregulation of IL-1 receptor, TLR, and TNF-α associated pathways. Food Res. Int. 132, 109097. https://doi.org/10.1016/j.foodres.2020.109097.

Luzardo-Ocampo, I., Ramírez-Jiménez, A.K., Cabrera-Ramírez, Á.H., Rodríguez-Castillo, N., Campos-Vega, R., Loarca-Piña, G., Gaytán-Martínez, M., 2020. Impact of cooking and nixtamalization on the bioaccessibility and antioxidant capacity of phenolic compounds from two sorghum varieties. Food Chem. 309, 125684. https://doi.org/https://doi.org/10.1016/j.foodchem.2019.125684.

- **M**

Maron, D. M. and Ames, B. N. (1983) 'Revised methods for the Salmonella mutagenicity test', *Mutation Research/Environmental Mutagenesis and Related Subjects*, 113(3–4), pp. 173–215. doi: 10.1016/0165-1161(83)90010-9.

Mayer, A. M. S. and Gustafson, K. R. (2003) 'Marine pharmacology in 2000: Antitumor and cytotoxic compounds', *International Journal of Cancer*, 105(3), pp. 291–299. doi: 10.1002/ijc.11080.

- **N**

Nenadis, N., Wang, L.-F. F., Tsimidou, M., & Zhang, H.-Y. Y. (2004). Estimation of scavenging activity of phenolic compounds using the ABTS • + assay. Journal of Agricultural and Food Chemistry, 52(15), 4669–4674. https://doi.org/10.1021/jf0400056

Noguera-Artiaga, L., Salvador, M.D., Fregapane, G., Collado-González, J., Wojdyło, A., López-Lluch, D., Carbonell-Barrachina, Á.A., 2019. Functional and sensory properties of pistachio nuts as affected by cultivar. J. Sci. Food Agric. 99, 6696–6705. https://doi.org/10.1002/jsfa.9951

- **P**

Paredes-Lario, A., Blanco-García, C. and Echenique-Elizondo, M. (2006) 'Expresión de proteínas relacionadas con resistencia a Múltiples Drogas (MDR-Proteínas) y resistencia a la quimioterapia en el cáncer de pulmón.', *Gaceta Médica de Bilbao*, 103(3), pp. 105–117. doi: 10.1016/S0304-4858(06)74536-X.

Plummer, M. *et al.* (2016) 'Global burden of cancers attributable to infections in 2012: a synthetic analysis', *The Lancet Global Health*, 4(9), pp. e609–e616. doi: 10.1016/S2214-109X(16)30143-7.

- **R**

Rajasekharan Nair, J. *et al.* (2011) 'Cephalopod research and bioactive substances',

Indian Journal of Marine Sciences, 40(1), pp. 13–27.

RoyChoudhury, S., More, T.H., Chattopadhyay, R., Lodh, I., Ray, C.D., Bose, G., Sarkar, H.S., Chakravarty, B., Rapole, S., Chaudhury, K., 2017. Polycystic ovary syndrome in Indian women: a mass spectrometry based serum metabolomics approach. Metabolomics 13, 115. https://doi.org/10.1007/s11306-017-1253-4

- **S**

Sadayan, P., Thiyagarajan, S. and Balakrishnan, B. (2013) 'Inhibitory Activity of Ink and Body Tissue Extracts of Euprymna Stenodactyla and Octopus Dollfusi Aganist Histamine Producing Bacteria', *Middle-East Journal of Scientific Research*, 16(4), pp. 514–518. doi: 10.5829/idosi.mejsr.2013.16.04.11155.

Saleem, M. Z., Nisar, M. A., Alshwmi, M., Din, S. R. U., Gamallat, Y., Khan, M., & Ma, T. (2020). Brevilin a inhibits STAT3 signaling and induces ros-dependent apoptosis, mitochondrial stress and endoplasmic reticulum stress in MCF-7 breast cancer cells. OncoTargets and Therapy, 13, 435–450. https://doi.org/10.2147/OTT.S228702.

- **T**

Taylor, W.F., Moghadam, S.E., Moridi Farimani, M., N. Ebrahimi, S., Tabefam, M., Jabbarzadeh, E., 2019. A multi-targeting natural compound with growth inhibitory and anti-angiogenic properties re-sensitizes chemotherapy resistant cancer. PLoS One 14, e0218125. https://doi.org/10.1371/journal.pone.0218125

Tsai, C.-J. and Sun Pan, B. (2012) 'Identification of Sulfoglycolipid Bioactivities and Characteristic Fatty Acids of Marine Macroalgae', *Journal of Agricultural and Food Chemistry*. American Chemical Society, 60(34), pp. 8404–8410. doi: 10.1021/jf302241d.

Turgeon, D. D. *et al.* (1998) 'Common and scientific names of aquatic invertebrates from the United States and Canada: Mollusks'. Available at: https://pubs.er.usgs.gov/publication/70162654 (Accessed: 24 May 2018).

- **V**

Van Vuuren, R.J., Botes, M., Jurgens, T., Joubert, A.M., Van Den Bout, I., 2019. Novel sulphamoylated 2-methoxy estradiol derivatives inhibit breast cancer migration by disrupting microtubule turnover and organization. Cancer Cell Int. 19.

https://doi.org/10.1186/s12935-018-0719-4.

Von Mering, C., Jensen, L.J., Kuhn, M., Chaffron, S., Doerks, T., Kruger, B., Snel, B., Bork, P., Krüger, B., Snel, B., Bork, P., 2007. STRING 7 - Recent developments in the integration and prediction of protein interactions. Nucleic Acids Res. 35, 358–362. https://doi.org/10.1093/nar/gkl825

- **W**

WHO, 2020. Cancer [WWW Document]. Cancer. URL https://www.who.int/health-topics/cancer#tab=tab_1 (accessed 4.7.20).

AGRADECIMIENTOS

AGRADECIMIENTOS

Agradezco al Dr. Ángel Antonio Carbonell Barrachina por su generosidad al aceptarme en su equipo de investigación, por brindarme la oportunidad de ser su alumno y por depositar plena confianza en mí que, además de desempeñar un papel fundamental como mentor, quiero agradecerle por su vasta experiencia educativa e investigativa al formar parte de mi comité de tesis y por su valiosa contribución al desarrollo de mi tema de investigación. Su hospitalidad al recibirme en su centro de investigación, donde pude interactuar con un grupo de trabajo excepcional, no solo me permitió conocer colegas de laboratorio, sino que también forjó amistades perdurables, por lo cual estoy profundamente agradecido.

Asimismo, extiendo mi gratitud a la Universidad Miguel Hernández por proporcionarme sus instalaciones de vanguardia, recursos y una educación de primer nivel, que resultaron esenciales en el desarrollo de esta investigación.

No puedo pasar por alto mi reconocimiento al Departamento de Investigación y Posgrado en Alimentos por permitirme llevar a cabo mis estudios dentro de un Programa Nacional de Posgrados de Calidad y por facilitarme las aulas y laboratorios necesarios para ello.

Mi reconocimiento se extiende al Dr. Pablo Taboaba Antelo, quien, a pesar de no conocernos previamente, accedió a formar parte de mi comité y dirección de tesis, aportando su vasta experiencia y toma de decisiones cruciales en el desarrollo de mi investigación, incluyendo estudios y valiosas ideas que fueron fundamentales para la culminación de este proyecto.

Mi gratitud profunda se dirige a la Dra. Josafat Marina Ezquerra Brauer por brindarme su apoyo, orientación y financiamiento desde el inicio de mis estudios de posgrado. Sus consejos y motivación desempeñaron un papel determinante en la realización y finalización de este importante proyecto.

También deseo expresar mi agradecimiento a la Dra. Ema Carina Rosas Burgos, quien ha desempeñado un papel fundamental en mi investigación desde mis estudios de maestría, siempre dispuesta a ayudarme a encontrar soluciones a los métodos y técnicas utilizados en mi trabajo de investigación.

La Dra. Hisila del Carmen Santacruz Ortega merece un agradecimiento especial, ya que su vasta experiencia ha sido esencial no solo en el desarrollo de esta investigación, sino también en la obtención de resultados y reconocimientos que esta investigación ha recibido.

Agradezco a la Dra. María Guadalupe Burboa Zazueta por su colaboración y al depositar su confianza al proporcionarme sus instalaciones e insumos para llevar a cabo esta investigación.

Al Dr. Ivan Luzardo Ocampo, amigo y colaborador, le agradezco profundamente sus enseñanzas y contribuciones fundamentales en el desarrollo de la investigación, que han sido esenciales para la obtención de los resultados y su difusión.

No puedo dejar de mencionar mi agradecimiento al Dr. Luis Noguera y la Dra. Paola Sánchez por recibirme y brindarme el apoyo necesario durante mi estadía en España, así como por abrir las puertas de su hogar y ofrecerme su valiosa amistad.

Al Dr. Joel García Romo, amigo y compañero, le agradezco su apoyo y el tiempo compartido en este proceso de preparación y desarrollo de investigación.

Asimismo, al Dr. Juan Manuel Martínez Soto, amigo y colaborador en este proceso de investigación, le agradezco su valiosa experiencia en este campo científico.

Mi reconocimiento se extiende al M.C. Edgar Sandoval Petris por su conocimiento y apoyo en el desarrollo de los experimentos llevados a cabo en esta investigación.

Quiero expresar mi gratitud a mis compañeros y compañeras de laboratorio: Joel, Carolina, Jesús, José Miguel, Leontina, Dania y Héctor. No solo me permitieron trabajar junto a ellos, sino que también compartimos experiencias y forjamos amistades que perdurarán a lo largo de los años. A todos ellos, muchas gracias.

Por último, pero no menos importante, deseo expresar mi profundo agradecimiento al Dr. Armando Burgos Hernández, quien desde el principio me brindó la oportunidad de llevar a cabo mi investigación en su proyecto y me aceptó como su estudiante para realizar mis estudios de posgrado. Le agradezco por su apoyo, consejo y motivación, y por ser mi guía en este proceso de preparación. ¡Muchas gracias a todos!

A mi esposa; Beatriz H. Gallego

A mis padres; Maria de los Angeles y Martin

A mi hermana; Priscila